

**Investigating the Efficacy of
Radiofrequency Renal Artery
Denervation: From Bench to
Bedside**

Dr Sara I. Al Raisi

A thesis submitted in fulfilment of the requirements for the degree of

Doctor of Philosophy (PhD)

Department of Cardiology, Westmead Clinical School

Faculty of Medicine
The University of Sydney
June 2019

Preface

This thesis is submitted for the degree of Doctor of Philosophy. The research was performed in the Cardiology Department at Westmead Hospital and the University of Sydney, NSW, Australia, under the supervision of Associate Professor Pramesh Kovoor and Dr Jim Poulipoulos. I certify that the intellectual content of this thesis is the product of my own work and that all assistance received in preparing this thesis and sources have been acknowledged. This thesis does not exceed the length of 100,000 words. Studies involving human subjects were conducted under the supervision and approval of Western Sydney Local Health District Human Ethics Research Committee at Westmead Hospital.

Dr Sara I. Al Raisi

Department of Cardiology, Westmead Hospital

University of Sydney,

NSW, Australia

Acknowledgments

This work would not have been possible without the help and support of many people to whom I am indebted. I am tremendously grateful to my supervisor, Associate Professor Pramesh Kovoov, for giving me the opportunity to conduct this work. He has been a great mentor, and a constant source of encouragement and inspiration. I have been fortunate to have him guide me through this process. I would like to convey my deepest appreciation to my co-supervisor, Dr Jim Pouliopoulos. He has always been generous with his time and eager to help and teach. Much of the experimental work would not have been possible without the assistance of my colleagues Tony Barry and Juntang Lu who I sincerely thank. I also thank Dr. John Swinnen for his assistance in the procedural work, Dr. Thiagalingam for his valuable comments and suggestions, Dr Karen Byth for her assistance in the statistical work and data analysis and Ms. Patricia King for her help in patients' follow-up. I thank my colleagues and friends Jun, Abhi, Loan, Pierre, Arun and Mary for their help and support and many shared memories over endless coffee/ tea sessions. I dedicate this work to my loving family. My father, who is my role model. His diligence and hard work set an example for great work ethics. My mother whose positivity and ambitiousness are infectious. Thank you both for making me value learning and education and for respecting the choices I made. My precious sisters (Abeer, Sana, Amira, Maryam and Esra), thank you for believing in me and for being my best friends. Finally, I thank my dear husband for being there for me every step of the way. I love you and I could not have done this without your endless love and support.

Table of Contents

Preface	I
Acknowledgments	II
Abstract	V
Publications/ Manuscripts	VI
Conference Abstracts	VIII
Authorship Attribution.....	X
Abbreviations	XIII
Chapter 1: Introduction	1
1.1 Background.....	2
1.2 Aims of Thesis	3
Chapter 2: Literature Review	4
2.1 Review Article (submitted for publication).....	5
2.2 Background to chapters 3-6	39
2.3 Supplementary methods (chapter 3-6)	40
Chapter 3: Evaluation of First Generation Symplicity and EnligHTN Renal Artery Denervation Systems Using A Renal Artery Phantom Model	46

3.1	Manuscript 1 (published).....	47
Chapter 4: Assessment of New Generation Symplicity and EnligHTN Renal Artery Denervation Systems Using A Renal Artery Phantom Model		
		55
4.1	Manuscript 2 (published).....	56
Chapter 5: The Clinical Efficacy of Two Different Radiofrequency Ablation Systems for Renal Artery Denervation		
		62
5.1	Manuscript 3 (Accepted for publication)	63
Chapter 6: Assessment of Renal Artery Branch Denervation Using A Phantom Model		
		70
6.1	Manuscript 4 (under review).....	71
Chapter 7: Discussion		
		89
7.1	Summary.....	90
7.2	Conclusion	92
7.3	Future Directions	93
Bibliography.....		95

Abstract

Hypertension is a prevalent condition affecting one third of the adult population worldwide. Medications alone have failed to control the blood pressure (BP) in a large proportion of the hypertensive population. Therefore, renal artery denervation (RAD) was developed for the management of resistant hypertension. However, its efficacy was found to be inconsistent in clinical trials. Delivery of effective ablation that results in sufficient nerve injury is one important criterion for a successful procedure. This thesis focuses on evaluation of various commercially available RAD devices and understanding their unique properties and limitations. Using an in-house built renal artery phantom model, we demonstrated that single electrode Symplicity Flex produced larger lesions, in depth and width compared to multi-electrode EnligHTN when both systems were used under identical experimental conditions, and with optimal vessel wall contact. Clinically, in a small cohort of patients who underwent RAD using either systems, we found no significant difference in office BP reduction between the two systems and both groups had a significant reduction in office BP, which persisted up to 4 years. When the new generation multi-electrode Symplicity Spyral and multi-electrode EnligHTN systems were assessed in the same model, EnligHTN lesions were larger in depth. However, lesion depth of the new generation devices was reduced by 30-40% compared to older generation devices. In a phantom model of branch renal artery, Symplicity Spyral produced lesion that were of similar size and with bigger circumferential coverage compared to main vessel phantom model. No overheating at the electrode-tissue interface occurred during branch ablation. Overall, this thesis broadens our knowledge in the field of RAD with respect to information regarding properties and limitation of different RAD systems and it aids in refining the procedure in order to achieve the best clinical outcome.

Publications/ Manuscripts

Review Article (under review)

Al Raisi SI, Pouliopoulos J, Swinnen J, Thiagalingam A, Kovoov A. Renal Artery Denervation in Resistant Hypertension: The Good, The Bad and the Future. Submitted to *Heart Lung Circ.* **[Chapter 2]**

Manuscript 1 (published)

Al Raisi SI, Pouliopoulos J, Barry MT, Swinnen J, Thiagalingam A, Thomas SP, Sivagangabalan G, Chow C, Chong J, Kizana E, Kovoov P. Evaluation of lesion and thermodynamic characteristics of Symplicity and EnligHTN renal denervation systems in a phantom renal artery model. *EuroIntervention.* 2014;10:277-84. This manuscript was accompanied with an Editorial. **[Chapter 3]**

Manuscript 2 (published)

Al Raisi SI, Barry MT, Qian P, Bhaskaran A, Pouliopoulos J, Kovoov P. Comparison of new generation renal artery denervation systems: Assessing lesion size and thermodynamics using a thermochromic liquid crystal phantom model. *EuroIntervention.* 2017;13:1242-1247. **[Chapter 4]**

Manuscript 3 (Epub ahead of print)

Al Raisi SI, Pouliopoulos J, Qian P, King P, Byth K, Barry MT, Swinnen J, Thiagalingam A, Kovoov P. Comparison of two different radiofrequency ablation systems for renal artery denervation: Evaluation of short-term and long-term follow up. *Catheter Cardiovasc Interv* 2018.doi:10.1002/ccd.28038 **[Chapter 5]**

Manuscript 4 (under review)

Al Raisi SI, Pouliopoulos J, Barry MT, Qian P, Thiagalingam A, Swinnen J, Kovoov P. Renal artery branch denervation: Evaluation of lesion characteristics using a thermochromic liquid crystal phantom model. Submitted to *Heart Lung Circ.* [**Chapter 6**]

Conference Abstracts

1. Sara I. Al Raisi, Jim Pouliopoulos, Michael T. Barry, Pierre Qian, Aravinda Thiagalingam, John Swinnen, Pramesh Kovoor. Renal artery branch denervation: Evaluation of lesion characteristics using a thermochromic liquid crystal phantom model.

Moderated poster presentation at the European Society of Cardiology Congress. August 2018, Munich, Germany.

2. Sara I. Al Raisi, Jim Pouliopoulos, Pierre Qian, Patricia King, Karen Byth, Michael T. Barry, John Swinnen, Aravinda Thiagalingam, Pramesh Kovoor. Comparison of two different radiofrequency ablation systems for renal artery denervation: evaluation of short-term and long-term follow-up.

E-Poster presentation at EuroPCR Annual Scientific Meeting. May 2018, Paris, France.

3. Sara I. Al Raisi, Michael T. Barry, Pierre Qian, Abhishek Bhaskaran, Jim Pouliopoulos, Pramesh Kovoor. Comparison of New Generation Renal Artery Denervation Systems: Assessing Lesion Size and Thermodynamics Using a Thermochromic Liquid Crystal Phantom Model.

Oral presentation at EuroPCR Annual Scientific Meeting. May 2016, Paris, France.

4. Sara I. Al Raisi, Jim Pouliopoulos, Tony Barry, Pramesh Kovoor. Evaluation of Lesion and Thermodynamic Characteristics of Symplicity and EnlighTn Renal Denervation Systems in a Phantom Renal Artery Model.

Poster presentation at the European Society of Cardiology Congress. August 2014, Barcelona, Spain.

5. Sara I. Al Raisi, Jim Pouliopoulos, Tony Barry, Pramesh Kovoor. Evaluation of Lesion and Thermodynamic Characteristics of Symplicity and EnligHTN Renal Denervation Systems in a Phantom Renal Artery Model.

Oral presentation at the World Congress of Cardiology. May 2014, Melbourne, Australia.

Authorship Attribution

1. **Chapter 3 is published as: Al Raisi SI, Pouliopoulos J, Barry MT, Swinnen J, Thiagalingam A, Thomas SP, Sivagangabalan G, Chow C, Chong J, Kizana E, Kovoov P.** Evaluation of lesion and thermodynamic characteristics of Symplicity and EnligHTN renal denervation systems in a phantom renal artery model. *EuroIntervention*. 2014;10:277-84.
 - P Kovoov, J Pouliopoulos and S Al Raisi designed the research methodology. S Al Raisi conducted the experiments, collected the data, analysed the results and wrote the manuscripts. J Pouliopoulos assisted in the statistical analysis. T Barry assisted in setting up the phantom model. The co-authors assisted in editing the manuscript and providing valuable comments.

2. **Chapter 4 is published as: Al Raisi SI, Barry MT, Qian P, Bhaskaran A, Pouliopoulos J, Kovoov P.** Comparison of new generation renal artery denervation systems: Assessing lesion size and thermodynamics using a thermochromic liquid crystal phantom model. *EuroIntervention*. 2017;13:1242-1247.
 - P Kovoov, J Pouliopoulos and S Al Raisi designed the research methodology. S Al Raisi conducted the experiments, collected the data, analysed the results and wrote the manuscripts. Tony Barry and assisted in setting up the phantom model. P Qian, A Bhaskaran, J Pouliopoulos and P Kovoov assisted in editing the manuscript and providing valuable comments.

3. **Chapter 5 is published as: Al Raisi SI, Pouliopoulos J, Qian P, King P, Byth K, Barry MT, Swinnen J, Thiagalingam A, Kovoov P.** Comparison of two different radiofrequency ablation systems for renal artery denervation: Evaluation of short-term

and long-term follow up. *Catheter Cardiovasc Interv* 2018. doi:10.1002/ccd.28038.

[Epub ahead of print]

- P Kovoov, J Pouliopoulos and S Al Raisi designed the research methodology. J Swinnen, P Kovoov and S Al Raisi performed the procedural work. S Al Raisi collected the data and wrote the manuscripts. K Byth performed the statistical analysis. J Pouliopoulos. T Barry assisted in procedural technical aspects. P King performed patients follow up. The co-authors assisted in editing the manuscript and providing valuable comments. I would also like to thank S zaman for her assistance with ethics and Janice Sullivan for her assistance with data collection and patients follow up.

4. **Chapter 6 has been submitted for publication as: Al Raisi SI**, Pouliopoulos J, Barry MT, Qian P, Thiagalingam A, Swinnen J, Kovoov P. Renal artery branch denervation: Evaluation of lesion characteristics using a thermochromic liquid crystal phantom model. *Heart Lung Circ*. Under review

- S Al Raisi designed the research methodology. S Al Raisi conducted the experiments, collected the data, analysed the results and wrote the manuscripts. J Pouliopoulos assisted in the statistical analysis. T Barry assisted in setting up the phantom model. The co-authors assisted in editing the manuscript and providing valuable comments.

In addition to the statements above, permission to include the published material has been granted by the corresponding author.

Dr Sara Al Raisi



Signature

Date:11/09/2019

As the supervisor for the candidature upon which this thesis is based, I confirm that the authorship attribution statements above are correct.

A Prof Pramesh Kovoor



Signature

8 September 2019

Date

Abbreviations

BP	blood pressure
RAD	renal artery denervation
RF	radiofrequency
TLC	thermochromic liquid crystal
SBP	systolic blood pressure
NE	norepinephrine
IV	intravenous
eGFR	estimated glomerular filtration rate
MI	myocardial infarction
CVA	cerebrovascular accident
PPM	permanent pacemaker
ICD	implantable cardioverter-defibrillator
RNS	renal nerve stimulation
US	ultrasound
HIFU	high intensity focused ultrasound
ISH	isolated systolic hypertension
SSAHT	standardised stepped-care antihypertensive treatment
LIMA	left internal mammary artery
SS	Symplicity Spyril
NGE	new-generation EnligHTN
CT	computed tomography
TIA	transient ischaemic attack
DBP	diastolic blood pressure
BMI	body mass index

ACEi	angiotensin-converting-enzyme inhibitor
ARB	angiotensin receptor blocker
BB	beta blocker
CCB	calcium channel blocker
IHD	ischaemic heart disease
OSA	obstructive sleep apnoea

Chapter 1

Introduction

INTRODUCTION

1.1 Background

Hypertension is a major health concern globally, which is associated with serious cardiovascular and cerebrovascular complications. For decades, pharmacotherapy was the only available treatment option for hypertension. However, amongst the hypertensive population, a large proportion of patients remain untreated, undertreated or resistant to treatment on medication alone [1, 2]. In recent years, management of hypertension using non-pharmacological therapy including minimally invasive renal artery denervation (RAD) has been explored [3]. The rationale for this procedure was supported by a good volume of evidence, which demonstrated that renal afferent and efferent sympathetic nerves are crucial players in hypertension development [4-14]. In RAD, injury of nerves located around the renal artery is achieved through the application of various energy modes, most commonly radiofrequency (RF) onto the intimal surface via an intra-arterial catheter-based approach [3]. Early clinical trials demonstrated significant blood pressure (BP) reduction after RAD [3, 15]. However, the randomised sham-controlled trial, Symplicity HTN-3 showed no difference in BP reduction between the RAD and the sham control arms [16]. The negative results of this clinical trial highlighted the complexity of RAD and the importance of further research in this area. Procedural efficacy, defined by achieving a clinical response is affected by multiple factors including patient selection, anatomy of the target (renal nerves), the technique, and proceduralist skills. Careful assessment of each of those factors enhances our overall understanding and aids in refining the procedure in order to improve the clinical outcome.

1.2 Aims of Thesis

The overall objective of this thesis is to improve our understanding of the differences and limitations of various RF systems utilised in RAD by evaluating lesion characteristics and thermal properties of each system, and to understand the implications of these findings on RAD efficacy through both bench and clinical work. This has been illustrated through four manuscripts (chapter 3-6).

The specific aims of the thesis are:

- 1- To construct a gel based phantom model of the renal artery involving thermochromic liquid crystal (TLC) technology for evaluating various RF devices utilised in RAD. [Chapter 3]
- 2- To evaluate and compare the spatiotemporal lesion growth and ablation characteristics between single electrode Symplicity Flex and multi-electrode EnligHTN RF systems using the TLC model of the renal artery. [Chapter 3]
- 3- To assess and compare RF lesion dimensions and thermodynamics of the multi-electrode Symplicity Spyral versus the new generation multi-electrode EnligHTN systems using the TLC model. [Chapter 4]
- 4- To assess short-term and long-term BP response to RAD using two different RF systems in a cohort of patients with resistant hypertension. [Chapter 5]
- 5- To evaluate the extent of thermal injury (lesion depth, width and circumferential coverage) of RF ablation using the multi-electrode Symplicity Spyral system in the TLC model of a renal artery branch and to determine the electrode-tissue interface temperature for branch ablation in the TLC model. [Chapter 6]
- 6- To Compare the extent of thermal injury for main vessel versus branch renal artery RF ablation in the TLC model using the same RF system. [Chapter 6]

Chapter 2

Literature Review

Al Raisi SI, Pouliopoulos J, Swinnen J, Thiagalingam A, Kover A. Renal Artery Denervation in Resistant Hypertension: The Good, The Bad and the Future. Submitted to *Heart, Lung and Circulation*.

Renal Artery Denervation in Resistant Hypertension: The Good, The Bad and the Future

‘Review article’

Authors: Sara I. Al Raisi ^{a,b}, MB Bch, FRACP; Jim Pouliopoulos ^{a,b}, PhD; John Swinnen ^c, MBBS, FRACS; Aravinda Thiagalingam ^{a,b}, MBBS, PhD; Pramesh Kovoor ^{a,b*}, MBBS, PhD

^aDepartment of Cardiology, Westmead Hospital, Sydney, NSW, Australia,

^bUniversity of Sydney, NSW, Australia,

^cDepartment of Vascular Surgery, Westmead Hospital, NSW, Australia

***Correspondence and Reprints Requests: Word count: 7427**

A/Professor Pramesh Kovoor

Senior Staff Specialist, Department of Cardiology

PO Box 533, Westmead Hospital

Cnr of Hawkesbury and Darcy Road

NSW, 2145, Australia Phone: (+612) 8890 6030, Fax: (+612) 8890 8323

E-mail: pramesh.kovoor@sydney.edu.au

Declarations of Interest: None

Abstract

Early studies of renal artery denervation (RAD), Symplicity HTN-1 & 2, demonstrated efficacy in treating resistant hypertension patients with significant reduction in office blood pressure (BP). This resulted in a growing enthusiasm in the field and a rapid evolution of technology with expanding procedural indications. However, the first randomised sham-controlled trial, Symplicity HTN-3, failed to demonstrate a significant difference in BP reduction between the RAD and the sham-controlled arm, which subsequently led to a major reduction in the clinical application of this procedure. Additionally, the results generated further interest into understanding the mechanism and factors affecting procedural success and identifying the limitations within the field. Many lessons were learned from the Symplicity HTN-3 trial, and with recent evidence emerging for RAD in hypertension treatment, the field continues to be refined.

Keywords: Hypertension, renal denervation, blood pressure

Introduction

Hypertension affects one third of the adult population worldwide [1]. It is one of the major risk factors for ischaemic heart disease and cerebrovascular disease, both of which are main contributors to cardiovascular mortality [2]. It was demonstrated that a 20 mm Hg rise in systolic blood pressure (SBP) doubles the mortality risk for heart disease, stroke or any other vascular disease [3]. In contrast, a 10 mm Hg fall in SBP resulted in a reduction in stroke rate by 41% [4]. Of note, only about 50% of patients with hypertension have their blood pressure (BP) controlled on medical therapy [5], and 20-30% develop resistant hypertension (BP>140/90 despite three antihypertensive medications of different class including a diuretic) [6]. In the last decade, renal artery denervation (RAD) became available as a treatment option for refractory hypertension [7]. Despite conflicting efficacy results in clinical trials, the rationale for its application in hypertension treatment remains valid. Previous studies in different models of hypertension provide strong evidence for the implication of renal afferent and efferent sympathetic nerves in hypertension pathogenesis [8-19]. Moreover, the effectiveness of surgical sympathectomy in reducing BP at the time of limited medical therapy supports the use of RAD in hypertension treatment [20-28]. Therefore, recent effort has been focused on optimising the procedure by selecting appropriate patients and applying new methods and technologies guided by a better understanding of renal nerve anatomy. In this review we discuss the anatomy of renal nerves, the implication of renal sympathetic nerves in hypertension, the technology applied, and the clinical evidence, both old and new, for RAD.

Anatomy of renal nerves

Renal artery denervation is a minimally invasive procedure that specifically targets the renal nerves located in the adventitial layer of the renal arteries, which are derived from the celiac plexus, the lumbar splanchnic nerves and the superior mesenteric ganglion [10]. Postganglionic nerve fibres form a plexus around the renal artery (renal plexus) and run parallel to it (Figure 1A & 1B). They enter the kidney with the renal artery, renal vein and the ureter, branching in the renal cortex and medulla to supply the arterioles, the tubules and the juxtaglomerular apparatus. Due to the proximity of renal nerves to the renal artery intima, nerve injury through an endovascular approach via the renal artery was theoretically possible.

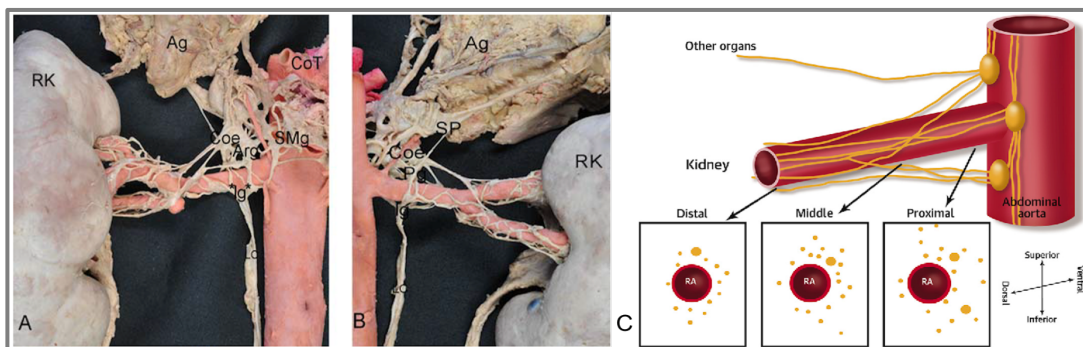


Figure 1. Renal nerve anatomy. Gross anatomy of renal sympathetic nerves demonstrating the ganglionic neural structures and the renal plexus; (A) anterior view of a right kidney, (B) Posterior view of a right kidney. An illustration showing the distribution of renal nerve fibres around the proximal, middle and distal segments of the renal artery (C). RK; right kidney, Ag; adrenal gland, Coe; coeliac ganglion, Arg; aorticorenal ganglion, Ig; renal inferior ganglion, LC; lumbar chain, SMg; superior mesenteric ganglion, CoT; coeliac trunk, Pg; posterior ganglion, SP; thoracic splanchnic nerves.

Nonetheless, detailed understanding of the anatomy and distribution of renal nerves was limited until recent years. Both animal and human post-mortem studies demonstrated that nerve fibres are more abundant in the proximal compared to the distal segment of the renal artery. In addition, about 50% of the nerve fibres around the main

vessel were located within 2.5 mm from the intima [29, 30]. However, fibres in the distal segments were found closer to the intima compared to those in the proximal segments, with 79% of fibres that are distal to the bifurcation occurring within 2 mm from the lumen (Figure 1C) [30]. These findings were of particular importance as they had led to exploration of new procedural methods in order to maximise the clinical outcome [31-33].

The role of renal sympathetic nerves in hypertension

It has been well established from previous experimental models, that both renal efferent sympathetic and afferent nerves contribute to the pathogenesis of human essential hypertension [8-10]. Efferent sympathetic nerves exert their effect by increasing renal tubular sodium and water reabsorption, activation of the renin-angiotensin system, and inducing renal vasoconstriction leading to a reduction in glomerular filtration rate and renal blood flow [8]. Augmented renal efferent sympathetic nerve activity in human essential hypertension has been demonstrated by higher level of renal norepinephrine (NE) spillover (a marker for renal efferent sympathetic nerve activity) in essential hypertension patients compared to healthy normotensive subjects [13]. Afferent sensory nerves on the other hand activate the central sympathetic system by transmitting signals from mechanoreceptors and chemoreceptors in the kidney to BP regulatory centres in the hypothalamus, which subsequently stimulates the sympathetic outflow to various organs including the heart, the skeletal muscles, the vasculature and the kidneys [9]. The contribution of afferent renal nerves to hypertension pathogenesis was well evident in animal studies. Bilateral dorsal rhizotomy (T10-L2) in the 5/6 nephrectomised rats diminished BP elevation [16, 17]. This was associated with a reduction in NE turnover rate in areas responsible for sympathetic BP control [16].

Furthermore, in the same model, intrarenal infusion of 10% phenol resulted in BP elevation and increase in NE secretion from the posterior hypothalamus. Dorsal rhizotomy (T12-L2) prevented this response supporting the connection between the afferent renal nerves and the brain and the role of afferent nerves in BP regulation in this model [18]. Moreover, in one-kidney one-clip hypertensive rats, Katholi demonstrated a reduction in peripheral sympathetic nerve activity after renal denervation, which wasn't associated with alteration in renin activity suggesting that afferent renal nerves are responsible for the development of hypertension in this model [19].

Renal artery denervation procedure

The procedure was initially indicated for patients with office SBP of ≥ 160 mm Hg and who are on \geq three antihypertensive medications including a diuretic. Main inclusion and exclusion criteria from major clinical trials are summarised in Table 1 [7, 34, 35]. In general, prior to referral for RAD, patients with resistant hypertension should undergo careful evaluation. True resistance must be confirmed by assessment of office and home BP as well as 24-hr ambulatory BP and monitoring of medication adherence. A secondary cause of hypertension must also be excluded. After lifestyle modification, medication escalation is usually practiced. In particular, the addition of a thiazide diuretics and mineralocorticoid receptor antagonists should be considered [36].

Table 1. Summary of inclusion and exclusion criteria from major clinical trials

Inclusion Criteria
<ul style="list-style-type: none"> • Office SBP of ≥ 160 mmHg, and on ≥ 3 antihypertensive medications including a diuretic (≥ 150 mmHg in patients with type 2 diabetes) • 24- hour ambulatory SBP of ≥ 135 mmHg * • Age between 18 and 85 years
Exclusion Criteria
<ul style="list-style-type: none"> • Known secondary cause for hypertension • Significant renal failure (eGFR < 45 ml/min/7.3 m²) • Hemodynamically significant valvular disease, MI or CVA in the previous six months • Implanted PPM or ICD • Type 1 diabetes • Pregnant • Renal artery stenosis of $> 50\%$, renal artery aneurysm or previous renal artery intervention • Multiple or small renal arteries (diameter < 4 mm and length < 20 mm) • On clonidine, moxonidine, rilmenidine or warfarin • More than one hospitalisation for hypertensive emergency in the previous year
<p>Abbreviations: SBP; systolic blood pressure, eGFR; estimated glomerular filtration rate, MI; myocardial infarction, CVA; cerebrovascular accident, PPM; permanent pacemaker, ICD; implantable cardioverter- defibrillator. * Symplivity HTN 3</p>

The procedure is often performed under conscious intravenous (IV) sedation. Two-dimensional fluoroscopic x-ray imaging is utilized to guide the ablation catheter into the renal artery via femoral arterial access. Each renal artery is selectively engaged using a guiding catheter and arteriography is subsequently performed to assess anatomical suitability. If suitable, the catheter is advanced into the artery and positioned distally to deliver the ablation. Prior to energy delivery, a prophylactic dose of IV glyceryl trinitrate is often administered to prevent arterial spasm. A final arteriogram is performed after ablation to confirm vessel wall integrity and to exclude severe vasospasm. Patients are usually discharged home the following day on their usual antihypertensive treatment [7].

Assessment of response to renal artery denervation

Clinical response to RAD is measured by a reduction in either office or 24-hr ambulatory BP (≥ 10 mmHg and ≥ 5 mmHg, respectively). Early RAD trials used office BP as an efficacy endpoint and showed a significant reduction up to three years [37, 38]. Nonetheless, using office BP as a primary endpoint can lead to inclusion of patients with pseudoresistance. Therefore, the use of 24-hr ambulatory BP at baseline and follow up became mandatory in later trials, as it offers more accurate assessments of BP and enables the exclusion of those with pseudoresistance. Whilst BP reduction as a surrogate endpoint has been shown to correlate with risk of death and cardiovascular mortality in antihypertensive medications trials, BP response to RAD is not immediate and can take up to 3 to 6 months [7, 34, 39-43]. Therefore, biomarkers that are specific for renal nerve activity have been used to measure RAD success. Measurement of Renal NE spillover rate, a marker for renal efferent sympathetic nerve activity pre and post RAD was used in a proportion of patients in Symplicity HTN1[7]. However, radiotracer

technique of measuring NE spillover rate is meticulous and is not widely available in clinical practice. Thus, intraprocedural veno-arterial NE gradient has been performed as an alternative [44]. Moreover, renin activity has also been used as marker for efferent renal sympathetic nerve activity [45]. Other biomarkers that have been used and are associated with afferent renal nerve activity include muscle sympathetic nerve activity, baroreflex sensitivity, and heart rate variability [46]. More recently, the use of electrical renal nerve stimulation (RNS) to guide RAD has been reported. A clinical study by Gal et al. demonstrated a significant increase in SBP after RNS, a response that was blunted after RAD [47]. This blunting of BP response to RNS was found to correlate with BP reduction at three to six months in these patients in a subsequent study [48]. More clinical studies are currently underway to evaluate RNS as a method to guide RAD (SMART study NCT03288142, and CONFIDENT study NCT02777216).

Evolution of renal artery denervation technology

The first system used in RAD was the Symplicity Flex (Medtronic, Minneapolis, MN, USA) radiofrequency (RF) system [7]. This system used low power output (8 W) to deliver RF ablation into the intraluminal surface of the renal artery via a single electrode catheter. Four to six RF ablations of 120 secs were delivered in a spiral pattern into each renal artery [7]. The ability to achieve circumferential ablation using this system was challenging and required operator experience. Therefore, new devices that used multi-electrode catheter design became readily available. The EnligHTN system (St. Jude Medical, now Abbott, Chicago, IL, USA) was one of the earliest multi-electrode RF system used in RAD [49]. The design required less catheter manipulation to achieve circumferential ablation and offered better vessel wall contact compared to Symplicity Flex. It used four electrodes mounted on an expandable basket and separated both

longitudinally and rotationally to deliver four 90sec ablations sequentially, resulting in an overall shorter procedure. The first-generation EnligHTN was later replaced by a new generation EnligHTN system that further reduced procedural duration by simultaneously delivering RF ablation via all four electrodes for a shorter duration (60 sec) [50]. Moreover, the maximum electrode-tip temperature was also reduced to 70 °C (from 75 °C) in order to minimise intimal damage, as microthrombus formation and intimal disruption has been reported previously with the first-generation device [51]. Concurrently, Symplicity Flex was replaced with a new generation multi-electrode (x4) Symplicity Spyral [52]. Each RF ablation using the Spyral system delivers a maximum power of 6.5 W for a duration of 60 secs. In addition, systems that used alternative energy modalities were also developed including ultrasound (US) and chemical denervation. Both of which enabled deeper ablation while sparing the endothelium [53, 54]. Ease of use, less operator dependency and shorter procedure duration were objectives for the newer generation devices [55]. A list of devices that were tested or used in RAD and their technical specifications are summarised in Table 2.

Tables 2. Summary of technologies that have been tested and utilised for renal artery denervation

Technology	System/ Catheter	Design	Evidence available
RF	Symplicity Flex	Single electrode, unipolar, 6fr	Symplicity HTN-1, 2, 3, DENERHTN [7, 35, 56, 57]
	EnligHTN	Multielectrode, basket, unipolar, 8fr	EnligHTN I, II [49, 50]
	Symplicity Spyral	Multielectrode, over wire, unipolar, 6fr	Spyral feasibility study, Spyral HTN-Off MED/On MED [52, 58, 59]
	Iberis	Single electrode, radial or ulnar approach, unipolar, 4fr	Case reports only [60]
	One-Shot	Balloon based, Irrigated, over the wire, unipolar, 6fr	In-man, RAPID [61]
	Vessix V2	Balloon based, over the wire Bipolar, 8fr	In-man, REDUCE-HTN [62]
	Paradise	Active cooling balloon, 6fr	Porcine model studies In-man, REDUCE, RADIANCE HTN SOLO [53, 63, 64]

US	Surround Sound System	Non-invasive	Feasibility study in canine, In-man 'WAVE I-IV'[65-67]
Chemical	Vincristine, Modified angioplasty catheter	Angioplasty balloon catheter Over the wire, 8fr	Swine model study, In-man single case report [68, 69]
	Alcohol, Peregrine system	Three-needle catheter, 7fr	Proof of concept in swine, Randomised comparison with RF in swine, First-in-man feasibility study [54, 70, 71]
Microwave	In-house build catheter	Irrigated catheter, 8.5fr	A proof of concept study in sheep [72]

Energy modalities used in renal artery denervation

Radiofrequency ablation

Radiofrequency ablation was the first and most commonly used energy source for RAD. The use of RF has been well established and extensively studied in ablation of

cardiac arrhythmia. In RF ablation, irreversible tissue damage occurs through thermal injury when tissue is heated up to 50°C [73]. In addition to Symplicity and the EnligHTN systems other RF systems that were used in RAD include the bipolar Vessix V2 system (Boston Scientific, Marlborough, MA, USA), Iberis (Terumo, Tokyo, Japan) and OneShot system (Covidien, Dublin, Ireland) [60-62, 74] (Table 2).

Differences in lesion size between various RF systems was demonstrated using a phantom model of the renal artery [75, 76]. Therefore, evaluation of individual systems is important in order to guide and inform clinicians regarding those devices.

Ultrasound

Both intraluminal and extracorporeal high intensity focused US (HIFU) have been studied and applied in RAD [53, 63-66]. The intravascular Paradise system (ReCor Medical Inc., Palo Alto, CA, USA) delivers high frequency acoustic energy from an US transducer centred in the artery using an expandable cooling balloon [53]. *In vivo* studies demonstrated endothelial surface sparing and a circumferential heating pattern with injury depth reaching 7 mm [53, 64]. Significant nerve injury and reduction in kidney NE level was achieved with at least two energy applications per artery [64]. However, cases of collateral injury including focal psoas muscle injury, colonic necrosis, and ureteric injury were also observed [53, 64]. Preliminary first-in-man REDUCE study demonstrated significant office and home BP reduction at three months. Minimal complications were reported including common occurrence of lower abdominal and back pain, as well as a single case of guide related renal artery dissection requiring stenting [63].

Non-invasive extracorporeal HIFU also has the advantage of reaching deeper targets whilst preserving the vascular endothelium. Moreover, it achieves this independent of

vessel dimension or anatomy. However, HIFU requires good quality images to visualise the target, which may be difficult in overweight patients. Although initial clinical evaluation using HIFU reported effectiveness in office BP reduction, the recently published randomised sham-controlled WAVE IV study showed no difference in office or 24-hr ambulatory BP reduction between the RAD arm and the sham control arm at 24 weeks [66, 67].

Chemical denervation

Chemical denervation uses neurotoxins like vincristine and alcohol, infused into the renal perivascular tissue resulting in neurolysis [68, 70]. Vincristine is an anti-neoplastic agent that produces giant axonal swelling and ultimately leads to peripheral nerve demyelination. In a swine model, RAD using vincristine delivered through a modified angioplasty catheter significantly decreased the number of renal nerves [68]. In-man experience is limited to a single case report in which the procedure resulted in significant office and 24-hr ambulatory BP reduction at four weeks without major adverse events [69].

In alcohol renal denervation, a dedicated 3-needles Peregrine catheter (Peregrine System, Ablative Solutions, Inc., Kalamazoo, MI, USA) was used to deliver alcohol into the perivascular space [70]. Studies in a swine model demonstrated significant reduction in renal NE content (up to 88% using 0.6 ml dose) at three months compared to saline control, without associated intimal and vascular wall injury on histology and angiography. Furthermore, no nephrotoxic effect was observed after direct injection of alcohol (0.6ml) into the artery [70, 77]. When compared to RF ablation in a randomised porcine study, alcohol denervation resulted in significantly deeper lesions (6.6 mm for 0.3 ml, 8.2 mm for 0.6 ml of alcohol versus 3.9 mm for RF) at 90 days [54]. A first-in-

man study (n=18) assessed the feasibility and safety of alcohol denervation at a dose of 0.3 ml. A significant change in office BP from baseline (-24/-12 mm Hg) was observed at six months with no procedural related adverse events [71].

Additional technologies that were tested for application in RAD include cryoablation with cryocatheter Freezor Xtra (Cryocath: Medtronic Inc., Minneapolis, MN, USA), and microwave energy using an in-house built irrigated microwave catheter [72, 78]. Although alternative energy modalities may have several benefits over RF including the capability of reaching deeper targets, sparing of the vascular endothelium, and the ability to negotiate challenging anatomy; comprehensive evaluation of their safety and efficacy is warranted prior to wide scale clinical utility.

The evidence: Before Symplicity HTN-3

Symplicity HTN-1 was the first non-randomised multi-centre proof of concept trial that included 50 patients of whom 45 underwent RAD [7]. Primary endpoints included safety and efficacy in lowering office BP. Mean baseline office BP was 177/101 mm Hg. The study demonstrated significant change in office BP from baseline and up to 12 months (-27/-17 mm Hg). Reports from a larger series of patients showed a similar and persistent office BP reduction at 24 and 36 months, with clinical response (reduction in SBP of ≥ 10 mm Hg) occurring in 85% at 12 months, 83% at 24 months, and 93% of patients at 36 months [7, 37, 79]. Moreover, in a subset of patients (n=10) from Symplicity HTN-1, RAD resulted in 47% reduction in NE spillover at six months, with corresponding average office BP reduction of 22/12 mm Hg; therefore, suggesting interruption of efferent sympathetic nerves [7].

Symplicity HTN-2 was a prospective multi-centre unblinded study that randomised 106 patients to either RAD (n=52) or control arm [34]. Similarly, there was a significant reduction in office BP in the RAD arm at six months (-32/-12 mm Hg) with 84% responders. In follow-up studies, significant office BP reduction was persistent at one (-28/-9.7 mm Hg, n = 49) and three years (-33/-14 mm Hg, n = 40) [38, 56].

Both Symplicity HTN-1 & 2 used the Symplicity Flex System. Notably, assessment of 24-hr ambulatory BP was not mandatory in both studies. However, subgroups of patients in each study underwent assessment of 24-hr ambulatory BP measurements at baseline and at 30 days or six months post denervation in Symplicity HTN-1 and 2, respectively. Reduction in 24-hr ambulatory BP was significant but less pronounced compared to office BP (-11 mm Hg, n = 9 for 24-hr ambulatory SBP and -11/-7 mmHg, n = 20 for 24-hr ambulatory BP in Symplicity HTN-1 and 2, respectively) [7, 34].

The small number of patients in both studies, and the lack of mandatory assessment of 24-hr ambulatory BP and sham control were drawbacks from the studies. Therefore, the Symplicity HTN-3 was designed to confirm the safety and efficacy results of RAD in resistant hypertension treatment.

Symplicity HTN-3

The Symplicity HTN-3 was a multi-centre single blinded trial that randomised 535 patients to either a bilateral RAD using Symplicity Flex or sham control arm (2:1 randomisation) [35]. The primary efficacy endpoint and secondary efficacy endpoint were the difference in office and 24-hr ambulatory BP reduction between the two groups at six months, respectively. Primary safety endpoint included major adverse events or renal artery stenosis >70% at six months identified by angiography. The study

showed no difference in office or 24-hr ambulatory BP reduction between the two arms (between-group difference in office SBP reduction of 2.39 mm Hg, $p= 0.26$ and in 24-hr ambulatory BP reduction of 1.96 mm Hg, $p= 0.98$) [35]. Despite a well-designed trial, it was criticised for its technical execution. Further analysis of the trial demonstrated a high failure rate of complete bilateral circumferential ablation (~75%), inexperienced operators in RAD, medications variability, and inclusion of patients with isolated systolic hypertension (ISH) that were later found to be poor responders [80, 81]. Therefore, it remains uncertain whether successful denervation was achieved in these patients.

The evidence: After Symplicity HTN-3

EnligHTN I was the first-in-man single arm, non-randomised multi-centre study utilising the multi-electrode EnligHTN system [49]. Mean office BP at baseline was 176/96 mm Hg ($n = 46$). The study demonstrated significant reduction in office and 24-hr ambulatory BP at six months (-26/-10 mm Hg and -10/-6 mm Hg, respectively), which was persistent in the 12 months follow-up study [49, 82]. Analysis of baseline 24-hr ambulatory BP identified patients with pseudoresistance ($n=5$) who had a more pronounced reduction in their office BP compared to true resistant patients (-36/-13 mm Hg versus -25/-10 mm Hg for pseudoresistant and true resistant patients, respectively at 12 months). However, they had minimal change to their 24-hr ambulatory BP (-2/-1 mm Hg versus -7/-5 mm Hg, respectively) [82]. This study highlighted the importance of 24-hr ambulatory BP assessment in hypertension studies as the apparent reduction in office BP could be attributed to pseudoresistant cases.

The DENERHTN study randomised 106 patients with true resistant hypertension (office BP $\geq 140/90$ mm Hg despite maximum tolerated doses of three antihypertensive medications and mean daytime ambulatory BP $\geq 135/85$ mm Hg) to RAD using Symplicity Flex, in addition to standardised stepped-care antihypertensive treatment (SSAHT) or SSAHT alone [83]. To reduce bias caused by medication variability, once initially stabilised on three antihypertensive medications, additional standardised medical therapy was added if home BP was $> 135/85$ mm Hg during monthly follow-ups. Between-group difference in daytime ambulatory SBP reduction (primary endpoint) was significant in favour of RAD with SSAHT arm (difference of 5.9 mm Hg) at six months. However, there were no significant differences in home or office SBP reduction between the two groups (difference of 3.6 mm Hg, $p=0.30$ and 5.6 mm Hg, $p=0.15$ for home and office SBP, respectively). Notably, drug testing at six months detected high rate of non-adherence to medications ($\sim 50\%$) in both groups. In the subgroup of patients who were completely nonadherent, between-group difference in daytime ambulatory SBP reduction was not significant. However, the number of patients in this subgroup was small for comparison [57].

Safety evidence

Though the clinical efficacy of RAD has been debatable, all studies to date demonstrated low complications and adverse events rate. Periprocedural complications were primarily related to vascular access injury occurring at a rate of 1-2 %, which included femoral haematomas and pseudoaneurysms [7, 34, 35, 37, 38, 49]. Additionally, renal artery dissection caused by the guiding catheter occurred in a few cases ($<1\%$) [7, 34]. Thus far, no significant renal artery stenosis occurred in any of the major trials that included assessment of renal vessels by invasive angiography,

magnetic resonance angiography or renal duplex sonography. However, isolated cases of significant *de novo* renal artery stenosis post RAD have been reported [84, 85]. Furthermore, no significant impact on renal function was observed [35, 37, 38].

Renal artery denervation: Post Symplicity HTN-3 era

The field of RAD after Symplicity HTN-3 has witnessed an improvement in knowledge concerning factors that implicate denervation efficacy. Histologically, Sakakura et al. (2014) have mapped out the distribution of renal nerves along the renal artery, and their findings highlighted the importance of energy application in the distal vessel segment [30]. As a result, combined branch and main vessel ablation was evaluated as a new technique for RAD. This approach resulted in a greater reduction in kidney NE content, and increased axonal injury compared to main vessel ablation alone using the Symplicity Spyral in a swine model [31]. In addition, a clinical study demonstrated improved BP reduction at three months using the combined method compared to main vessel ablation only [33].

Furthermore, it has been shown that a larger number of ablations correlated with better BP reduction [86]. Moreover, patients with ISH were less responsive to RAD compared to those with combined systolic and diastolic hypertension, which is likely related to an increased arterial stiffness in ISH patients [80, 87, 88]. Therefore, recently designed studies involved larger number of ablations, and excluded patients with ISH [58, 59].

New evidence for renal artery denervation

SPYRAL HTN-OFF MED and ON MED studies

In light of the shortcomings of previous RAD trials and concerns regarding its efficacy, two randomised, single blinded sham-controlled trials, SPYRAL HTN-OFF MED and

SPYRAL HTN-ON MED, were carefully designed as new proof of concept studies [58, 59]. Both trials assessed BP response to RAD in patients with mild to moderate combined (systolic and diastolic) hypertension (SBP between 150-180 mm Hg, 24-hr ambulatory SBP between 140-170 mm Hg and DBP \geq 90 mm Hg). To overcome medication variability and patients compliance bias, those enrolled in the SPYRAL HTN-OFF MED were either medication naïve or had their antihypertensives withheld for the trial period. Whilst the SPYRAL HTN-ON MED assessed patients who were on one to three antihypertensive medications. Drug testing was performed in both studies to confirm either the absence of or adherence to medications.

The initial three month analysis of the SPYRAL HTN-OFF MED demonstrated a significant reduction in both office and 24-hr ambulatory BP from baseline in the treatment arm (-10/-5.3 mm Hg and -5.5/-4.8 mm Hg, respectively) with significant between-group differences in favour of RAD (difference of 7.7/4.9 mm Hg, and 5.0/4.4 mm Hg, respectively) [58]. Significant BP reduction in the RAD arm was also reported in the recently published SPYRAL HTN-ON MED study at six months (-9.4/-5.2 mm Hg and -9.0/-6.0 mm Hg for office and 24-hr ambulatory BP, respectively) [59]. Similar to previous reports, the study confirmed high medication non-adherence rate amongst patients in hypertension trial (~50%), which could affect the assessment of BP reducing effect of RAD. However, there was no difference in medication adherence between the two groups [59].

Compared to previous RAD trials, the magnitude of BP reduction in the SPYRAL HTN trials was smaller [7, 34]. It has been suggested that this could be due to a lesser degree of sympathetic activity in those with mild to moderate resistant hypertension compared to severe resistant hypertension. Of note, rigorous procedural technique was adopted in this study, including more extensive ablations using the contemporary method of

combined main vessel and branch ablation. The larger number of ablations was not associated with an increased rate of major complications or significant adverse events in the short-term [58, 59].

RADIANCE-HTN SOLO

Another recently published multi-centre, single-blinded, randomised sham-controlled trial assessing endovascular US for RAD using the Paradise system is the RADIANCE-HTN SOLO trial [89]. The study randomised 146 patients with mild to moderate combined hypertension (daytime ambulatory BP of $\geq 135/85$ mm Hg and $< 170/105$ mm Hg), who were off their antihypertensive medications for four weeks prior to enrolment to RAD versus sham control arm. The primary endpoint was daytime ambulatory SBP reduction at two months in the intention-to-treat population. In the RAD arm, at least two US treatments (7 secs each) were delivered in the main renal artery, bilaterally. At two months, the intention-to-treat analysis demonstrated a significant BP reduction from baseline in the RAD arm (-8.5 mmHg) and significant between-group difference in daytime ambulatory SBP in favour of RAD (6.3 mmHg). No major complications were reported. However, > 50% of patients in the RAD arm were commenced on antihypertensive medication after two months due to uncontrolled hypertension, and of those who completed six months follow-up (n = 94), a single patient in the RAD arm underwent renal artery stenting due to progression of pre-existing renal artery stenosis [89].

The magnitude of change in 24-hr ambulatory BP in the RADIANCE HTN SOLO was similar to that reported in the SPYRAL HTN studies [58, 59]. It may be possible that the effect of RAD in these patients is delayed. Furthermore, functional nerve

regeneration may also occur; therefore, longer follow up of patients is necessary in order to confirm sustained reduction in BP.

Conclusions

The available evidence to date suggests that RAD could be effective in carefully selected patients with hypertension. Clinically, careful patient assessment is necessary in order to exclude secondary causes of hypertension, insure compliance to medication, and recognise those who are less likely to respond, including ISH and older patients with increased arterial stiffness. With regards to the procedural technique, the delivery of a large number of ablations including distal to the bifurcation may be necessary when using the currently available RF system. In contrast, ablation proximal to the bifurcation alone may be effective in US renal denervation. Nonetheless, regardless of the ablation method and modality, RAD has been shown to be safe with a low complication rate. Finally, trials designed should include a sham-control arm, in addition to an assessment of ambulatory BP, and monitoring of medication adherence as these help in the accurate assessment of BP reduction, thereby delineating confounding factors that can affect our understanding of RAD efficacy, which has been shown in the most recent trials.

References

1. Kearney PM, Whelton M, Reynolds K, Muntner P, Whelton PK, He J. Global burden of hypertension: analysis of worldwide data. *Lancet* 2005;365:217-23.
2. Benjamin EJ, Blaha MJ, Chiuve SE, Cushman M, Das SR, Deo R, et al. Heart Disease and Stroke Statistics-2017 Update: A Report From the American Heart Association. *Circulation* 2017;135:e146-e603.
3. Lewington S, Clarke R, Qizilbash N, Peto R, Collins R. Age-specific relevance of usual blood pressure to vascular mortality: a meta-analysis of individual data for one million adults in 61 prospective studies. *Lancet* 2002;360:1903-13.
4. Pezzini A, Grassi M, Lodigiani C, Patella R, Gandolfo C, Zini A, et al. Predictors of long-term recurrent vascular events after ischemic stroke at young age: the Italian Project on Stroke in Young Adults. *Circulation* 2014;129:1668-76.
5. Roger VL, Go AS, Lloyd-Jones DM, Benjamin EJ, Berry JD, Borden WB, et al. Heart disease and stroke statistics--2012 update: a report from the American Heart Association. *Circulation* 2012;125:e2-e220.
6. Calhoun DA, Jones D, Textor S, Goff DC, Murphy TP, Toto RD, et al. Resistant hypertension: diagnosis, evaluation, and treatment: a scientific statement from the American Heart Association Professional Education Committee of the Council for High Blood Pressure Research. *Circulation* 2008;117:e510-26.
7. Krum H, Schlaich M, Whitbourn R, Sobotka PA, Sadowski J, Bartus K, et al. Catheter-based renal sympathetic denervation for resistant hypertension: a multicentre safety and proof-of-principle cohort study. *Lancet* 2009;373:1275-81.
8. DiBona GF. Physiology in perspective: The Wisdom of the Body. Neural control of the kidney. *Am J Regul, Integr Comp Physiol* 2005;289:R633-41.
9. DiBona GF. Sympathetic nervous system and the kidney in hypertension. *Curr Opin Nephrol Hypertens* 2002;11:197-200.
10. DiBona GF, Kopp UC. Neural control of renal function. *Physiol Rev* 1997;77:75-197.

11. Esler M, Willett I, Leonard P, Hasking G, Johns J, Little P, et al. Plasma noradrenaline kinetics in humans. *Journal of the Autonomic Nervous System*. 1984;11:125-44.
12. Esler M, Jennings G, Korner P, Willett I, Dudley F, Hasking G, et al. Assessment of human sympathetic nervous system activity from measurements of norepinephrine turnover. *Hypertension*. 1988;11:3-20.
13. Esler M, Jennings G, Lambert G. Noradrenaline release and the pathophysiology of primary human hypertension. *Am J Hypertens*. 1989;2:140S-6S.
14. Esler M, Jennings G, Korner P, Blombery P, Sacharias N, Leonard P. Measurement of total and organ-specific norepinephrine kinetics in humans. *Am J Physiol*. 1984;247:E21-8.
15. DiBona GF. Functionally specific renal sympathetic nerve fibers: role in cardiovascular regulation. *Am J Hypertens*. 2001;14:163s-70s.
16. Campese VM, Kogosov E. Renal afferent denervation prevents hypertension in rats with chronic renal failure. *Hypertension*. 1995;25:878-82.
17. Campese VM, Kogosov E, Koss M. Renal afferent denervation prevents the progression of renal disease in the renal ablation model of chronic renal failure in the rat. *Am J kidney Dis* 1995;26:861-5.
18. Ye S, Ozgur B, Campese VM. Renal afferent impulses, the posterior hypothalamus, and hypertension in rats with chronic renal failure. *Kidney Int*. 1997;51:722-7.
19. Katholi RE, Winternitz SR, Oparil S. Decrease in peripheral sympathetic nervous system activity following renal denervation or unclipping in the one-kidney one-clip Goldblatt hypertensive rat. *J clin invest*. 1982;69:55-62.

20. Whitelaw GP, Kinsey D, Smithwick RH. Factors influencing the choice of treatment in essential hypertension: Surgical, medical or a combination of both. *Am J Surg*. 1964;107:220-31.
21. Palmer RS, Loofbourow D, Doering CR. Prognosis in essential hypertension; 8-year follow-up study of 430 patients on conventional medical treatment. *N Engl J Med*. 1948;239:990-4.
22. Peet MM. Hypertension and its surgical treatment by bilateral supradiaphragmatic splanchnicectomy. *Am J Surg*. 1948;75:48-68.
23. Whitelaw GP, Smithwick RH. Effect of extensive sympathectomy upon blood pressure responses and levels. *Angiology*. 1951;2:157-72.
24. Smithwick RH, Thompson JE. Splanchnicectomy for essential hypertension; results in 1,266 cases. *J Am Med Assoc*. 1953;152:1501-4.
25. Grimson KS, Orgain ES, Anderson B, D'Angelo GJ. Total thoracic and partial to total lumbar sympathectomy, splanchnicectomy and celiac ganglionectomy for hypertension. *Ann Surg*. 1953;138:532-47.
26. Thorpe JJ, Welch WJ, Poindexter CA. Bilateral thoracolumbar sympathectomy for hypertension; a study of 500 cases. *Am J Med*. 1950;9:500-15.
27. Morrissey DM, Brookes VS, Cooke WT. Sympathectomy in the treatment of hypertension; review of 122 cases. *Lancet*. 1953;1:403-8.
28. Smithwick RH. Surgical treatment of hypertension. *Am J Med*. 1948;4:744-59.
29. Tellez A, Rousselle S, Palmieri T, Rate Wr, Wicks J, Degrange A, et al. Renal artery nerve distribution and density in the porcine model: biologic implications for the development of radiofrequency ablation therapies. *Transl Res* 2013;162:381-9.

30. Sakakura K, Ladich E, Cheng Q, Otsuka F, Yahagi K, Fowler DR, et al. Anatomic assessment of sympathetic peri-arterial renal nerves in man. *J Am Coll Cardiol*. 2014;64:635-43.
31. Mahfoud F, Tunev S, Ewen S, Cremers B, Ruwart J, Schulz-Jander D, et al. Impact of Lesion Placement on Efficacy and Safety of Catheter-Based Radiofrequency Renal Denervation. *J Am Coll Cardiol*. 2015;66:1766-75.
32. Mahfoud F, Pipenhagen CA, Boyce Moon L, Ewen S, Kulenthiran S, Fish JM, et al. Comparison of branch and distally focused main renal artery denervation using two different radio-frequency systems in a porcine model. *Int J Cardiol*. 2017;241:373-8.
33. Fengler K, Ewen S, Hollriegel R, Rommel KP, Kulenthiran S, Lauder L, et al. Blood Pressure Response to Main Renal Artery and Combined Main Renal Artery Plus Branch Renal Denervation in Patients With Resistant Hypertension. *J Am Heart Assoc*. 2017;6(8).
34. Esler MD, Krum H, Sobotka PA, Schlaich MP, Schmieder RE, Bohm M. Renal sympathetic denervation in patients with treatment-resistant hypertension (The Symplicity HTN-2 Trial): a randomised controlled trial. *Lancet*. 2010;376:1903-9.
35. Bhatt DL, Kandzari DE, O'Neill WW, D'Agostino R, Flack JM, Katzen BT, et al. A controlled trial of renal denervation for resistant hypertension. *N Engl J Med*. 2014;370:1393-401.
36. Grassi G, Calhoun DA, Mancia G, Carey RM. Resistant Hypertension Management: Comparison of the 2017 American and 2018 European High Blood Pressure Guidelines. *Curr hypertens rep*. 2019;21:67.

37. Krum H, Schlaich MP, Sobotka PA, Bohm M, Mahfoud F, Rocha-Singh K, et al. Percutaneous renal denervation in patients with treatment-resistant hypertension: final 3-year report of the Symplicity HTN-1 study. *Lancet*. 2014;383:622-9.
38. Esler MD, Bohm M, Sievert H, Rump CL, Schmieder RE, Krum H, et al. Catheter-based renal denervation for treatment of patients with treatment-resistant hypertension: 36 month results from the SYMPPLICITY HTN-2 randomized clinical trial. *Eur heart j*. 2014;35:1752-9.
39. Muntner P, Davis BR, Cushman WC, Bangalore S, Calhoun DA, Pressel SL, et al. Treatment-resistant hypertension and the incidence of cardiovascular disease and end-stage renal disease: results from the Antihypertensive and Lipid-Lowering Treatment to Prevent Heart Attack Trial (ALLHAT). *Hypertension*. 2014;64:1012-21.
40. Kostis JB, Davis BR, Cutler J, Grimm RH, Jr., Berge KG, Cohen JD, et al. Prevention of heart failure by antihypertensive drug treatment in older persons with isolated systolic hypertension. SHEP Cooperative Research Group. *Jama*. 1997;278:212-6.
41. Einhorn PT, Davis BR, Wright JT, Jr., Rahman M, Whelton PK, Pressel SL. ALLHAT: still providing correct answers after 7 years. *Curr Opin Cardiol*. 2010;25:355-65.
42. Beckett NS, Peters R, Fletcher AE, Staessen JA, Liu L, Dumitrascu D, et al. Treatment of hypertension in patients 80 years of age or older. *N Eng J med*. 2008;358:1887-98.
43. Wright JT, Jr., Williamson JD, Whelton PK, Snyder JK, Sink KM, Rocco MV, et al. A Randomized Trial of Intensive versus Standard Blood-Pressure Control. *N. Eng J med*. 2015;373:2103-16.

44. Tiroch K, Sause A, Szymanski J, Nover I, Leischik R, Mann JF, et al. Intraprocedural reduction of the veno-arterial norepinephrine gradient correlates with blood pressure response after renal denervation. *EuroIntervention*. 2015;11:824-34.
45. Schlaich MP, Sobotka PA, Krum H, Lambert E, Esler MD. Renal sympathetic-nerve ablation for uncontrolled hypertension. *N Eng J Med*. 2009;361:932-4.
46. Sobotka PA, Harrison DG, Fudim M. The endpoint on measuring the clinical effects of renal denervation: what are the best surrogates. In: Heuser R SM, Sievert H, editor. *Renal Denervation*. London: Springer, London; 2015.
47. Gal P, de Jong MR, Smit JJ, Adiyaman A, Staessen JA, Elvan A. Blood pressure response to renal nerve stimulation in patients undergoing renal denervation: a feasibility study. *J hum hypertens*. 2015;29:292-5.
48. de Jong MR, Adiyaman A, Gal P, Smit JJ, Delnoy PP, Heeg JE, et al. Renal Nerve Stimulation-Induced Blood Pressure Changes Predict Ambulatory Blood Pressure Response After Renal Denervation. *Hypertension*. 2016;68:707-14.
49. Worthley SG, Tsioufis CP, Worthley MI, Sinhal A, Chew DP, Meredith IT, et al. Safety and efficacy of a multi-electrode renal sympathetic denervation system in resistant hypertension: the EnligHTN I trial. *Eur heart J* 2013;34:2132-40.
50. Worthley SG, Wilkins GT, Webster MW, Montarello JK, Delacroix S, Whitbourn RJ, et al. Safety and performance of the second generation EnligHTN Renal Denervation System in patients with drug-resistant, uncontrolled hypertension. *Atherosclerosis*. 2017;262:94-100.
51. Templin C, Jaguszewski M, Ghadri JR, Sudano I, Gaehwiler R, Hellermann JP, et al. Vascular lesions induced by renal nerve ablation as assessed by optical coherence tomography: pre- and post-procedural comparison with the Simplicity catheter system

and the EnligHTN multi-electrode renal denervation catheter. *Eur heart.*2013;34(28):2141-8, 8b.

52. Whitbourn R, Harding SA, Walton A. Symplicity multi-electrode radiofrequency renal denervation system feasibility study. *EuroIntervention.* 2015;11:104-9.

53. Sakakura K, Roth A, Ladich E, Shen K, Coleman L, Joner M, et al. Controlled circumferential renal sympathetic denervation with preservation of the renal arterial wall using intraluminal ultrasound: a next-generation approach for treating sympathetic overactivity. *EuroIntervention.* 2015;10:1230-8.

54. Bertog S, Fischel TA, Vega F, Ghazarossian V, Pathak A, Vaskelyte L, et al. Randomised, blinded and controlled comparative study of chemical and radiofrequency-based renal denervation in a porcine model. *EuroIntervention.* 2017;12e1898-e906.

55. Bunte MC, Infante de Oliveira E, Shishehbor MH. Endovascular treatment of resistant and uncontrolled hypertension: therapies on the horizon. *JACC Cardiovasc Interv* 2013;6:1-9.

56. Esler MD, Krum H, Schlaich M, Schmieder RE, Bohm M, Sobotka PA. Renal sympathetic denervation for treatment of drug-resistant hypertension: one-year results from the Symplicity HTN-2 randomized, controlled trial. *Circulation.* 2012;126:2976-82.

57. Azizi M, Pereira H, Hamdidouche I, Gosse P, Monge M, Bobrie G, et al. Adherence to Antihypertensive Treatment and the Blood Pressure-Lowering Effects of Renal Denervation in the Renal Denervation for Hypertension (DENERHTN) Trial. *Circulation.* 2016;134:847-57.

58. Townsend RR, Mahfoud F, Kandzari DE, Kario K, Pocock S, Weber MA, et al. Catheter-based renal denervation in patients with uncontrolled hypertension in the

absence of antihypertensive medications (SPYRAL HTN-OFF MED): a randomised, sham-controlled, proof-of-concept trial. *Lancet*. 2017;390:2160-70.

59. Kandzari DE, Bohm M, Mahfoud F, Townsend RR, Weber MA, Pocock S, et al. Effect of renal denervation on blood pressure in the presence of antihypertensive drugs: 6-month efficacy and safety results from the SPYRAL HTN-ON MED proof-of-concept randomised trial. *Lancet*. 2018;391:2346-2355.

60. Jiang XJ, Dong H, Liang T, Zou YB, Xu B, Gao RL. First-in-man report of a novel dedicated radiofrequency catheter for renal denervation via the transulnar approach. *EuroIntervention*. 2013;9:684-6.

61. Verheye S, Ormiston J, Bergmann MW, Sievert H, Schwindt A, Werner N, et al. Twelve-month results of the rapid renal sympathetic denervation for resistant hypertension using the OneShot™ ablation system (RAPID) study. *EuroIntervention*. 2015;10:1221-9.

62. Sievert H, Schofer J, Ormiston J, Hoppe UC, Meredith IT, Walters DL, et al. Renal denervation with a percutaneous bipolar radiofrequency balloon catheter in patients with resistant hypertension: 6-month results from the REDUCE-HTN clinical study. *EuroIntervention*. 2015;10:1213-20.

63. Mabin T, Sapoval M, Cabane V, Stemmett J, Iyer M. First experience with endovascular ultrasound renal denervation for the treatment of resistant hypertension. *EuroIntervention*. 2012;8:57-61.

64. Pathak A, Coleman L, Roth A, Stanley J, Bailey L, Markham P, et al. Renal sympathetic nerve denervation using intraluminal ultrasound within a cooling balloon preserves the arterial wall and reduces sympathetic nerve activity. *EuroIntervention*. 2015;11:477-84.

65. Wang Q, Guo R, Rong S, Yang G, Zhu Q, Jiang Y, et al. Noninvasive renal sympathetic denervation by extracorporeal high-intensity focused ultrasound in a pre-clinical canine model. *J Am Coll Cardiol*. 2013;61:2185-92.
66. Neuzil P, Ormiston J, Brinton TJ, Starek Z, Esler M, Dawood O, et al. Externally Delivered Focused Ultrasound for Renal Denervation. *JACC Cardiovasc Interv*. 2016;9:1292-9.
67. Schmieder RE, Ott C, Toennes SW, Bramlage P, Gertner M, Dawood O, et al. Phase II randomized sham-controlled study of renal denervation for individuals with uncontrolled hypertension - WAVE IV. *J Hypertens*. 2018;36:680-9.
68. Stefanadis C, Toutouzas K, Synetos A, Tsioufis C, Karanasos A, Agrogiannis G, et al. Chemical denervation of the renal artery by vincristine in swine. A new catheter based technique. *Int J Cardiol*. 2013;167:421-5.
69. Stefanadis C, Toutouzas K, Vlachopoulos C, Tsioufis C, Synetos A, Pietri P, et al. Chemical denervation of the renal artery with vincristine for the treatment of resistant arterial hypertension: first-in-man application. *Hellenic J Cardiol*. 2013;54:318-21.
70. Fischell TA, Vega F, Raju N, Johnson ET, Kent DJ, Ragland RR, et al. Ethanol-mediated perivascular renal sympathetic denervation: preclinical validation of safety and efficacy in a porcine model. *EuroIntervention*. 2013;9:140-7.
71. Fischell TA, Ebner A, Gallo S, Ikeno F, Minarsch L, Vega F, et al. Transcatheter Alcohol-Mediated Perivascular Renal Denervation With the Peregrine System: First-in-Human Experience. *JACC Cardiovasc Interv*. 2016;9:589-98.
72. Qian PC, Barry MA, Al-Raisi S, Kovoov P, Pouliopoulos J, Nalliah CJ, et al. Transcatheter non-contact microwave ablation may enable circumferential renal artery

denervation while sparing the vessel intima and media. *EuroIntervention*. 2017;12:e1907-e15.

73. Haines DE. The biophysics of radiofrequency catheter ablation in the heart: the importance of temperature monitoring. *Pacing Clin Electrophysiol*. 1993;16:586-91.

74. Ormiston JA, Watson T, van Pelt N, Stewart R, Haworth P, Stewart JT, et al. First-in-human use of the OneShot renal denervation system from Covidien. *EuroIntervention*. 2013;8:1090-4.

75. Al Raisi SI, Pouliopoulos J, Barry MT, Swinnen J, Thiagalingam A, Thomas SP, et al. Evaluation of lesion and thermodynamic characteristics of Symplicity and EnligHTN renal denervation systems in a phantom renal artery model. *EuroIntervention*. 2014;10:277-84.

76. Al Raisi SI, Barry MT, Qian P, Bhaskaran A, Pouliopoulos J, Kovoov P. Comparison of new-generation renal artery denervation systems: assessing lesion size and thermodynamics using a thermochromic liquid crystal phantom model. *EuroIntervention*. 2017;13:1242-7.

77. Fischell TA, Fischell DR, Ghazarossian VE, Vega F, Ebner A. Next generation renal denervation: chemical "perivascular" renal denervation with alcohol using a novel drug infusion catheter. *Cardiovasc Revasc Med*. 2015;16:221-7.

78. Prochnau D, Figulla HR, Romeike BF, Franz M, Schubert H, Bischoff S, et al. Percutaneous catheter-based cryoablation of the renal artery is effective for sympathetic denervation in a sheep model. *Int J Cardiol*. 2011;152:268-70.

79. Catheter-based renal sympathetic denervation for resistant hypertension: durability of blood pressure reduction out to 24 months. *Hypertension*. 2011;57:911-7.

80. Mahfoud F, Bakris G, Bhatt DL, Esler M, Ewen S, Fahy M, et al. Reduced blood pressure-lowering effect of catheter-based renal denervation in patients with isolated

systolic hypertension: data from SYMPLICITY HTN-3 and the Global SYMPLICITY Registry. *Eur Heart J*. 2017;38:93-100.

81. Esler M. Illusions of truths in the Symplicity HTN-3 trial: generic design strengths but neuroscience failings. *J Am Soc Hypertens*. 2014;8:593-8.

82. Papademetriou V, Tsioufis CP, Sinhal A, Chew DP, Meredith IT, Malaiapan Y, et al. Catheter-based renal denervation for resistant hypertension: 12-month results of the EnlighTn I first-in-human study using a multielectrode ablation system. *Hypertension*. 2014;64:565-72.

83. Azizi M, Sapoval M, Gosse P, Monge M, Bobrie G, Delsart P, et al. Optimum and stepped care standardised antihypertensive treatment with or without renal denervation for resistant hypertension (DENERHTN): a multicentre, open-label, randomised controlled trial. *Lancet*. 2015;385:1957-65.

84. Diego-Nieto A, Cruz-Gonzalez I, Martin-Moreiras J, Rama-Merchan JC, Rodriguez-Collado J, Sanchez-Fernandez PL. Severe Renal Artery Stenosis After Renal Sympathetic Denervation. *JACC Cardiovasc Interv*. 2015;8:e193-4.

85. Chandra AP, Marron CD, Puckridge P, Spark JI. Severe bilateral renal artery stenosis after transluminal radiofrequency ablation of renal sympathetic nerve plexus. *J Vasc Surg*. 2015;62:222-5.

86. Kandzari DE, Bhatt DL, Brar S, Devireddy CM, Esler M, Fahy M, et al. Predictors of blood pressure response in the SYMPLICITY HTN-3 trial. *Eur Heart J*. 2015;36:219-27.

87. Ewen S, Ukena C, Linz D, Kindermann I, Cremers B, Laufs U, et al. Reduced effect of percutaneous renal denervation on blood pressure in patients with isolated systolic hypertension. *Hypertension*. 2015;65:193-9.

88. Okon T, Rohnert K, Stiermaier T, Rommel KP, Muller U, Fengler K, et al. Invasive aortic pulse wave velocity as a marker for arterial stiffness predicts outcome of renal sympathetic denervation. *EuroIntervention*. 2016;12:e684-92.
89. Azizi M, Schmieder RE, Mahfoud F, Weber MA, Daemen J, Davies J, et al. Endovascular ultrasound renal denervation to treat hypertension (RADIANCE-HTN SOLO): a multicentre, international, single-blind, randomised, sham-controlled trial. *Lancet*. 2018;391:2335-2345.

2.2 Background to Chapters 3- 6

During the early phase of RAD, reports on ablation characteristics and lesion size for RAD systems were lacking. Despite this, the technology evolved rapidly with numerous devices became available within a short period of time. The single electrode Symplicity Flex was the most studied system. It was unclear if various systems exhibited a class effect. Therefore, we developed a phantom model of the renal artery to enable assessment of various devices under controlled experimental settings. In Chapter 3, 4 and 6, we utilised this model to study and compare the characteristics of old and new generation devices, and to understand the differences between main vessel and branch ablation with respect to effect on lesion characteristics and thermodynamics. Using this model, we were the first to report on lesion dimension of RF ablations using first generation Symplicity and EnligHTN systems. Later, data from animal model studies reporting on lesion depth based on tissue injury depth on histology for different systems became available [17-20]. However, our phantom model allows assessment of devices under controlled experimental settings without confounding variables, and within a short period of time. In addition, it enables temporal assessment of lesion formation and visualisation of thermal profile in real-time, which is difficult to achieve *in-vivo*.

2.3 Supplementary methods (Chapter 3-6)

Thermochromic liquid crystal phantom model (Chapter 3, 4 & 6)

A previously described myocardial RF ablation model was modified to construct the renal artery phantom model [21]. The system comprised of a transparent block of gel that contained a temperature sensitive TLC sheet (Hallcrest, LCR, Connah's Quay, United Kingdom) onto which RF ablations were performed, and a large tank where the gel was placed (Figure 2).

The tank was made of polycarbonate, which is shatter resistant. To simulate blood flow, a pump/heater (Thermomix 1441, B. Braun) was used to circulate saline solution in the tank and into the lumen of the phantom renal artery from an external bath. Flow into the phantom was controlled using a high-volume flowmeter. The fluid temperature was regulated by the heater and maintained at 37 °C. Saline temperature was also controlled and monitored during the experiments using a thermometer.

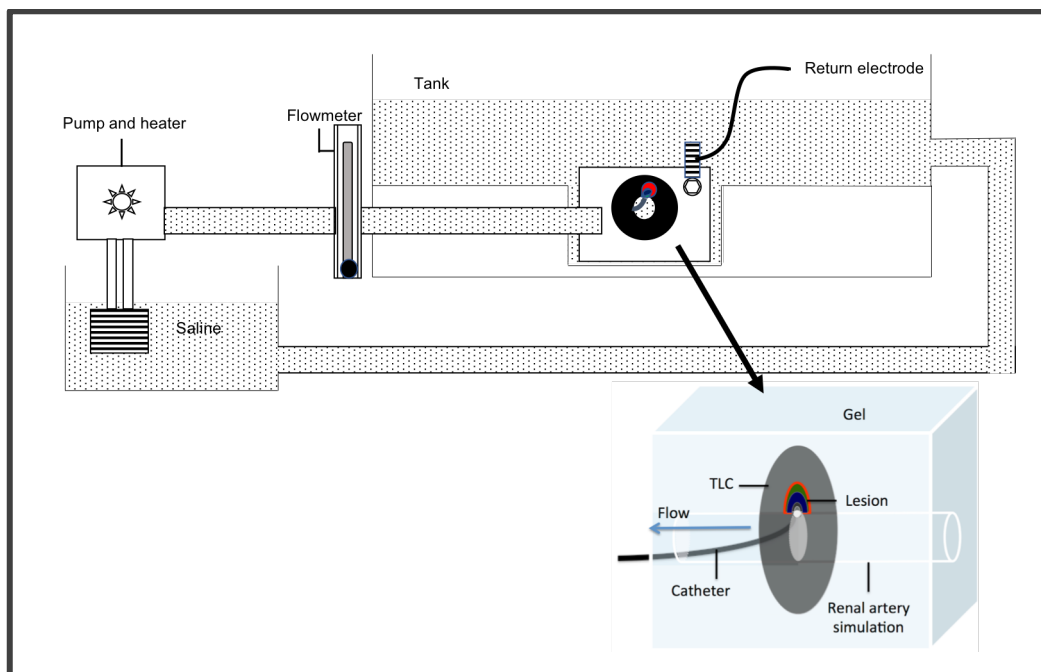


Figure 2. A schematic diagram of the renal artery phantom model setup.

The impedance and conductivity of the saline solution was titrated to that of blood at 37 °C (conductivity of 15750 us). Saline conductivity was measured using a conductivity probe (COND-BTA, Vernier Instruments) and monitored at a regular interval throughout the experiments (every 10 ablations).

The gel block was made by dissolving 1 gram of agar-based gel (Phytigel; Merck, St. Louis, MO, USA) in a mixture of normal saline and distilled water (30 ml and 70 ml, respectively). The solution was heated up to 90 °C. The temperature of the mix was monitored with a thermometer as shown in Figure 3A. The mix was allowed to cool at room temperature until it reached 70 °C. It was then poured into a pre-made well that contained a 5 mm or 3 mm cylindrical former. A TLC sheet was placed vertically in the former prior to gel pouring (Figure 3B). Once poured, the gel was left to cool down in room temperature for 30 minutes, after which it was placed in ice for 15 minutes to allow further solidification. After gel solidification, the former was removed, and the gel block was then placed in the tank where it can adequately be visualised by a camera (Canon 5DMKII, Canon Inc, Japan) positioned in front of the tank (Figure 3C).

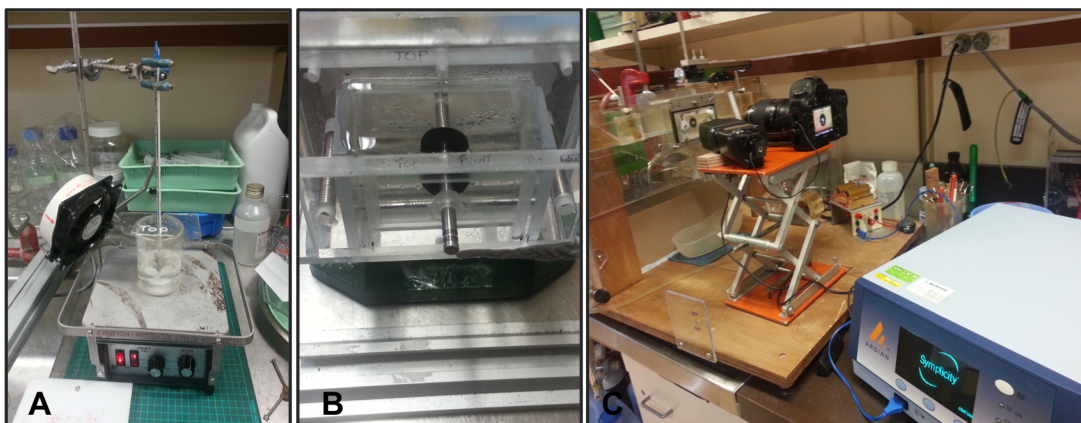


Figure 3. Preparation and set up of the phantom model. Gel heating (a), placement of TLC sheet in the well (b). Placement of the well in the tank with the TLC sheet directly facing the camera (c).

The TLC film was shaped as a disc with 5 mm or 3 mm circular hole in the centre, where ablations were delivered. It changed colour in response to temperature change with a resolution of 10-20 micron per sample unit, and a thermal accuracy within 0.5 °C (Figure 4 A). We used TLC with temperature sensitivity range between 50-78 °C (Chapter 3 & 4) or dual range TLC, with temperature sensitivity between 50-77 °C and 80-103 °C (Chapter 6). The TLC colour gradient starts with red for the lower range and ends with black (clearing) at the highest range (Figure 4C).

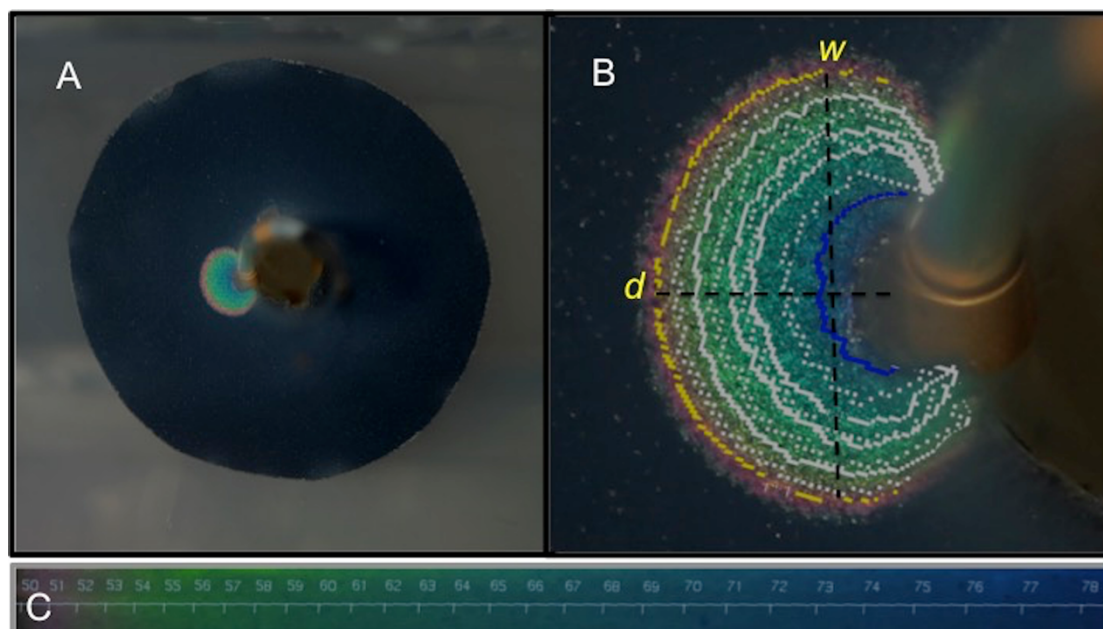


Figure 4. Images of RF colour gradient on the TLC during RF ablation. TLC colour gradient at 60sec with RF ablation using Symplicity Spyril (a). Superimposed isotherm drawn on the lesion after analysis by software (b). d; lesion depth, w; lesion width

The ablation catheter was advanced through a guiding catheter into the lumen of the phantom vessel and held in position using a positioning tool. Placement of electrode against the TLC/gel surface was confirmed by direct visualisation or by zoomed image through the camera positioned in front of the tank. At least one electrode had to have adequate contact with the

wall of the phantom vessel and placed on plane with the TLC film (Figure 4A & B). The return electrode for the circuit was located on the gel well (circuit impedance of 100 Ω).

Image acquisition and analysis (Chapter 3,4 & 6)

The camera and the macro lens (USM EF 100 mm Canon Inc, Japan) used to acquire the images provided image resolution of ~90 pixel/mm, which is higher than the resolution for the TLC grain. Images during RF ablations were taken at prespecified intervals, and at the end of each RF ablation. Images were then loaded onto an in-house built software (i-Chorme) for analysis and assignment of hue to temperature isotherms. A pre-made calibrated hue to temperature conversion chart was used in the software for lesion analysis and drawing the isotherms. The isotherm of interest is highlighted by the software (Figure 4B). Lesion depth was measured as the length of a line between the electrode/TLC interface and the isotherm of interest that is perpendicular to the electrode surface. Lesion depth was measured as the maximum length of the isotherm of interest that is perpendicular to the depth line.

Renal artery denervation procedure (Chapter 5)

Renal artery denervation procedures were performed by an interventional cardiologist and a vascular surgeon, under conscious intravenous sedation using midazolam and fentanyl. Intra-arterial Heparin was administered in all cases at a dose of 50units/kg. A 6Fr (Symplicity) or 8Fr (EnligHTN) sheaths were introduced into the right femoral artery for access. Selective right and left renal arteriograms using a 6Fr LIMA guiding catheter (Symplicity) or EnligHTN guiding catheter (EnligHTN) was done to assess vessel anatomy for denervation suitability. Prior to RF application, a 200mcg bolus of glyceryl trinitrate was administered into each renal artery to prevent arterial spasm. RF ablations in a spiral fashion were delivered into each renal

artery wall starting distally and using the clinically recommended settings for both systems. A final angiogram was performed at the end of ablation to exclude complications including severe spasms, perforation or dissection. The femoral arterial access site was closed with a ProGlide closure device if suitable. The following day, patients were reviewed for any adverse events or complications and discharged home if well. All patients were advised to continue the same antihypertensive medications, unless advised otherwise by their treating cardiologist or nephrologist.

Radiofrequency ablation using Symplicity Flex (Chapter 5)

The Symplicity Flex catheter was positioned distally in the renal artery just proximal to the bifurcation. The tip was flexed to establish contact with the vessel wall. The first ablation was then delivered for 2 minutes. After delivery of the first ablation, the catheter was pulled (0.5mm) more proximally and rotated 45 degrees to deliver the next ablation. This process was repeated along the renal artery (maintaining the rotation in single direction) until four to six successful ablations were delivered into each renal artery depending on its length.

Radiofrequency ablation using EnligHTN (Chapter 5)

The EnligHTN catheter was positioned distally in the renal artery just proximal to the bifurcation. Once in position, the basket was deployed. Impedance monitoring in the system detects appropriate vessel wall contact. Once vessel wall contact was confirmed, ablations were commenced. After delivery of the first set of ablations, the basket was collapsed, and the catheter was withdrawn 10mm and rotated 45 degrees. and the process was repeated in the new

position. A minimum of 4-8 ablations were performed. In instances where the vessel was long, additional ablations were performed.

Chapter 3

Evaluation of First Generation Symplicity and EnligHTN Renal Artery Denervation Systems Using A Renal Artery Phantom Model

Al Raisi SI, Pouliopoulos J, Barry MT, Swinnen J, Thiagalingam A, Thomas SP, Sivagangabalan G, Chow C, Chong J, Kizana E, Kovoov P. Evaluation of lesion and thermodynamic characteristics of Symplicity and EnligHTN renal denervation systems in a phantom renal artery model. *EuroIntervention*. 2014;10:277-84.

Evaluation of lesion and thermodynamic characteristics of Symplicity and EnligHTN renal denervation systems in a phantom renal artery model

Sara I. Al Raisi^{1,2}, MBBS; Jim Pouliopoulos^{1,3}, PhD; Michael T. Barry^{1,3}, BSc; John Swinnen^{2,3}, MBBS, FRACS; Aravinda Thiagalingam^{1,3}, MBBS, PhD; Stuart P. Thomas^{1,3}, MBBS, PhD; Gopal Sivagangabalan^{1,3}, MBBS, PhD; Clara Chow^{1,4}, MBBS, PhD; James Chong^{1,3}, MBBS, PhD; Eddy Kizana^{1,3}, MBBS, PhD; Pramesh Kovoov^{1,3*}, MBBS, PhD

1. Department of Cardiology, Westmead Hospital, Sydney, NSW, Australia; 2. Department of Vascular Surgery, Westmead Hospital, Sydney, NSW, Australia; 3. University of Sydney, NSW, Australia; 4. The George Institute for International Health, Sydney, NSW, Australia

KEYWORDS

- renal disease
- risk factors
- safety

Abstract

Aims: Radiofrequency renal artery denervation has been used effectively to treat resistant hypertension. However, comparison of lesion and thermodynamic characteristics for different systems has not been previously described. We aimed to assess spatiotemporal lesion growth and ablation characteristics of Symplicity and EnligHTN systems.

Methods and results: A total of 39 ablations were performed in a phantom renal artery model using Symplicity (n=17) and EnligHTN (n=22) systems. The phantom model consisted of a hollowed gel block surrounding a thermochromic liquid crystal (TLC) film, exhibiting temperature sensitivity of 50-78°C. Flow was simulated using 37°C normal saline with impedance equal to blood. Radiofrequency ablations with each system were delivered with direct electrode tip contact to the TLC. Lesion size was interpreted from the TLC as the maximum dimensions of the 51°C isotherm. Mean lesion depth was 3.82 mm±0.04 versus 3.44 mm±0.03 (p<0.001) for Symplicity and EnligHTN, respectively. Mean width was 7.17 mm±0.08 versus 6.23 mm±0.07 (p<0.001), respectively. With EnligHTN, steady state temperature was achieved 20 sec earlier, and was 15°C higher than Symplicity.

Conclusions: In this phantom model, Symplicity formed larger lesions compared to EnligHTN with lower catheter-tip temperature. The clinical significance of our findings needs to be explored further.

*Corresponding author: Cardiac Services, PO Box 533, Westmead Hospital, Cnr of Hawkesbury and Darcy Road, Sydney, NSW, 2145, Australia. E-mail: pramesh.kovoov@sydney.edu.au

Introduction

Refractory hypertension affects about 10-30% of hypertensive patients¹. Renal artery denervation has resulted in a significant and sustained blood pressure reduction in patients with resistant hypertension as demonstrated by clinical trials^{2,3}. The procedure aims to interrupt the neurohormonal impulses arising from the kidneys, which have been implicated in the pathogenesis of essential hypertension⁴⁻⁷. Nerves responsible for these signals lie within the adventitia of the renal artery with about 90% of nerve fibres occurring within 2 mm from the intimal surface⁸. Endovascular denervation of the renal arteries has been performed through different energy modalities, including radiofrequency, cryoablation, ultrasound, and chemical denervation⁹⁻¹³. At present, the two most widely utilised systems are the radiofrequency Symplicity™ (Medtronic, Minneapolis, MN, USA) and EnligHTN (St. Jude Medical, St. Paul, MN, USA) systems. Radiofrequency energy causes tissue destruction by means of thermal injury¹⁴, when tissue temperature is raised above 45-50°C¹⁵. Both systems are optimised to operate with unique ablation settings summarised in **Table 1**.

Table 1. Clinical settings for the Symplicity and EnligHTN systems.

System parameters	Symplicity	EnligHTN
Monitoring	Temperature and impedance-based algorithm	Temperature-controlled algorithm
Number of electrodes	1	4
Maximal power (W)	8	6
Maximal temperature (°C)	70	75
Ablation duration (sec)	120	90

A predetermined algorithm is utilised for each system to ensure ablation safety. The goal is to achieve reasonably large lesions affecting the target nerves, whilst limiting the injury to the renal artery in order to minimise the risk of renal artery stenosis. It is therefore important to understand the basic biophysical properties for each system in relation to factors that may affect lesion formation. Assessment of the thermal characteristics of cardiac radiofrequency ablation using *in vivo* and *in vitro* models has been described previously^{16,17}. Previous studies have demonstrated good correlation between radiofrequency ablation lesions performed in myocardium, and a Phytigel™ based myocardial phantom model incorporating a TLC film (LCR Hallcrest, Flintshire, UK)¹⁷. The study demonstrated the ability of TLC to map the dynamics of lesion formation, based on the 50°C isotherm, in high spatial and temporal resolution. Herein, we provide the first report to evaluate ablation characteristics for two renal denervation systems using a TLC phantom model of the human renal artery.

Editorial, see page 178

Methods

PHANTOM RENAL ARTERY MODEL

A renal artery model was prepared as per Chik¹⁷. Briefly, 1 gram of gel (Phytigel™; Sigma-Aldrich, St. Louis, MO, USA) was

dissolved in a mixture of distilled water and normal saline at a pre-specified concentration (70% distilled water and 30% normal saline). The mix was then brought to a temperature of 90°C, and poured into a well once cooled down to 75°C. The gel well was immersed in a tank that pumped saline at a constant temperature (37°C). Impedance of saline used in the tank was matched to that of blood at 37°C. To mimic the renal artery with a comparable diameter and physiological blood flow rate in a human renal artery¹⁸, specific modifications to the model were applied. In summary, this was achieved by pouring the gel around a 5 mm diameter metal rod holding a vertical TLC disc (colour bandwidth from 50-78°C) at the centre of the gel well. The rod was retrieved after gel cooling to form a hollowed tube in the centre of the gel simulating a renal artery lumen (**Figure 1**). The diameter of the phantom renal artery was kept constant (5 mm) for all gel blocks used in the experiment. A flow meter was used to maintain the rate of saline pumped into the phantom renal artery at 500 ml/min.

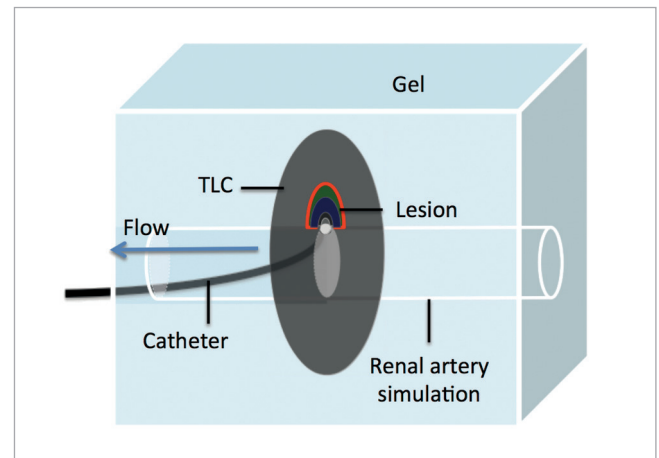


Figure 1. Schematic diagram of radiofrequency ablation in a renal artery phantom model.

RADIOFREQUENCY ABLATION ON TLC

An average of eight radiofrequency ablations per system were delivered on each gel block (n=3). A new TLC disc was used per gel block to avoid damage to the TLC by repeated heating. The order in which each system was tested was altered randomly with every new gel. To deliver radiofrequency ablations, the catheter (Symplicity or EnligHTN) was advanced through the phantom renal artery and positioned in plane with the TLC film. Contact was confirmed by direct visualisation, as the gel was transparent. Radiofrequency ablation was then applied to the gel using the recommended clinical parameters for each system as indicated in **Table 1**. In the case of EnligHTN, the small size basket was used to match the diameter of our phantom renal artery.

LESION MEASUREMENTS AND ANALYSIS

Photographs of the TLC colour gradient were taken at baseline and at 5 sec intervals during ablation using a digital camera (Canon EOS 5D Mark II; Canon Inc., Tokyo, Japan) and a light source (Canon

Speedlite 580EX; Canon Inc.). In-house software was used to analyse the pictures and measure lesion dimensions at several ablation intervals (initially every 5 sec, then every 10 sec) as described previously¹⁷. Lesion size was defined using the 51°C isotherm. Lesion depth was measured from the gel electrode surface to the isotherm of interest (51°C). Lesion width was defined as the maximal width of the 51°C isotherm parallel to the electrode gel surface (Figure 2).

ELECTRODE SURFACE AREA IN CONTACT WITH GEL

For all ablations a cavity was created in the TLC and the gel to simulate endothelial tissue depression during electrode tip contact. The surface area in contact with the electrode was estimated to be about 50% of the total ablation electrode surface area for all energy applications. Measurements of electrode dimensions were carried out using a vernier scale (Figure 3).

1. For Symplicity, total electrode surface area was calculated as follows:

Total surface area (A_{TS})=Surface area 1 (A_1)+Surface area 2 (A_2)

Given that $r=0.62$ mm and $h=1.02$ mm

$$A_1=4 \pi r^2 / 2=2.42 \text{ mm}^2$$

$$A_2=2 \pi r h=3.97 \text{ mm}^2, \text{ hence,}$$

$$A_{TS}=6.39 \text{ mm}^2$$

Therefore, Symplicity electrode area in contact with gel=3.2 mm².

2. For EnligHTN, total surface area (A_{TE})= $2L\pi\sqrt{0.5(a^2+b^2)}$ =3.7 mm², where $L=0.97$ mm, $a=0.42$, $b=0.75$ mm

Therefore, EnligHTN electrode area in contact with gel=1.85 mm².

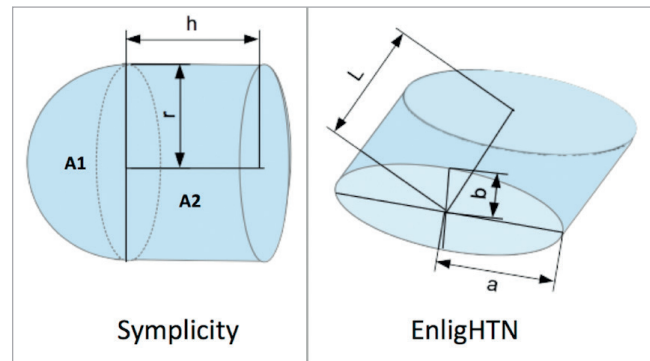


Figure 3. Schematic diagram of Symplicity and EnligHTN electrode tip measurements.

Statistical analysis

Based on preliminary data from gel 1 experiments, a total sample size of six ablations (three per catheter modality) was required to detect a mean difference of 0.66 mm for depth, and 1.54 mm for width with a power of 95% between each catheter modality when $\alpha=0.05$ (two-tailed). As sufficient power was achieved to detect differences between modalities in the first experiment (gel 1), additional experimentation using multiple gels was performed to negate the effect of variation in the gel substrate, which may occur due to external factors (gel heating and solidification time). Mean depth and width for each system were determined using an unpaired

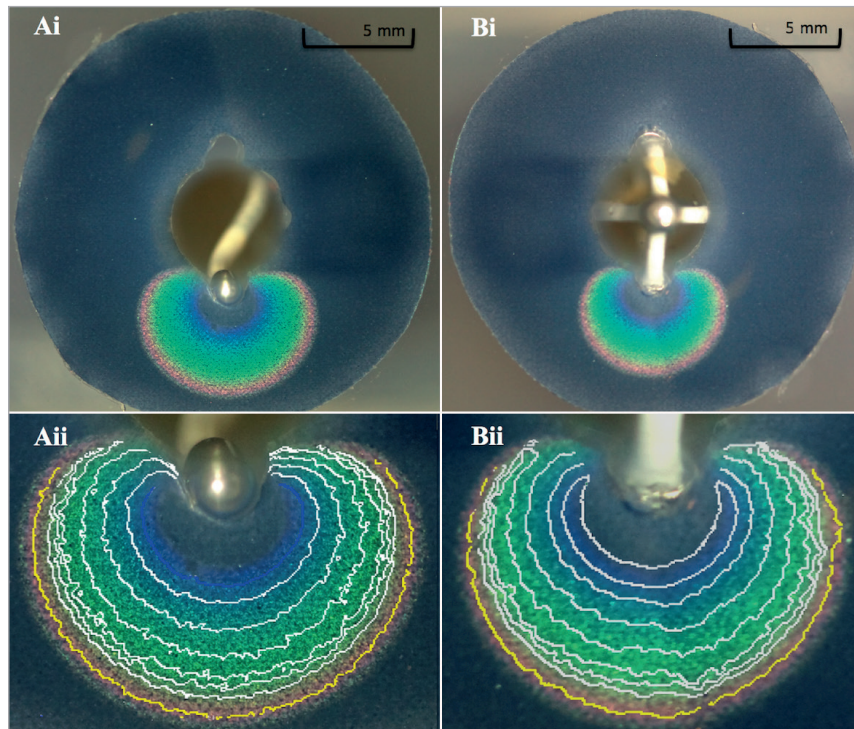


Figure 2. Coronal image of gel with Symplicity (Ai) and EnligHTN (Bi) radiofrequency ablation of TLC film with related isotherm gradient at 120 sec and 90 sec, respectively, and their magnifications (Aii & Bii). The isotherm of interest (51°C) is highlighted in yellow (Aii & Bii).

two-tailed Student's t-test. Each gel experiment for lesion dimensions (depth and width) was analysed using a two-way ANOVA. Pearson's correlation was used to assess the relationship between lesion dimensions (depth and width) with time, and power with time. Statistics were performed on GraphPad Prism 6.0 (GraphPad Software, San Diego, CA, USA). A linear mixed effects model was used to calculate the rate of temperature rise over time for the two systems. S-PLUS Version 8 was used to fit linear mixed effects models to the catheter temperature. In these models, ablation repetition and gel were considered as random factorial effects and time as a random continuous variable. Catheter type, time (continuous) and catheter by time interaction term were considered as fixed effects.

Results

A total of 52 ablations were performed on the phantom renal artery model, comprising 26 ablations for each system. A total of eight ablations using Symplicity and four ablations using EnligHTN were excluded from the analysis due to incorrect plane alignment between the catheter tip and TLC plate. Incorrect plane alignment refers to a catheter positioned inadequately on the TLC surface, but which could still be in contact with the gel. Therefore, the centre of the ablation zone (where maximal lesion dimension could be measured) occurs either behind or in front of the TLC, which will subsequently lead to underestimation of lesion dimensions. The exclusion

rate for the Symplicity catheter was much higher because catheter positioning was technically more difficult with the Symplicity catheter compared to EnligHTN. Radiofrequency ablation parameters are summarised in **Table 2**.

LESION DIMENSION

Mean lesion depth was $3.82 \text{ mm} \pm 0.04$ and $3.44 \text{ mm} \pm 0.03$ ($p < 0.001$) for Symplicity and EnligHTN, respectively. Mean width was $7.17 \text{ mm} \pm 0.08$ versus $6.23 \text{ mm} \pm 0.07$ ($p < 0.001$), respectively (**Figure 4Ai**, **Figure 4Aii**). Variability in lesion characteristics (range

Table 2. Parameters for Symplicity and EnligHTN ablations on the phantom model.

Ablation characteristics	Symplicity	EnligHTN	<i>p</i>
Number of ablations analysed	17	22	–
Mean maximal electrode temperature (°C)	55.11 ± 1.04	68.91 ± 0.94	< 0.001
Mean baseline impedance (Ω)	199.9 ± 1.12	216.2 ± 1.28	< 0.001
Mean baseline temperature (°C)	37.24 ± 0.14	37.18 ± 0.16	0.80
Mean power (W)	6.23 ± 0.7	5.18 ± 0.5	0.26
Electrode surface area in contact (mm ²)	3.2	1.85	–
Ablation duration (sec)	120	90	–

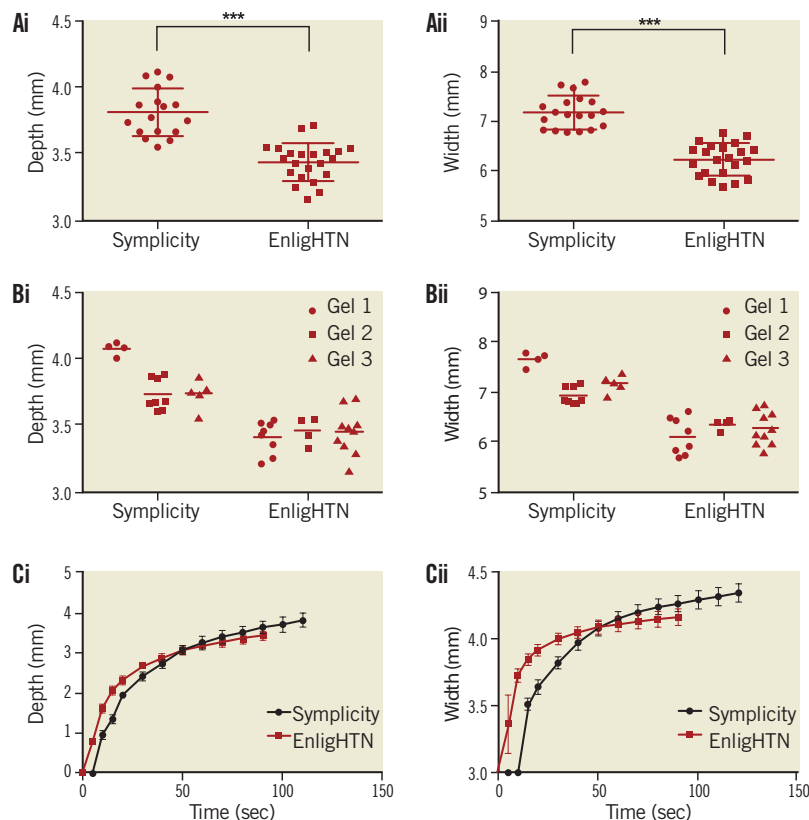


Figure 4. Scatter plots comparing lesion depth (Ai) and width (Aii) for Symplicity and EnligHTN for all three gels combined and each gel separately (Bi, Bii). Graph of lesion growth, depth (Ci) and width (Cii), over duration of radiofrequency application with both systems.

of width, and depth in mm) was observed between gels but, despite this, statistical significance between ablation systems was achieved (**Figure 4Bi, Figure 4Bii**). This variability could be attributed to minor differences in the gel and TLC set-up, as well as electrode-TLC contact.

When analysed at 90 sec, there was no significant difference in lesion depth between the Symplicity and EnligHTN, with mean depth of $3.51 \text{ mm} \pm 0.04$ versus $3.44 \text{ mm} \pm 0.03$ ($p=0.16$). However, at 90 sec the difference in lesion width remained significant with mean width of $6.76 \text{ mm} \pm 0.07$ versus $6.23 \text{ mm} \pm 0.07$ ($p<0.001$) for Symplicity and EnligHTN, respectively. During Symplicity ablation, lesions continued to grow gradually over time, whereas lesion growth appeared to trend towards a plateau with EnligHTN at an earlier time point than Symplicity (**Figure 4Ci, Figure 4Cii**).

ABLATION THERMODYNAMICS

Using EnligHTN, steady state temperature was achieved within 20-30 sec, while Symplicity took longer (50 sec) (**Figure 5A**). This trend was consistent with the power output curve, whereby maximal power was reached within 10 sec for EnligHTN compared to a more gradual increase with Symplicity (**Figure 5B**). This delay in heating with the Symplicity system may be due to an automated algorithm used to increase ablation safety. The maximal power output limit for each system was reached with all ablations. Within the first 20 sec of ablation, the rate of Symplicity electrode temperature rise was 0.2°C per sec (SE 0.065) faster than EnligHTN ($p<0.0024$). Additionally, EnligHTN had a higher electrode temperature at steady state 68°C compared to 55°C for Symplicity, $p<0.001$.

Discussion

Renal artery denervation is a promising treatment option for patients with resistant hypertension. However, a lot of questions remain unanswered regarding this treatment approach, as has been outlined recently¹⁹. One of the unknown factors is the safety and efficacy across different ablation systems and energy modalities. The present study is the first to compare ablation characteristics of two commercially available radiofrequency renal artery denervation systems directly using a phantom renal artery model. We found that Symplicity created lesions that were significantly

deeper and wider than EnligHTN when duration of radiofrequency energy delivery was 120 sec and 90 sec, respectively, as recommended by the manufacturers. When ablation time was capped at 90 sec, lesion depths were similar between systems but remained significantly wider using Symplicity.

Thermal necrosis of tissue using radiofrequency energy occurs as a result of resistive and conductive heating²⁰. During radiofrequency ablation resistive heating occurs within 1 mm of the myocardial-electrode interface, whereas deeper tissue heating results from slower thermal conduction which occurs in a radial pattern away from the resistive zone. Factors that lead to a larger volume of resistive heating or higher current density at the electrode tissue interface will similarly increase the temperature radial gradient area and subsequently lesion size²⁰. These include ablation power, ablation duration, electrode surface area in contact with tissue, and ablation temperature.

In general, power increase leads to a greater current density at the electrode tissue interface. Therefore, lesion size is proportional to ablation power. An *in vivo* closed chest endocardial ablation study by Wittkampf demonstrated an increase in lesion size with higher power settings²¹. Similar results were obtained during *ex vivo* ablations of a bovine left ventricle under superfusate flow (1 L/min)²². The amount of power delivered to the target tissue is however affected by tissue impedance and power dissipation into the blood pool, which varies between different positions within one patient and also between different patients. Both Symplicity and EnligHTN systems operate at low power settings compared to cardiac radiofrequency ablation generators and are regulated by a catheter tip-temperature and impedance feedback mechanism. In our phantom model, mean power delivered during radiofrequency ablation was comparable for both systems. Hence, differences in lesion dimensions between the two systems cannot be explained by differences in power output.

Lesion growth rate for radiofrequency ablation follows a monoexponential function with a rapid initial phase occurring locally to the area of resistive heating. Thereafter, growth reaches a steady state without subsequent increase in lesion size^{21,23}. A study that compared cardiac lesion size at two ablation time points (60 and 120 sec), utilising low ablation power

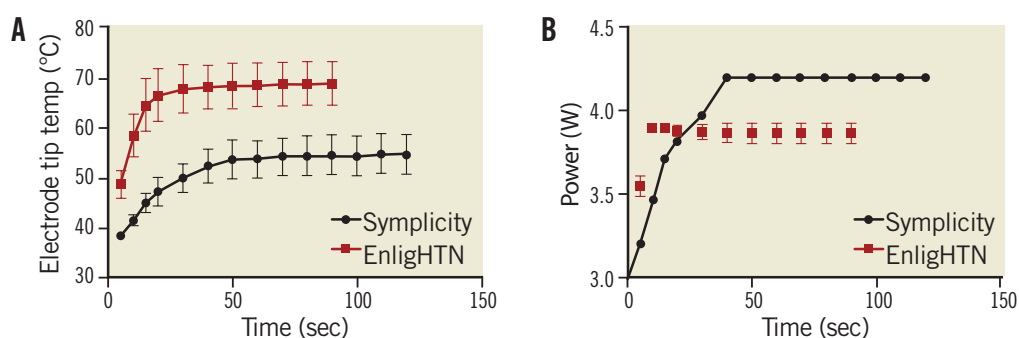


Figure 5. Graph showing temperature change (A) and power output (B) over the duration of radiofrequency application for Symplicity and EnligHTN.

ranging from 20-50 W and superfusate flow, showed that larger lesions occurred at 120 sec compared to 60 sec²². Based on that study, we postulate that the relatively longer ablation time applied using Symplicity was a significant factor in the observed increase in lesion size compared to EnligHTN. In support of this, neither system reached growth steady state, which is probably due to the high flow rate accounting for dissipation of power and reduction in power delivered to the tissue. This suggests that longer duration of ablation could potentially result in larger lesion size with both systems.

Lesion size is also affected by electrode tissue interface area. Haines described a linear relationship between electrode radius and lesion radius under constant electrode tissue interface temperature using a thermodynamic model. His model was validated using perfused and superfused canine right ventricular free wall²⁴. Larger electrode radius formed bigger lesions when power density and tissue interface temperature remained constant. Nevertheless, higher overall power was required to maintain a similar power density. Additionally, lesion dimensions increase with increasing electrode length provided contact is adequate^{25,26}. It has been demonstrated that increases in electrode tissue interface area and area exposed to convective cooling by blood are both responsible for increase in lesion size with larger electrodes²⁷. Thus, the larger Symplicity electrode tissue interface area may have contributed to the difference in lesion size between the two catheters. Of note, the Symplicity system is based on a temperature and impedance algorithm, while the EnligHTN system has a temperature-controlled algorithm. The difference in system operation could also influence lesion size.

During temperature-controlled radiofrequency ablation, lesion size is directly proportional to electrode tissue interface temperature²⁰. Temperature monitoring devices (thermocouple or thermistor) embedded within the ablation electrode monitor electrode tip temperature during radiofrequency ablation. However, a discrepancy between catheter tip temperature and tissue temperature can occur due to various factors including convective cooling by blood or irrigation. Whilst EnligHTN ablations reached higher electrode tip temperature compared to Symplicity for all ablations, Symplicity lesions were larger. This is probably due to the contribution of other factors discussed above affecting lesion size. Moreover, temperatures at the TLC electrode interface for all ablations were higher than those detectable by the TLC sheet (indicated by colour clearing, **Figure 2**), suggesting that the temperature measured by the electrode tip during renal artery ablation was lower than that of the electrode tissue interface. This difference was probably due to cooling of the electrode tip by high flow rate in the renal artery.

Thrombus formation and intimal disruption have been reported in a study using optical coherence tomography during renal artery denervation, more frequently with EnligHTN²⁸. It is unclear if this is due to the higher temperature achieved during ablation and more rapid temperature increase with EnligHTN observed in our study.

Clinical implications

With numerous emerging technologies and catheter designs for renal artery denervation, it is critical to understand the basic biophysics of radiofrequency ablation for each device and the affect of that design on lesion formation. Moreover, identifying the unique characteristics of each renal denervation system is of pivotal importance in order to optimise ablation safety and efficacy. Each system needs to be evaluated further in clinical trials to establish its clinical safety and efficacy.

In the present study, adequate contact between the catheter tip and the TLC was confirmed by direct visualisation. However, in clinical practice this is difficult to establish and maintain, especially with the single electrode Symplicity catheter. This is important, as adequate electrode tissue contact is imperative for lesion formation²⁹. In addition, despite the statistical difference in lesion size, it is difficult to anticipate the clinical significance of this finding.

Study limitations

The phantom renal artery used for our study does not replicate the heterogeneity of renal arterial layers, which have unique conduction properties and are also surrounded by fat. This may consequently affect the distribution of thermal injury. Nonetheless, the two systems were compared under an identical controlled environment with no confounding variables. This model also has the advantage of allowing the evaluation of temporal progression of lesions, which is difficult to assess *in vivo*. To allow for the comparison between the two systems, the flow rate and the renal artery diameter were kept constant; therefore, the effect of alteration in flow rate, arterial spasms and vessel wall oedema that can occur during the application of radiofrequency energy could not be simulated. In addition, EnligHTN lesions were more consistent in size compared to Symplicity lesions, as seen in **Figure 4B**. This could be as a result of variations in the electrode contact area with the gel-TLC surface, which were carefully placed but were more difficult to establish between the Symplicity experiments. Evaluation of collateral damage using the phantom model is not possible; however, a preclinical safety trial conducted with the Symplicity system reported no collateral damage to kidneys or nearby structures³⁰. Finally, the TLC film used in the phantom had a colour change sensitivity range between 50-78°C; therefore, we were unable to detect temperatures beyond this range.

Conclusion

Lesion size was larger for the Symplicity renal artery denervation system compared to EnligHTN when radiofrequency ablation was performed on a phantom renal artery model. The difference in lesion size was more pronounced for lesion width, with a smaller difference in lesion depth. This was achieved with a gradual increase in temperature and lower electrode tip temperature at steady state with the Symplicity system. It is likely that the larger electrode surface area and longer ablation duration with Symplicity could have accounted for the difference in lesion size.

Impact on daily practice

One important criterion for successful renal artery denervation is the delivery of safe and effective ablation lesions. Currently, different systems are being used to deliver these ablations in patients with resistant hypertension. Understanding the biophysical properties of the systems and the differences in lesions formed is essential to improve the techniques and clinical outcome. The renal artery phantom model described here provided a platform to identify lesion properties from two different systems under specific conditions. This model can be applied to available and future renal denervation systems, thereby providing a preclinical simulation that would objectively inform the clinical parameters for the lesions created.

Conflict of interest statement

The authors have no conflicts of interest to declare.

References

- Calhoun DA, Jones D, Textor S, Goff DC, Murphy TP, Toto RD, White A, Cushman WC, White W, Sica D, Ferdinand K, Giles TD, Falkner B, Carey RM; American Heart Association Professional Education Committee. Resistant hypertension: diagnosis, evaluation, and treatment: a scientific statement from the American Heart Association Professional Education Committee of the Council for High Blood Pressure Research. *Circulation*. 2008;117:e510-26.
- Krum H, Schlaich M, Whitbourn R, Sobotka PA, Sadowski J, Bartus K, Kapelak B, Walton A, Sievert H, Thambar S, Abraham WT, Esler M. Catheter-based renal sympathetic denervation for resistant hypertension: a multicentre safety and proof-of-principle cohort study. *Lancet*. 2009;373:1275-81.
- Esler MD, Krum H, Schlaich M, Schmieder RE, Bohm M, Sobotka PA. Renal sympathetic denervation for treatment of drug-resistant hypertension: one-year results from the Symplicity HTN-2 randomized, controlled trial. *Circulation*. 2012;126:2976-82.
- DiBona GF. Physiology in perspective: The Wisdom of the Body. Neural control of the kidney. *Am J Physiol Regul Integr Comp Physiol*. 2005;289:R633-41.
- Esler M, Jennings G, Lambert G. Noradrenaline release and the pathophysiology of primary human hypertension. *Am J Hypertens*. 1989;2:140S-146S.
- Campese VM, Kogosov E, Koss M. Renal afferent denervation prevents the progression of renal disease in the renal ablation model of chronic renal failure in the rat. *Am J Kidney Dis*. 1995;2:861-5.
- Katholi RE, Winternitz SR, Oparil S. Decrease in peripheral sympathetic nervous system activity following renal denervation or unclipping in the one-kidney one-clip Goldblatt hypertensive rat. *J Clin Invest*. 1982;69:55-62.
- Atherton DS, Deep NL, Mendelsohn FO. Micro-anatomy of the renal sympathetic nervous system: a human postmortem histology study. *Clin Anat*. 2012;25:628-33.
- Honton B, Pathak A, Sauguet A, Fajadet J. First report of transradial renal denervation with the dedicated radiofrequency Iberis catheter. *EuroIntervention*. 2014;9:1385-8.
- Fischell TA, Vega F, Raju N, Johnson ET, Kent DJ, Ragland RR, Fischell DR, Almany SL, Ghazarossian VE. Ethanol-mediated perivascular renal sympathetic denervation: preclinical validation of safety and efficacy in a porcine model. *EuroIntervention*. 2013;9:140-7.
- Heuser RR, Mhatre AU, Buelna TJ, Berci WL, Hubbard BS. A novel non-vascular system to treat resistant hypertension. *EuroIntervention*. 2013;9:135-9.
- Ormiston JA, Watson T, van Pelt N, Stewart R, Stewart JT, White JM, Doughty RN, Stewart F, Macdonald R, Webster MW. Renal denervation for resistant hypertension using an irrigated radiofrequency balloon: 12-month results from the Renal Hypertension Ablation System (RHAS) trial. *EuroIntervention*. 2013;9:70-4.
- Mabin T, Sapoval M, Cabane V, Stemmett J, Iyer M. First experience with endovascular ultrasound renal denervation for the treatment of resistant hypertension. *EuroIntervention*. 2012;8:57-61.
- Erez A, Shitzer A. Controlled destruction and temperature distributions in biological tissues subjected to monoactive electrocoagulation. *J Biomech Eng*. 1980;102:42-9.
- Cosman ER Jr, Cosman ER Sr. Electric and thermal field effects in tissue around radiofrequency electrodes. *Pain Med*. 2005;6:405-24.
- Nakagawa H, Yamanashi WS, Pitha JV, Arruda M, Wang X, Ohtomo K, Beckman KJ, McClelland JH, Lazzara R, Jackman WM. Comparison of in vivo tissue temperature profile and lesion geometry for radiofrequency ablation with a saline-irrigated electrode versus temperature control in a canine thigh muscle preparation. *Circulation*. 1995;91:2264-73.
- Chik WW, Barry MA, Thavapalachandran S, Midekin C, Pouliopoulos J, Lim TW, Sivagangabalan G, Thomas SP, Ross DL, McEwan AL, Kovoov P, Thiagalingam A. High spatial resolution thermal mapping of radiofrequency ablation lesions using a novel thermochromic liquid crystal myocardial phantom. *J Cardiovasc Electrophysiol*. 2013;24:1278-86.
- Wolf RL, King BF, Torres VE, Wilson DM, Ehman RL. Measurement of normal renal artery blood flow: cine phase-contrast MR imaging vs clearance of p-aminohippurate. *AJR Am J Roentgenol*. 1993;161:995-1002.
- Tsioufis C, Mahfoud F, Mancia G, Redon J, Damascelli B, Zeller T, Schmieder RE. What the interventionalist should know about renal denervation in hypertensive patients: a position paper by the ESH WG on the interventional treatment of hypertension. *EuroIntervention*. 2014;9:1027-35.
- Nath S, DiMarco JP, Haines DE. Basic aspects of radiofrequency catheter ablation. *J Cardiovasc Electrophysiol*. 1994;5:863-76.
- Wittkampf FH, Hauer RN, Robles de Medina EO. Control of radiofrequency lesion size by power regulation. *Circulation*. 1989;80:962-8.
- Guy DJ, Boyd A, Thomas SP, Ross DL. Increasing power versus duration for radiofrequency ablation with a high superfusate

flow: implications for pulmonary vein ablation? *Pacing Clin Electrophysiol.* 2003;26:1379-85.

23. Haines DE. Determinants of lesion size during radiofrequency catheter ablation: the role of electrode-tissue contact pressure and duration of energy delivery. *J Cardiovasc Electrophysiol.* 1991;2:509-15.

24. Haines DE, Watson DD, Verow AF. Electrode radius predicts lesion radius during radiofrequency energy heating. Validation of a proposed thermodynamic model. *Circ Res.* 1990;67:124-9.

25. Langberg JJ, Gallagher M, Strickberger SA, Amirana O. Temperature-guided radiofrequency catheter ablation with very large distal electrodes. *Circulation.* 1993;88:245-9.

26. Kovoov P, Daly M, Campbell C, Dewsnap B, Eipper V, Uther J, Ross D. Intramural radiofrequency ablation. *Pacing Clin Electrophysiol.* 2004;27:719-25.

27. Otomo K, Yamanashi WS, Tondo C, Antz M, Bussey J, Pitha JV, Arruda M, Nakagawa H, Wittkamp FH, Lazzara R, Jackman WM. Why a large tip electrode makes a deeper

radiofrequency lesion: effects of increase in electrode cooling and electrode-tissue interface area. *J Cardiovasc Electrophysiol.* 1998;9:47-54.

28. Templin C, Jaguszewski M, Ghadri JR, Sudano I, Gaehwiler R, Hellermann JP, Schoenenberger-Berzins R, Landmesser U, Erne P, Noll G, Lüscher TF. Vascular lesions induced by renal nerve ablation as assessed by optical coherence tomography: pre- and post-procedural comparison with the Simplicity catheter system and the EnligHTN multi-electrode renal denervation catheter. *Eur Heart J.* 2013;34:2141-8, 2148b.

29. Haines DE, Watson DD. Tissue heating during radiofrequency catheter ablation: a thermodynamic model and observations in isolated perfused and superfused canine right ventricular free wall. *Pacing Clin Electrophysiol.* 1989;12:962-76.

30. Rippey MK, Zarins D, Barman NC, Wu A, Duncan KL, Zarins CK. Catheter-based renal sympathetic denervation: chronic preclinical evidence for renal artery safety. *Clin Res Cardiol.* 2011;100:1095-101.

Chapter 4

Assessment of New Generation Symplicity and EnligHTN Renal Artery Denervation Systems Using A Renal Artery Phantom Model

Al Raisi SI, Barry MT, Qian P, Bhaskaran A, Pouliopoulos J, Kovoov P. Comparison of new generation renal artery denervation systems: Assessing lesion size and thermodynamics using a thermochromic liquid crystal phantom model. *EuroIntervention*. 2017;13:1242-1247.

Comparison of new-generation renal artery denervation systems: assessing lesion size and thermodynamics using a thermochromic liquid crystal phantom model



Sara I. Al Raisi^{1,2}, MB Bch, FRACP; Michael T. Barry^{1,2}, B.Sc; Pierre Qian^{1,2}, MBBS, FRACP; Abhishek Bhaskaran², MBBS, FRACP; Jim Pouliopoulos^{1,2}, PhD; Pramesh Kovoor^{1,2*}, MBBS, PhD

1. Department of Cardiology, Westmead Hospital, Sydney, NSW, Australia; 2. University of Sydney, Sydney, NSW, Australia

KEYWORDS

- catheter ablation
- renal sympathetic denervation
- resistant hypertension

Abstract

Aims: The aim of this study was to evaluate and compare lesion dimensions and thermodynamics of the new-generation multi-electrode Symplicity Spyral and the new-generation multi-electrode EnligHTN renal artery denervation systems, using a thermochromic liquid crystal phantom model.

Methods and results: A previously described renal artery phantom model was used as a platform for radiofrequency ablation. A total of 32 radiofrequency ablations were performed using the multi-electrode Symplicity Spyral (n=16) and the new-generation EnligHTN systems (n=16). Both systems were used as clinically recommended by their respective manufacturer. Lesion borders were defined by the 51°C isotherm. Lesion size (depth and width) was measured and compared between the two systems. Mean lesion depth was 2.15±0.02 mm for the Symplicity Spyral and 2.32±0.02 mm for the new-generation EnligHTN (p-value <0.001). Mean lesion width was 3.64±0.08 mm and 3.59±0.05 mm (p-value=0.61) for the Symplicity Spyral and the new-generation EnligHTN, respectively.

Conclusions: The new-generation EnligHTN system produced lesions of greater depth compared to the Symplicity Spyral under the same experimental conditions. Lesion width was similar between both systems. Achieving greater lesion depth by use of the new-generation EnligHTN may result in better efficacy of renal artery denervation.

*Corresponding author: Department of Cardiology, PO Box 533, Westmead Hospital, Cnr of Hawkesbury and Darcy Road, Sydney, NSW, 2145, Australia. E-mail: pramesh.kovoor@sydney.edu.au

Abbreviations

BP	blood pressure
RAD	renal artery denervation
RF	radiofrequency
TLC	thermochromic liquid crystal
SS	Symplicity Spyral
NGE	new-generation EnligHTN

Introduction

Following the encouraging results of the Symplicity HTN-1 and Symplicity HTN-2 trials, which demonstrated significant blood pressure (BP) reduction after renal artery denervation (RAD), endovascular radiofrequency (RF) ablation of the renal arteries was considered an acceptable treatment for drug refractory hypertension^{1,2}. Later, the randomised controlled SYMPPLICITY HTN-3 trial failed to show a significant difference in BP reduction between the RAD treatment arm and the sham control arm³. Nevertheless, the implication of renal sympathetic nerves in the pathogenesis of resistant hypertension has been well described and demonstrated in previous animal and human studies⁴⁻⁸. Several factors have been proposed that may have limited the denervation efficacy in SYMPPLICITY HTN-3⁹. A better understanding of the basic mechanisms of denervation and factors affecting procedural success including patient selection, renal nerve anatomy and the biophysics of the various renal denervation systems through further preclinical studies is pivotal to achieving the desired results.

Previously, we developed a thermochromic liquid crystal (TLC) model and validated it *in vivo* for cardiac RF ablation¹⁰. Subsequently, we modified this model for renal denervation. In our previous study, we assessed and compared lesion size and thermodynamic properties of the single-electrode Symplicity (Flex) renal denervation system (Medtronic, Minneapolis, MN, USA) versus the first-generation multi-electrode EnligHTN system (St. Jude Medical, St. Paul, MN, USA) using the TLC renal artery phantom model¹¹. Recently, in the new-generation systems, several modifications have been applied to both the EnligHTN and Symplicity renal denervation systems in order to overcome some of the technical procedural challenges, and to reduce overall procedural duration, either of which could ultimately impact on ablation efficacy. Therefore, in this study we aimed to evaluate and

assess the performance of the new-generation Symplicity Spyral (SS) and the new-generation EnligHTN (NGE) renal denervation systems using the previously described renal artery phantom model. **Table 1** summarises the differences between the old and the new Symplicity and EnligHTN systems.

Methods

Radiofrequency ablations for both the SS and NGE systems were performed in the renal artery phantom model using clinically recommended ablation settings (**Table 1**). Temporal changes in lesion dimensions (depth and width) for the two systems were measured and compared.

THERMOCHROMIC LIQUID CRYSTAL PHANTOM RENAL ARTERY MODEL

The renal artery phantom model was prepared as previously described¹¹. In summary, a mixture of saline and an agar substitute powder (Phytigel™; Sigma-Aldrich [now Merck], St. Louis, MO, USA) was heated to 90°C in a preformed cast encompassing a 5 mm diameter cylindrical former. Once cooled, the former was removed to create a transparent block of gel with a 5 mm diameter lumen to simulate the renal artery. A TLC film that has temperature sensitivity between 50-78°C (Hallcrest LCR, Connah's Quay, United Kingdom) was embedded within the gel prior to solidification. The gel block was placed in a tank, which pumped saline around the gel and into the phantom renal artery lumen at a rate of 500 ml/min and a temperature of 37°C.

RADIOFREQUENCY ABLATION

The ablation catheter for the system was introduced into the phantom renal artery under direct visualisation. The Spyral catheter was advanced into the phantom lumen over a (0.014-inch) guidewire as clinically recommended. Once within the lumen of the phantom renal artery, the guidewire was pulled back to allow spiral configuration of the catheter. In the case of the EnligHTN catheter, a small diameter basket size (recommended for vessel diameters between 4 and 6 mm) was used and the catheter was deployed on a single instance per gel to limit abrasion of the gel surface. At least one electrode was positioned in plane with the TLC sheet. Only the electrode in contact with the TLC sheet was activated for each RF ablation (one electrode per run). All ablations were performed with

Table 1. Summary of the technical specifications and a comparison between the new and old Symplicity and EnligHTN renal denervation systems.

System	Old systems		New systems	
	Symplicity (Flex)	EnligHTN old generation	Symplicity (Spyral)	EnligHTN new generation
Generator	Symplicity G2	1 st generation	Symplicity G3	2 nd generation
Number of electrodes	1	4	4	4
Ablation duration (sec)	120	90	60	60
Maximum power per electrode (W)	8	6	6.5	8
Electrode surface area (mm ²)*	6.39	3.7	5.9	3.7

* Measured in-house.

a flow rate of 500 ml/min through the phantom renal artery, and an ablation duration of 60 sec. The gel was allowed to cool down for five minutes between RF ablations and the catheter was moved to a new position after four runs of ablation.

LESION MEASUREMENTS AND ANALYSIS

A digital camera (Canon EOS 5D Mark II; Canon Inc., Tokyo, Japan) with a light source (Canon Speedlite 580EX; Canon) was placed in front of the phantom model to capture images at different ablation time points (at baseline, 20 sec, 30 sec, 40 sec, 50 sec and 60 sec). Heating of the gel at the TLC surface produced a colour gradient on the TLC sheet (**Figure 1A**), which was utilised to calculate the isotherms following thermochromic calibration using in-house developed software (**Figure 1B**). The 51°C isotherm was used as an arbitrary measure to define lesion borders, as irreversible neural tissue injury occurs at temperatures greater than 45–50°C^{12,13}. Lesion depth (*d*) was measured as the length of a line between the electrode/gel interface and the 51°C isotherm perpendicular to the electrode tip. Lesion width (*w*) was defined as the maximum width of the 51°C isotherm perpendicular to *d* (**Figure 1B**).

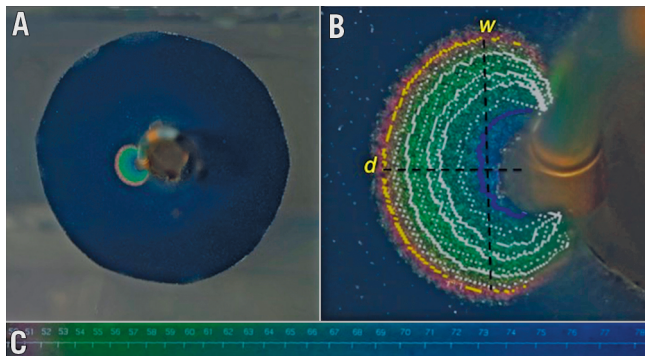


Figure 1. Image taken during radiofrequency ablation on the phantom renal artery model at 60 sec using the Symplicity Spyrax system in this case. A) Colour gradient on the TLC sheet during RF ablation. B) Lesion post analysis with superimposed isotherms. Yellow line highlights the 51°C isotherm. C) Colour gradient with the corresponding temperature in °C. d: lesion depth; w: lesion width; TLC: thermochromic liquid crystal

STATISTICAL ANALYSIS

Based on previous work in the same phantom model, RF ablation in replicates of three per catheter were required to detect a significant difference in lesion size, with a power of 95% and $\alpha=0.05$ (two-tailed), for each parameter tested¹¹. Mean lesion depth and width for each system were compared using an unpaired two-tailed Student's t-test. Data were expressed as mean±standard deviation. The relationship between lesion growth (depth and width) and time was assessed using Spearman's correlation. Values of $p<0.05$ were considered significant. Data analysis was performed with GraphPad Prism software 6.0 (GraphPad Software Inc., La Jolla, CA, USA) and SPSS, Version 24 (IBM Corp., Armonk, NY, USA).

Results

A total of 32 RF ablations (16 ablations per system) were performed on the phantom renal artery model. All ablations were carried out under similar phantom conditions whereby parameters, including phantom vessel diameter, flow rate and gel temperature, were adjusted to within normal physiological ranges of 5 mm, 500 ml/min and 37°C, respectively. **Table 2** summarises the ablation parameters for both systems.

Table 2. Ablation parameters for Symplicity Spyrax and new-generation EnligHTN systems.

System	Symplicity Spyrax	New-generation EnligHTN	p-value
Ablation number	16	16	–
Mean power (V)	6.5±0.00 (maximum power)	5.3±0.07 (average power)	–
Mean baseline impedance (Ω)	174.3±0.88	199.1±0.88	<0.001
Mean electrode tip temperature (°C)	45.56±0.66 (maximum temperature)	52.50±0.98 (average temperature)	–
Ablation duration (sec)	60	60	–

LESION SIZE AND GROWTH

Thirty-one RF ablation lesions (16 for SS and 15 for NGE) were analysed at 60 sec to determine final lesion size. A single data point for the NGE group was unavailable due to photographic aberration. Immediately prior to termination of RF ablation (60 sec), mean lesion depth for SS was 2.15±0.02 mm versus 2.32±0.02 mm for NGE (p -value <0.001) (**Figure 2A**). Mean lesion width was 3.64±0.08 mm and 3.59±0.04 mm (p -value=0.61) for SS and NGE, respectively (**Figure 2B**).

In addition, temporal analysis of lesion dimensions was performed to demonstrate the thermodynamics of each ablation system (**Figure 3**). A Spearman correlation test demonstrated a strong positive correlation between the duration of RF ablation and lesion size (depth and width), which was statistically significant for both systems. The correlation coefficient (r_s) for ablation duration versus lesion depth was 0.91 ($p<0.001$) for SS and 0.86 ($p<0.001$) for NGE. The correlation coefficient (r_s) for ablation duration versus lesion width was 0.606 ($p<0.001$) and 0.726 ($p<0.001$) for SS and NGE, respectively.

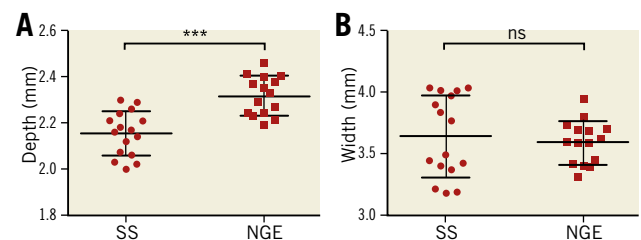


Figure 2. Scatter plots comparing lesion depth and width for the Symplicity Spyrax and new-generation EnligHTN systems at end of radiofrequency ablation (60 sec). A) Lesion depth. B) Lesion width. NGE: new-generation EnligHTN; SS: Symplicity Spyrax

Graphs of lesion depth and width over time (**Figure 3**) suggest that prolonging the ablation duration could potentially increase lesion size, as a plateau phase has not been reached. Nonetheless, analysis of lesion size at different ablation time points demonstrated that about 70-80% of lesion growth occurred within the first 20 sec of RF delivery with a lesion growth rate of 0.076 mm/sec for depth and 0.147 mm/sec for width with SS, and 0.094 mm/sec for depth and 0.124 mm/sec for width with NGE during the initial 20 sec ablation phase. Lesion growth rate slows down thereafter to 0.012 mm/sec for depth and 0.01 mm/sec for width with SS and 0.009 mm/sec for depth and 0.008 mm/sec for width with NGE in the last 20 sec of RF ablation. Thus, increasing ablation time beyond 60 sec may result in only a small increase in lesion size. **Table 3** summarises lesion dimensions at 20, 40 and 60 seconds of RF ablation and the percentage of lesion growth (depth and width) at each time point.

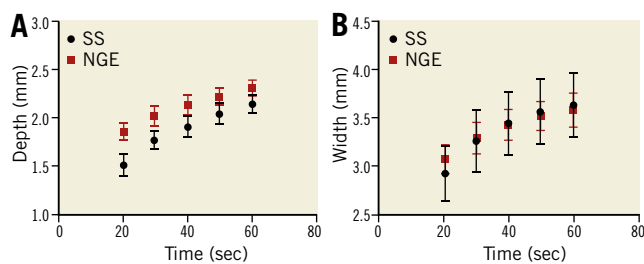


Figure 3. Graph demonstrating the relationship between radiofrequency ablation duration and lesion growth for the Symplixity Spyral and new-generation EnligHTN systems. A) Lesion depth versus time. B) Lesion width versus time. NGE: new-generation EnligHTN; SS: Symplixity Spyral

Discussion

Using the TLC renal artery phantom model, the NGE renal denervation system achieved greater lesion depth compared to the multi-electrode SS system. However, there was no difference in lesion width between the two systems. RF ablation with both systems was performed under consistent experimental settings (i.e., consistent gel impedance, gel temperature, vessel diameter and flow rate) and optimal electrode/gel contact as confirmed by direct visualisation. Our phantom model allows direct comparison due to the ability to control variables, which is difficult to achieve clinically.

In our previous study, we compared the lesion dimensions and thermal properties of the single-electrode Symplixity Flex

versus the first-generation multi-electrode EnligHTN renal artery denervation system, utilising the same renal artery phantom model¹¹. The present study is the first to compare the new-generation multi-electrode Spyral system to the new-generation EnligHTN system using the TLC/gel phantom model. In RF ablation, only about 1 mm of tissue adjacent to the electrode (area of resistive heating) is heated directly. Deeper tissue is heated by conduction of thermal energy from the resistive heating zone¹⁴.

Therefore, increased heating at the electrode tissue interface leads to more heat being conducted through the tissue and subsequently larger lesions. This is affected by several factors including ablation power, electrode size, electrode area in contact with tissue, contact force, convective cooling and ablation duration^{14,15}. Whilst the SS electrode surface area is larger compared to the NGE (**Table 1**), lesions produced by the SS were comparatively smaller in depth. It has been demonstrated that increased electrode surface area results in larger lesions. Nonetheless, electrodes with a larger surface area usually require higher power delivery to maintain the same current density at the electrode tissue interface¹⁶⁻¹⁹. The maximum power generated by the SS and NGE is 6.5 W and 8 W, respectively. Conversely, a larger electrode area leads to more heat loss in the blood pool by convection and, therefore, reduces heating efficiency. Power lost in the blood pool is even greater when electrode-tissue contact is reduced¹⁵. It is possible that the greater contact force produced by the EnligHTN catheter upon deployment results in more optimal and stable gel contact, and therefore deeper lesions. It is important to note that for all ablations careful placement of the electrode tip against the TLC/gel surface was consistent and confirmed. Haines demonstrated in an *in vitro* model that greater contact pressure produced deeper lesions as long as electrode-tissue contact was maintained and electrode-tissue temperature kept constant by adjusting power. In his study, lesion width showed no significant difference with increased contact force²⁰. Consistent with this finding, we found no difference in width between the two systems. Although not directly measured, it is likely to be the design of the EnligHTN catheter that has the advantage of producing more consistent contact force. This could also explain the lower electrode tip temperature achieved by the SS (**Table 2**).

Of note, when the old-generation systems were used in the same model, the lesions produced were deeper (3.8 mm and 3.4 mm for Symplixity and EnligHTN, respectively)¹¹. A recent animal study also suggested a thermal injury depth of 3.9 mm when the Symplixity

Table 3. Lesion size and the percentage of growth at 20, 40 and 60 sec during radiofrequency ablation for Symplixity Spyral and new-generation EnligHTN.

Ablation time (sec)	Depth (mm)		p-value	Width (mm)		p-value	% Depth:width of maximum	
	SS	NGE		SS	NGE		SS	NGE
20	1.52±0.03	1.87±0.02	<0.001	2.93±0.07	3.08±0.04	0.10	70.7:80.7	80.6:85.8
40	1.92±0.03	2.14±0.03	<0.001	3.45±0.08	3.44±0.04	0.86	89.3:95.0	92.2:95.8
60	2.15±0.02	2.32±0.02	<0.001	3.63±0.08	3.59±0.05	0.61	100:100	100:100

NGE: new-generation EnligHTN; SS: Symplixity Spyral

Flex was used²¹. Although the old- and the new-generation systems were not directly compared, the conditions of the phantom model were consistent between time points, suggesting a difference in performance between the old- and the new-generation systems. In the case of the SS, a 50% reduction in ablation duration with lower power output compared to the old Symplicity system may have resulted in reduced net current density at the electrode-tissue interface despite the marginally smaller electrode surface area of this system. In addition, increased contact force at the tip of the Symplicity Flex catheter due to the ability to deflect the tip vector towards the gel interface could have produced a degree of contact force that minimised heat loss. For the NGE, smaller depth compared to the old EnligHTN system is probably partially due to shorter ablation duration.

Lesion size is one of several important elements for achieving clinical efficacy in RAD. Deeper lesions may translate into more effective denervation, as more nerve bundles could be targeted. Clinically, successful denervation is important in order to achieve a significant BP reduction after RAD. Evidence from post-mortem and animal studies has demonstrated that about 50% of renal nerves proximal to the bifurcation are located at a depth of greater than 2.44 mm^{22,23}. Therefore, given the findings of the present study, ablation using the new-generation systems may potentially result in denervation of <50% of renal nerves at those sites, thus limiting the efficacy of the procedure. When assessing nerves at different vessel segments, it has been shown that most of the nerve bundles are located within the proximal and middle segments of the renal arteries. However, they are found at a greater depth in the proximal segment compared to the distal segment of the vessel (3.4 mm proximally versus 2.6 mm distally), which renders the proximal nerve bundles more difficult to ablate endovascularly using the currently available denervation systems²². In distal segments (before the bifurcation), the 50th percentile of nerves was found to be at 1.81 mm from the lumen; 79% of nerves found distal to the bifurcation are located within 2 mm from the lumen²². The limited depth of heating and the current knowledge of renal nerve distribution highlight the importance of distal segment ablation. This was demonstrated in a porcine model study by Mahfoud et al, where the addition of ablation distal to the bifurcation using the SS resulted in more effective denervation as measured by a reduction in cortical norepinephrine content and axonal density compared to main vessel ablation only²⁴.

While the focus now has been directed towards more distal denervation (distal segment and distal to the bifurcation), improving ablation systems to reach deeper targets may also be beneficial, if this could be attained safely. Initial experimental studies using alternative energy modalities, including microwave ablation and chemical denervation, reported on lesion depth of 5-8 mm^{21,25}. However, until additional research is conducted to evaluate the efficacy and safety of such modalities further, their use remains experimental.

Study limitations

Ablation conditions on the phantom renal artery model used in this study do not represent the complete spectrum of physiological

conditions and acute response to RF ablation during renal denervation. In addition, the design of the current model allows assessment of heating pattern on a single plane only. Therefore, we were unable to assess heating of all four electrodes simultaneously, which may have an effect on heating pattern. However, the ability to control different variables and standardise the model allows us to compare the two systems under identical settings. Moreover, the effect of altering different parameters on lesion size could be assessed using this model in future studies. Lastly, we have chosen the 51°C isotherm to define lesion dimension. However, if nerve injury occurs at temperatures above or below this threshold, the actual depth of thermal injury would be underestimated or overestimated. Nonetheless, for the application of RF ablation in neurosurgery it has been generally accepted that neural tissue destruction occurs at temperature ≥ 45 -50°C (lethal isotherm) and temperatures between 42-45°C showed reversible neural damage^{13,26}.

Conclusions

Increased lesion depth was achieved using the NGE renal denervation system compared to the SS system for ablation on the TLC phantom model, with no difference in lesion width. Whilst the difference in depth is small, it may have an impact on denervation efficacy.

Impact on daily practice

The relationship between the renal nerves as a target for radio-frequency ablation and ablation depth is one of several factors affecting denervation success. Information on different devices and technologies available with regard to their thermal properties and biophysics can guide clinicians as well as help us to understand the limitations of currently available systems and possible areas for improvement.

Funding

Symplicity Spyral and EnligHTN catheters were donated by Medtronic and St. Jude Medical. S. Al Raisi is supported by a Research Training Program Stipend scholarship (SC1999). P. Qian is supported by a National Health and Medical Research Council (NHMRC) and National Heart Foundation of Australia (NHF) co-funded postgraduate scholarship (NHMRC Scholarship No. 1114408, NHF Scholarship No. 101107).

Conflict of interest statement

P. Qian and M. Barry are inventors of a microwave catheter for renal artery denervation. The intellectual property is owned by the University of Sydney and Westmead Hospital, Australian Patent AU2015902225, issued 12-06-2015. The other authors have no conflicts of interest to declare.

References

1. Krum H, Schlaich M, Whitbourn R, Sobotka PA, Sadowski J, Bartus K, Kapelak B, Walton A, Sievert H, Thambar S, Abraham WT,

- Esler M. Catheter-based renal sympathetic denervation for resistant hypertension: a multicentre safety and proof-of-principle cohort study. *Lancet*. 2009;373:1275-81.
2. Symplicity HTN-2 Investigators, Esler M, Krum H, Sobotka PA, Schlaich MP, Schmieder RE, Böhm M. Renal sympathetic denervation in patients with treatment-resistant hypertension (The Symplicity HTN-2 Trial): a randomised controlled trial. *Lancet*. 2010;376:1903-9.
3. Bhatt DL, Kandzari DE, O'Neill WW, D'Agostino R, Flack JM, Katzen BT, Leon MB, Liu M, Mauri L, Negoita M, Cohen SA, Oparil S, Rocha-Singh K, Townsend RR, Bakris GL; SYMPLICITY HTN-3 Investigators. A controlled trial of renal denervation for resistant hypertension. *N Engl J Med*. 2014;370:1393-401.
4. DiBona GF. Physiology in perspective: The Wisdom of the Body. Neural control of the kidney. *Am J Physiol Regul Integr Comp Physiol*. 2005;289:R633-41.
5. Esler M, Jennings G, Lambert G. Noradrenaline release and the pathophysiology of primary human hypertension. *Am J Hypertens*. 1989;2:140S-146S.
6. Campese VM, Kogosov E, Koss M. Renal afferent denervation prevents the progression of renal disease in the renal ablation model of chronic renal failure in the rat. *Am J Kidney Dis*. 1995;26:861-5.
7. Katholi RE, Winternitz SR, Oparil S. Decrease in peripheral sympathetic nervous system activity following renal denervation or unclipping in the one-kidney one-clip Goldblatt hypertensive rat. *J Clin Invest*. 1982;69:55-62.
8. Esler M, Jennings G, Korner P, Blombery P, Sacharias N, Leonard P. Measurement of total and organ-specific norepinephrine kinetics in humans. *Am J Physiol*. 1984;247:E21-8.
9. Kandzari DE, Bhatt DL, Brar S, Devireddy CM, Esler M, Fahy M, Flack JM, Katzen BT, Lea J, Lee DP, Leon MB, Ma A, Massaro J, Mauri L, Oparil S, O'Neill WW, Patel MR, Rocha-Singh K, Sobotka PA, Svetkey L, Townsend RR, Bakris GL. Predictors of blood pressure response in the SYMPLICITY HTN-3 trial. *Eur Heart J*. 2015;36:219-27.
10. Chik WW, Barry MA, Thavapalachandran S, Midekin C, Pouliopoulos J, Lim TW, Sivagangabalan G, Thomas SP, Ross DL, McEwan AL, Kovoor P, Thiagalingam A. High spatial resolution thermal mapping of radiofrequency ablation lesions using a novel thermochromic liquid crystal myocardial phantom. *J Cardiovasc Electrophysiol*. 2013;24:1278-86.
11. Al Raisi SI, Pouliopoulos J, Barry MT, Swinnen J, Thiagalingam A, Thomas SP, Sivagangabalan G, Chow C, Chong J, Kizana E, Kovoor P. Evaluation of lesion and thermodynamic characteristics of Symplicity and EnligHTN renal denervation systems in a phantom renal artery model. *EuroIntervention*. 2014;10:277-84.
12. Cosman ER Jr, Cosman ER Sr. Electric and thermal field effects in tissue around radiofrequency electrodes. *Pain Med*. 2005;6:405-24.
13. Cosman ER Jr, Cosman ER Sr. Radiofrequency Lesions, in: Lozano AM, Gildenberg PL, Tasker RR, editors. Textbook of stereotactic and functional neurosurgery. 2nd ed. Berlin, Heidelberg, Germany: Springer Science & Business Media; 2009. p.1359-80.
14. Nath S, DiMarco JP, Haines DE. Basic aspects of radiofrequency catheter ablation. *J Cardiovasc Electrophysiol*. 1994;5:863-76.
15. Wittkampf FH, Nakagawa H. RF catheter ablation: Lessons on lesions. *Pacing Clin Electrophysiol*. 2006;29:1285-97.
16. Haines DE, Watson DD, Verow AF. Electrode radius predicts lesion radius during radiofrequency energy heating. Validation of a proposed thermodynamic model. *Circ Res*. 1990;67:124-9.
17. Otomo K, Yamanashi WS, Tondo C, Antz M, Bussey J, Pitha JV, Arruda M, Nakagawa H, Wittkampe F, Lazzara R, Jackman W. Why a large tip electrode makes a deeper radiofrequency lesion: effects of increase in electrode cooling and electrode-tissue interface area. *J Cardiovasc Electrophysiol*. 1998;9:47-54.
18. Kovoor P, Daly M, Campbell C, Dewsnap B, Eipper V, Uther J, Ross D. Intramural radiofrequency ablation: effects of electrode temperature and length. *Pacing Clin Electrophysiol*. 2004;27:719-25.
19. Langberg JJ, Gallagher M, Strickberger SA, Amirana O. Temperature-guided radiofrequency catheter ablation with very large distal electrodes. *Circulation*. 1993;88:245-9.
20. Haines DE. Determinants of Lesion Size During Radiofrequency Catheter Ablation: The Role of Electrode-Tissue Contact Pressure and Duration of Energy Delivery. *J Cardiovasc Electrophysiol*. 1991;2:509-15.
21. Bertog S, Fischel TA, Vega F, Ghazarossian V, Pathak A, Vaskelyte L, Kent D, Sievert H, Ladich E, Yahagi K, Virmani R. Randomised, blinded and controlled comparative study of chemical and radiofrequency-based renal denervation in a porcine model. *EuroIntervention*. 2017;12:e1898-906.
22. Sakakura K, Ladich E, Cheng Q, Otsuka F, Yahagi K, Fowler DR, Kolodgie FD, Virmani R, Joner M. Anatomic assessment of sympathetic peri-arterial renal nerves in man. *J Am Coll Cardiol*. 2014;64:635-43.
23. Tellez A, Rousselle S, Palmieri T, Rate WR 4th, Wicks J, Degrange A, Hyon CM, Gongora CA, Hart R, Grundy W, Kaluza GL, Granada JF. Renal artery nerve distribution and density in the porcine model: biologic implications for the development of radiofrequency ablation therapies. *Transl Res*. 2013;162:381-9.
24. Mahfoud F, Tunev S, Ewen S, Cremers B, Ruwart J, Schulz-Jander D, Linz D, Davies J, Kandzari DE, Whitbourn R, Böhm M, Melder RJ. Impact of Lesion Placement on Efficacy and Safety of Catheter-Based Radiofrequency Renal Denervation. *J Am Coll Cardiol*. 2015;66:1766-75.
25. Qian PC, Barry MA, Al Raisi S, Kovoor P, Pouliopoulos J, Nalliah CJ, Bhaskaran A, Chik W, Kurup R, James V, Verikatt W, McEwan A, Thiagalingam A, Thomas SP. Transcatheter non-contact microwave ablation may enable circumferential renal artery denervation while sparing the vessel intima and media. *EuroIntervention*. 2017;12:e1907-15.
26. Cosman ER Jr, Dolensky JR, Hoffman RA. Factors that affect radiofrequency heat lesion size. *Pain Med*. 2014;15:2020-36.


Chapter 5

The Clinical Efficacy of Two Different Radiofrequency Ablation Systems for Renal Artery Denervation

Al Raisi SI, Pouliopoulos J, Qian P, King P, Byth K, Barry MT, Swinnen J, Thiagalingam A, Koor P. Comparison of two different radiofrequency ablation systems for renal artery denervation: Evaluation of short-term and long-term follow up. *Catheterization and Cardiovascular Intervention*. Accepted for publication.

ORIGINAL STUDIES

Comparison of two different radiofrequency ablation systems for renal artery denervation: Evaluation of short-term and long-term follow up

Sara I. Al Raisi MB Bch, FRACP^{1,2} | Jim Pouliopoulos BSc, MSc, PhD^{1,2} |
 Pierre Qian MBBS, FRACP^{1,2} | Patricia King RN¹ | Karen Byth CStat RSS, PhD^{2,3} |
 Michael T. Barry BSc^{1,2} | John Swinnen MBBS, FRACS⁴ |
 Aravinda Thiagalingam MBBS, PhD^{1,2} | Pramesh Koor MBBS, PhD^{1,2} 

¹Department of Cardiology, Westmead Hospital, Sydney, New South Wales, Australia

²Sydney Medical School, University of Sydney, Sydney, New South Wales, Australia

³Research and Educational Network, Westmead Hospital, Sydney, New South Wales, Australia

⁴Department of Vascular Surgery, Westmead Hospital, Sydney, New South Wales, Australia

Correspondence

Pramesh Koor, Department of Cardiology, PO Box 533, Westmead Hospital, Cnr of Hawkesbury and Darcy Road, NSW 2145, Australia.

Email: pramesh.koor@sydney.edu.au

Funding information

National Health and Medical Research Council, Grant/Award Number: 1114408; National Heart Foundation of Australia, Grant/Award Number: 101107; Research Training Program Stipend scholarship, Grant/Award Number: SC1999

Abstract

Objectives: To assess the clinical efficacy of renal artery denervation (RAD) in our center and to compare the efficacy of two different radiofrequency (RF) systems.

Background: Several systems are available for RF renal denervation. Whether there is a difference in clinical efficacy among various systems remains unknown.

Methods: Renal artery denervation was performed on 43 patients with resistant hypertension using either the single electrode Symplicity Flex (n = 20) or the multi-electrode EnligHTN system (n = 23). Median post-procedural follow-up was 32.93 months. The primary outcome was post-procedural change in office blood pressure (BP) within 1 year (short-term follow-up). Secondary outcomes were change in office BP between 1 and 4 years (long-term follow-up) and the difference in office BP reduction between the two systems at each follow-up period.

Results: For the total cohort, mean baseline office BP (systolic/diastolic) was 174/94 mmHg. At follow-up, mean changes in office BP from baseline were -19.70/-11.86 mmHg ($P < 0.001$) and -21.90/-13.94 mmHg ($P < 0.001$) for short-term and long-term follow-up, respectively. The differences in office BP reduction between Symplicity and EnligHTN groups were 8.96/1.23 mmHg ($P = 0.42$ for systolic BP, $P = 0.83$ for diastolic BP) and 9.56/7.68 mmHg ($P = 0.14$ for systolic BP, $P = 0.07$ for diastolic BP) for short-term and long-term follow-up, respectively.

Conclusions: In our cohort, there was a clinically significant office BP reduction after RAD, which persisted up to 4 years. No significant difference in office BP reduction between the two systems was found.

KEYWORDS

catheter ablation, hypertension, renal artery intervention

1 | INTRODUCTION

The initial renal artery denervation (RAD) trials demonstrated significant blood pressure (BP) reduction, which persisted up to 3 years.¹⁻³ However, the randomized sham-controlled trial (Symplicity HTN-3) showed no significant difference in BP reduction between the RAD and the sham control arm.⁴ Inexperienced operators in RAD and lack

of bilateral circumferential denervation in most cases were possible reasons for insufficient denervation in Symplicity HTN-3.^{5,6} Since its first clinical application, RAD technology has evolved rapidly in consideration to different ablation modalities and energy delivery methods.⁷ Systems that utilize radiofrequency (RF) energy remain the most commonly used. Positive results were reported using both single electrode Symplicity Flex (Medtronic, Minneapolis, MN, USA) and

multi-electrode EnligHTN (Abbott, Chicago, IL, USA) RF systems.^{3,8-10} Nonetheless, studies on the clinical efficacy of single electrode versus multi-electrode systems have not been published. We previously compared the single electrode Symplicity Flex versus the multi-electrode EnligHTN in a gel based phantom renal artery model that allowed the spatiotemporal assessment of thermodynamics and lesion dimensions produced by each system.¹¹ In the gel model, Symplicity Flex produced larger lesions compared to EnligHTN. While the difference in lesion size was statistically significant, it was unclear if that difference would be clinically relevant. Moreover, it has been suggested that functional and anatomical reinnervation after RF renal denervation can occur and is likely to be complete by 11 months post procedure.¹² Therefore, we aimed to assess the efficacy of RAD in reducing office BP for a cohort of patients with refractory hypertension who underwent RAD using two RF systems (single electrode Symplicity Flex or multi-electrode EnligHTN system) within 1 year (short-term follow up), and to determine if BP reduction is persistent in the longer-term (between 1 and 4 years; long-term follow up) beyond the suggested time for reinnervation. We also aimed to compare office BP reduction between those two systems at each follow-up period.

2 | METHODS

We prospectively collected data for a total of 43 patients in whom RAD procedure was performed at our center between 2012 and 2015. Symplicity Flex was used in the first 20 consecutive patients, while EnligHTN was used in the subsequent 23 cases. Human Ethics Research Committee at Westmead Hospital approved the study and a written informed consent was obtained from all patients.

2.1 | Study population

Patients were referred for the procedure after an initial assessment by their treating cardiologist or nephrologist. Referral criteria included average baseline office systolic blood pressure (SBP) of ≥ 150 mmHg while on a minimum of three antihypertensive medications, or those with office SBP > 140 mmHg and intolerant to antihypertensive medications or had recurrent admissions with malignant hypertension. All patients reported compliance to their antihypertensive medications. They all had a CT renal angiogram prior to the procedure for anatomical assessment of their renal arteries and to exclude adrenal adenomas. Patients were excluded if they had significant bilateral renal artery stenosis, bilateral renal artery stenting or a small renal artery diameter (< 4 mm) bilaterally. Also, those with a secondary cause of hypertension were excluded.

Renal artery tortuosity index was calculated for each patient using the arc: chord ratio method, as described previously.¹³

2.2 | Renal artery denervation procedure

Renal artery denervation procedures were performed by an interventional cardiologist and a vascular surgeon, under conscious intravenous sedation using midazolam and fentanyl. Intra-arterial Heparin was administered in all cases at a dose of 50 units/kg. A 6 Fr

(Symplicity) or 8 Fr (EnligHTN) sheaths were introduced into the right femoral artery for access. Selective right and left renal arteriograms using a 6 Fr LIMA guiding catheter (Symplicity) or an 8 Fr EnligHTN guiding catheter (EnligHTN) were performed to assess vessel anatomy for denervation suitability. Prior to RF application, a 200 mcg bolus of glyceryl trinitrate was administered into each renal artery to prevent arterial spasm. Radiofrequency ablations in a spiral fashion were delivered into each renal artery wall starting distally and using the clinically recommended settings for both systems (Table 1). A final arteriogram was performed at the end of ablation to exclude complications including severe spasms, perforation, or dissection. The femoral arterial access site was closed with a ProGlide closure device if suitable. The following day, patients were reviewed for any adverse events or complications and discharged home if well. All patients were advised to continue the same antihypertensive medications, unless advised otherwise by their treating cardiologist or nephrologist.

2.3 | Follow-up

Data including office BP, antihypertensive medications, and adverse events including dizziness or postural hypotension, readmission with malignant hypertension, stroke or transient ischemic attack (TIA), cardiac events and all-cause mortality were collected through phone communication with patients or from clinic and medical record review. Each patient had multiple follow-ups to record BP measurements at different time-points. Office BP measurements were recorded by the treating doctors on follow-up. Mean office BP was determined during the short-term and long-term follow-up periods for each patient.

2.4 | Outcomes

The primary endpoint was overall change in office BP from baseline in the short-term follow-up. Secondary outcomes included; change in office BP in the long-term follow-up and the difference in office BP reduction between the Symplicity and the EnligHTN groups during the two follow-up periods. Secondary outcomes relating to safety included periprocedural complications and long-term adverse events (cardiac events, stroke or TIA, and death from any cause).

2.5 | Statistical analysis

Statistical analyses were performed in SPSS 24 (IBM Corp., Armonk, NY, USA) and S-PLUS 8.2 (TIBCO software Inc., Palo Alto, CA, USA)

TABLE 1 Summary of the clinical parameters for the Symplicity and EnligHTN renal denervation systems

System parameters	Symplicity	EnligHTN
Monitoring	Temperature and impedance based algorithm	Temperature controlled algorithm
Number of electrodes	1	4
Maximal power delivered (W)	8	6
Maximal temperature at electrode tip ($^{\circ}$ C)	70	75
Duration of each ablation (sec)	120	90

statistical software. Baseline characteristic for the two groups were compared using independent sample t-tests for continuous variables and Chi Square tests for categorical variables. Two-tailed tests with a significance level of 5% were used throughout. Data for baseline characteristics were expressed as the mean \pm standard deviation.

Linear mixed effect models were used to investigate the changes in SBP and diastolic blood pressure (DBP) post procedure during short-term and long-term follow-up periods, and to test for association (interaction) between the effect of time (three-level factor, pre-op baseline, short-term follow-up and long-term follow-up) and system (two-level factor). Linear mixed effect models were also used to test for association between the effect of time and each of the baseline or procedural covariates including baseline SBP, heart rate, body mass index (BMI), ablation time, ablation number, and tortuosity index. Patient identifier was considered as a random effect and the time factor as both a fixed effect and as a random effect with a general positive definite covariance structure. The procedural or baseline covariates and their two-way interactions with the time factor were considered as fixed effects. Parameter estimates (estimated mean) and their 95% confidence intervals (95% CI) were used to quantify the changes observed in both follow-up periods.

3 | RESULTS

3.1 | Study population

The study population baseline characteristics are summarized in Table 2. A total of 43 patients were followed up for a median of 32.93 months (IQR 29.43–42.87). For the total cohort, mean baseline office SBP was 174 ± 20 mmHg and mean baseline office DBP was 94 ± 16 mmHg. There was no significant difference in baseline office BP between the Symplicity and EnligHTN groups (Table 1). In both groups, patient enrolment rates were greater for males than females but not significantly different between groups ($P = 0.4$). Overall, there was no significant difference in baseline characteristics including risk factors between the two groups.

3.2 | Procedural parameters

Based on anatomical variation including vessel length and diameter, 4–12 RF ablations were delivered into each renal artery. Total ablation duration was similar between the two groups despite the longer duration per ablation with Symplicity system. This was due to the overall greater number of ablations in the EnligHTN group compared to Symplicity (Table 3). Four patients in total had unilateral denervation (one from the Symplicity group and three from the EnligHTN group). Reasons for unilateral denervation included difficult anatomy with failure to engage the vessel ($n = 1$), presence of previous renal artery stent unilaterally ($n = 1$), and a small renal artery diameter (≤ 3.5 mm) on one side ($n = 2$). Accessory renal arteries were present in five patients (one from the Symplicity group and four from the EnligHTN group). No ablation was performed in accessory renal arteries. Table 3 summarizes the procedural parameters for both groups.

TABLE 2 Summary of baseline characteristics for both Symplicity and EnligHTN groups

Baseline characteristics	Symplicity (n = 20)	EnligHTN (n = 23)	P-value
Age (years)	63.05 \pm 9.64	65.17 \pm 7.99	0.43
Gender-male (%)	13 (65%0.00)	13 (56.52%)	0.57
Baseline SBP (mmHg)	177.08 \pm 21.15	171.13 \pm 19.75	0.35
Baseline DBP (mmHg)	96.70 \pm 11.92	92.52 \pm 18.55	0.39
Number of BP medications at baseline	5.75 \pm 2.15	4.96 \pm 1.59	0.17
• BB	70.00%	60.90%	
• CCB	75.00%	69.50%	
• ACEi	50.00%	43.50	
• ARB	95.00%	73.90%	
• Thiazide	40.00%	52.20%	
• Loop diuretics	40.00%	13.00%	
• Vasodilators	35.00%	26.10%	
• Centrally	60.00%	56.50%	
• Aldosterone antagonist	20.00%	17.40.3%	
• Alpha blocker	45.00%	52.20%	
Hyperlipidemia (%)	8 (40.00%)	11 (47.83%)	0.61
Smoking (%)	5 (25.00%)	5 (21.74%)	0.80
OSA (%)	7 (35.00%)	9 (39.13%)	0.78
IHD (%)	6 (30.00%)	8 (34.78%)	0.74
Stroke or TIA (%)	4 (20.00%)	5 (21.74%)	0.89
BMI (kg/m ²)	34.15 \pm 8.64	32.65 \pm 7.37	0.54
eGFR (ml/min/1.73 m ²)	68.60 \pm 19.47	73.27 \pm 19.47	0.44

Abbreviations: ACEi, ACE inhibitor; ARB, angiotensin receptor blocker; BB, beta blocker; BMI, body mass index; BP, blood pressure; CCB, calcium channel blocker; DBP, diastolic blood pressure; eGFR, estimated glomerular filtration rate; IHD, ischemic heart disease; OSA, obstructive sleep apnea; SBP, systolic blood pressure; TIA, transient ischemic attack.

3.3 | Antihypertensive medications

The average number of antihypertensive medications for the total cohort at baseline was 5.33 ± 1.90 with no difference between the groups (Table 1). At follow-up, the average number of antihypertensive medications was 5.14 ± 2.05 (5.56 ± 2.31 versus 4.22 ± 0.83 for Symplicity and EnligHTN respectively, $P = 0.04$) and 4.56 ± 1.87 (4.80 ± 2.30 versus 4.33 ± 1.37 for Symplicity and EnligHTN, respectively, $P = 0.75$) for short-term and long-term follow-up, respectively (Figure 1A).

TABLE 3 Summary of procedural parameters for Symplicity and EnligHTN groups

Procedural parameters	Symplicity (n = 20)	EnligHTN (n = 23)	p-value
Total ablation time (min)	23.90 \pm 5.09	21.67 \pm 6.90	0.23
Number of ablations per patient	11.95 \pm 2.54	19.00 \pm 7.06	<0.001
Accessory renal artery (%)	1 (5%)	4 (17%)	0.21
Unilateral denervation (%)	1 (5%)	3 (13%)	0.37
Tortuosity index	0.30 \pm 0.07	0.30 \pm 0.09	0.91

In total, 33 patients (76.7%) had changes to their antihypertensive medications by their final follow-up. Half of the patients (53.6%) had a total decrease in medications number or dose, with or without class change, five patients (11.6%) had an increase in the number of antihypertensive medications, and five patients (11.6%) had a class change only.

3.4 | Outcomes

3.4.1 | Overall blood pressure reduction from baseline

For the entire study population, there was a significant reduction in both systolic and diastolic office BP within all follow-up periods (Figure 1B,C).

Mean change in office BP from baseline was $-19.70/-11.86$ mmHg (95% CI (SBP/DBP): $[-30.08, -9.34]/[-17.14, -6.58]$, $P < 0.001$ for SBP and DBP) and $-21.90/-13.94$ mmHg (95% CI: $[-28.38, -15.43]/[-17.14, -6.58]$, $P < 0.001$ for SBP and DBP) for short-term and long-term follow-up, respectively.

No association between the change in office SBP and baseline or procedural characteristics including heart rate, BMI, ablation duration, ablation number, and tortuosity index was found ($P = 0.33, 0.06, 0.17, 0.68,$ and 0.24 for association with each covariate, respectively). The only significant association was seen between baseline office SBP and the change in office SBP at 1 year ($P < 0.001$).

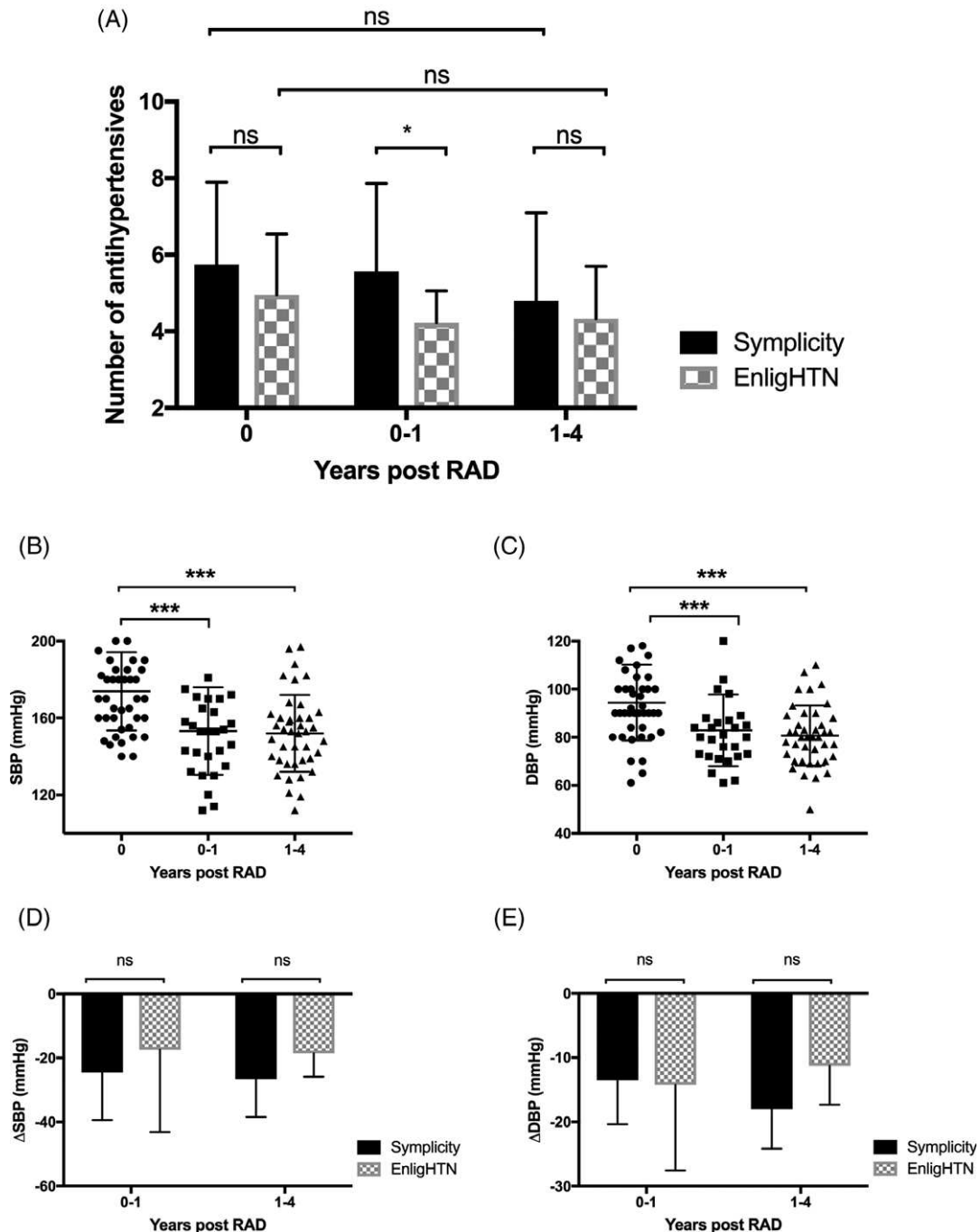


FIGURE 1 Number of antihypertensive medications per system at baseline and at each follow-up period (A). scatter plot of office BP at baseline and both follow-up time points for the total cohort of patients, (B) SBP and (C) DBP. Change in BP from baseline for Symplicity and EnligHTN groups at each follow-up time point, (D) SBP, (E) DBP

TABLE 4 Summary of periprocedural complications and adverse events for each group

Complications and adverse events	Symplicity	EnligHTN	Total	p-value
Femoral hematoma	1 (5%)	2 (8.70%)	3 (7%)	0.64
Contrast nephropathy	0	1 (4.35)	1 (2.33)	0.35
Length of stay (days)	1.05 ± 0.22	1.74 ± 1.68	1.40 ± 1.26	0.08
Postural hypotension	3 (15%)	5 (21.74%)	8 (18.60%)	0.57
Readmission with hypertension	2 (10%)	2 (8.70%)	4 (9.30%)	0.88
Cardiac events	3 (15%)	0	3 (7%)	0.05
Stroke or TIA	1 (5%)	0	1 (2.33%)	0.28
Mortality	0	2 (8.70%)	2 (4.65%)	0.17

Abbreviation: TIA, transient ischemic attack.

3.4.2 | Blood pressure reduction per system

There was no significant difference in post-procedural BP change between Symplicity and EnligHTN groups during any follow-up period (difference of $-8.96/-1.23$ mmHg, 95% CI (SBP/DBP): $[-30.86, 12.93]/[-12.61, 10.16]$, $P = 0.42$ for SBP, $P = 0.83$ for DBP, and $-9.56/-7.68$ mmHg, 95% CI: $[-22.39, 3.27]/[-15.89, 0.52]$, $P = 0.14$ for SBP, $P = 0.07$ for DBP), for short-term and long-term follow-up, respectively (Figure 1D,E).

However, both systems were effective in reducing office BP. For Symplicity group, mean change in office BP was $-24.48/-13.5$ mmHg (95% CI: $[-38.24, -10.71]/[-20.29, -6.63]$, $P < 0.001$ for SBP and DBP) and $-26.90/-17.92$ mmHg (95% CI: $[-36.14, -17.66]/[-23.85, -11.98]$, $P < 0.001$ for SBP and DBP) for short-term and long-term follow-up, respectively. With respect to the EnligHTN group, mean change in office SBP was not statistically significant during the short-term follow-up (-15.51 mmHg, 95% CI: $[-32.53, 1.50]$, $P = 0.07$). However, the change in office SBP became significant at the long-term follow-up (-17.34 mmHg, 95% CI: $[-26.23, -8.45]$, $P < 0.001$). Mean change in office DBP was -12.23 mmHg (95% CI: $[-15.90, -4.56]$, $P < 0.001$) and -10.23 mmHg (95% CI: $[-21.34, -3.12]$, $P = 0.01$) for short-term and long-term follow-up, respectively.

3.4.3 | Safety outcomes

All RAD procedures were performed safely with no major procedural complications. Minor complications included femoral hematoma managed conservatively in three patients (7%) and transient contrast nephropathy in a single patient who had mild renal impairment at baseline. Eight patients reported symptoms of postural hypotension on follow-up, and four patients had readmissions with hypertensive episodes. There was one case of recurrent stroke at 9 months and 45 months. Three patients had hospital admission for myocardial infarction and there were two mortalities of unknown cause. Table 4 summarizes procedural complications and adverse events for both groups.

4 | DISCUSSION

In this study, RAD resulted in a significant BP reduction within the first year, which persisted up to 4 years post procedure in our total cohort of patients who underwent the procedure using two different RF systems. When assessing each treatment group independently, mean

reduction in office SBP from baseline was significant at all follow-up periods for the Symplicity group. While mean reduction in office SBP for the EnligHTN group did not achieve significance within the short-term follow-up. A delayed effect on SBP occurred over the long-term follow-up. This could be due to increased lesion depth achieved with Symplicity Flex (3.8 mm) compared to EnligHTN (3.4 mm) as demonstrated in our previous work using the phantom model, given that both systems were tested under identical conditions including vessel diameter, flow rate and with optimal electrode contact.¹¹ Nonetheless, there was no significant difference in office systolic or diastolic BP reduction between the Symplicity and the EnligHTN group at any follow-up period. The lack of significant between-group differences in BP reduction may suggest a class effect of various RAD devices, whereby adequate injury to efferent and afferent nerve fibers was attained by both systems. Alternatively, it could be explained by the small number of patients in this study. Therefore, a larger study may be required in order to detect significant differences between the two systems.

Notably, the reduction in BP was not associated with an increase in the number of antihypertensive medications (Figure 1A). In fact, half of the total cohort had a reduction to the number or the dose of their antihypertensive medications. Thus, the BP reduction is unlikely to be related to medications.

The Symplicity HTN-3 trial also used Symplicity Flex;⁴ however, inadequate operator training and lack of experience in performing RAD had resulted in a high failure rate for achieving bilateral circumferential ablation (74% of cases).⁶ Therefore, it is likely that denervation in these cases was unsuccessful. While the Symplicity Flex may deliver greater heat energy penetration, catheter manipulation to achieve adequate contact and a circumferential ablation pattern is technically challenging, and thus requires rigorous training and greater operator experience compared to multi-electrode based systems. The primary proceduralist in our study had extensive experience in RF ablation and catheter manipulation.

Furthermore, it is still unclear what extent of denervation is required to result in a desired clinical response. In a subset of patients ($n = 10$) who underwent assessment of noradrenaline spillover (marker for efferent sympathetic nerve activity) in the Symplicity HTN-1 trial, there was a 47% reduction in noradrenaline spillover at 15–30 days post RAD, confirming the mechanistic effect of ablation on suppression of sympathetic activity. Mean reduction in office BP at 6 months in this subgroup was 22/12 mmHg,¹ suggesting that ablation to achieve a target noradrenaline spillover of about 50% could be

an adequate endpoint of long-term functional denervation. A post-mortem study demonstrated that for nerve fibers found within 10 mm depth from the renal artery intima, between 50% and 75% of fibers occurred at a depth between 2.44 and 4.28 mm in the main vessel.¹⁴ Therefore, both systems could cause injury to >50% but ≤75% of nerves providing that ablation is performed optimally by ensuring consistent electrode contact and energy delivery in a circumferential pattern along the artery wall.

The newer multi-electrode Symplicity Spyral is likely to offer a greater ablation consistency. However, it was found to have less heating depth than Symplicity Flex.^{15,16} Therefore, injury to 50% of nerve fibers may not be achievable when ablation is performed in the main vessel using Symplicity Spyral. Hence, RF ablation distal to the bifurcation in addition to the main vessel is now recommended when utilizing Symplicity Spyral, as nerve fibers are located closer to the intima in the branches compared to the main vessel.^{14,16}

Patient selection is another important factor that influences the clinical efficacy of RAD. In our study, the only factor that was associated with BP response within 1 year was office SBP at baseline. Nonetheless, it has become evident that patients with combined systolic and diastolic hypertension (SBP > 140 mmHg and DBP > 90 mmHg) respond better to RAD compared to those with isolated systolic hypertension (ISH).^{17,18} This is likely owing to the coexistence of arterial stiffness in patients with ISH. Increased arterial stiffness as measured by invasive pulse wave velocity was found to be a negative predictor of denervation response.¹⁹ Nonetheless, when stratifying patients with ISH according to their pulse wave velocity tertiles, those in the low tertile were found to have significant BP reduction after RAD, which was comparable to those with combined systolic and diastolic hypertension.²⁰ Therefore, arterial stiffness is likely to play a significant role in confounding the outcomes of RAD in this subgroup of patients, because the mechanism of hypertension may be complicated by the influence of structurally mediated vascular dysfunction, rather than, or in combination with vascular dysfunction mediated by sympathetic overstimulation. Therefore, not all those with ISH should be excluded from RAD.

Finally, as reported in major clinical trials our study illustrates that RAD remains a safe procedure with low periprocedural complication rates.

5 | LIMITATION

There are several limitations to our study. First, this was a non-randomized comparison of a small patient cohort from a single center without a sham control arm. However, the two groups were matched in all baseline characteristics. In addition, the sham effect was absent in recently published sham-controlled trials including the SPYRAL HTN and RADIANCE-HTN SOLO.²¹⁻²³ Second, no assessment of ambulatory BP at baseline and at follow-ups was carried out, which could lead to inclusion of patients with pseudoresistance and white-coat syndrome. Furthermore, all Symplicity procedures were performed first, followed by EnligHTN procedures consecutively. This could lead to bias, favoring the EnligHTN system, as the proceduralist was more experienced by that stage. Nonetheless, the primary

operator is an experienced interventionalist and electrophysiologist who is very familiar with RF ablation.

Moreover, longer follow-up period was available for Symplicity patients compared to EnligHTN. However, no difference in BP reduction was found between the two systems even when analysis was limited to 1 year. Finally, medication reduction during the study period could potentially mask treatment effect. Therefore, it is difficult to demonstrate superiority of one system over the other; however, this study demonstrates non-inferiority.

6 | CONCLUSION

Although the two RAD systems did not differ significantly, they have shown an overall reduction in office BP between selected timelines compared to baseline measurements. Our study further supports the role of RAD in treating appropriate patients with resistant hypertension.

ACKNOWLEDGMENTS

We thank Medtronic and St. Jude Medical for their cooperation with technical data collection during the procedures.

CONFLICT OF INTEREST

P. Qian and M Barry are inventors of a microwave catheter for renal artery denervation. The intellectual property is owned by the University of Sydney and Westmead Hospital. Australian Patent AU2015902225 issued December 6, 2015. J Swinnen received an unconditional grant from Medtronic for a drug eluting balloon study in restenosis of the native hemodialysis access fistula (2014–2017). The other authors have no conflict of interests.

ORCID

Pramesh Kovoov  <https://orcid.org/0000-0003-2455-5046>

REFERENCES

1. Krum H, Schlaich M, Whitbourn R, et al. Catheter-based renal sympathetic denervation for resistant hypertension: A multicentre safety and proof-of-principle cohort study. *Lancet*. 2009;373:1275-1281.
2. Esler M, Krum H, Sobotka PA, et al. Renal sympathetic denervation in patients with treatment-resistant hypertension (the Symplicity HTN-2 trial): A randomised controlled trial. *Lancet*. 2010;376:1903-1909.
3. Krum H, Schlaich MP, Sobotka PA, et al. Percutaneous renal denervation in patients with treatment-resistant hypertension: Final 3-year report of the Symplicity HTN-1 study. *Lancet*. 2014;383:622-629.
4. Bhatt DL, Kandzari DE, O'Neill WW, et al. A controlled trial of renal denervation for resistant hypertension. *N Engl J Med*. 2014;370:1393-1401.
5. Kandzari DE, Bhatt DL, Brar S, et al. Predictors of blood pressure response in the SYMPPLICITY HTN-3 trial. *Eur Heart J*. 2015;36:219-227.
6. Esler M. Illusions of truths in the Symplicity HTN-3 trial: Generic design strengths but neuroscience failings. *J Am Soc Hypertens*. 2014;8:593-598.
7. Bunte MC, Infante de Oliveira E, Shishehbor MH. Endovascular treatment of resistant and uncontrolled hypertension: Therapies on the horizon. *JACC Cardiovasc Interv*. 2013;6:1-90.

8. Esler MD, Krum H, Schlaich M, et al. Renal sympathetic denervation for treatment of drug-resistant hypertension: One-year results from the Symplicity HTN-2 randomized, controlled trial. *Circulation*. 2012;126:2976-2982.
9. Worthley SG, Tsioufis CP, Worthley MI, et al. Safety and efficacy of a multi-electrode renal sympathetic denervation system in resistant hypertension: The EnligHTN I trial. *Eur Heart J*. 2013;34:2132-2140.
10. Tsioufis CP, Papademetriou V, Dimitriadis KS, et al. Catheter-based renal denervation for resistant hypertension: Twenty-four month results of the EnligHTN I first-in-human study using a multi-electrode ablation system. *Int J Cardiol*. 2015;201:345-350.
11. Al Raisi SI, Pouliopoulos BMT, Swinnen J, et al. Evaluation of lesion and thermodynamic characteristics of Symplicity and EnligHTN renal denervation systems in a phantom renal artery model. *EuroIntervention*. 2014;10:277-284.
12. Booth LC, Nishi EE, Yao ST, et al. Reinnervation of renal afferent and efferent nerves at 5.5 and 11 months after catheter-based radiofrequency renal denervation in sheep. *Hypertension*. 2015;65(2):393-400.
13. Zaman S, Pouliopoulos J, Al Raisi S, et al. Novel use of NavX three-dimensional mapping to guide renal artery denervation. *EuroIntervention*. 2013;9:687-693.
14. Sakakura K, Ladich E, Cheng Q, et al. Anatomic assessment of sympathetic peri-arterial renal nerves in man. *J Am Coll Cardiol*. 2014;64:635-643.
15. Al Raisi SI, Barry MT, Qian P, Bhaskaran A, Pouliopoulos J, Kovoov P. Comparison of new generation renal artery denervation systems: Assessing lesion size and thermodynamics using a thermochromic liquid crystal phantom model. *EuroIntervention*. 2017;13:1242-1247.
16. Mahfoud F, Pipenhagen CA, Boyce Moon L, et al. Comparison of branch and distally focused main renal artery denervation using two different radio-frequency systems in a porcine model. *Int J Cardiol*. 2017;241:373-378.
17. Ewen S, Ukena C, Linz D, et al. Reduced effect of percutaneous renal denervation on blood pressure in patients with isolated systolic hypertension. *Hypertension*. 2014;65:193-199.
18. Mahfoud F, Bakris G, Bhatt DL, et al. Reduced blood pressure-lowering effect of catheter-based renal denervation in patients with isolated systolic hypertension: Data from SYMPPLICITY HTN-3 and the global SYMPPLICITY registry. *Eur Heart J*. 2017;38:93-100.
19. Okon T, Röhnert K, Stiermaier T, et al. Invasive aortic pulse wave velocity as a marker for arterial stiffness predicts outcome of renal sympathetic denervation. *EuroIntervention*. 2016;12:e684-e692.
20. Fengler K, Rommel KP, Hoellriegel R, et al. Pulse wave velocity predicts response to renal denervation in isolated systolic hypertension. *J Am Heart Assoc*. 2017;6. <https://doi.org/10.1161/JAHA.117.005879>.
21. Townsend RR, Mahfoud F, Kandzari DE, et al. Catheter-based renal denervation in patients with uncontrolled hypertension in the absence of antihypertensive medications (SPYRAL HTN-OFF MED): A randomised, sham-controlled, proof-of-concept trial. *Lancet*. 2017;390:2160-2170.
22. Kandzari DE, Bohm M, Mahfoud F, et al. Effect of renal denervation on blood pressure in the presence of antihypertensive drugs: 6-month efficacy and safety results from the SPYRAL HTN-ON MED proof-of-concept randomised trial. *Lancet*. 2018;391:2346-2355.
23. Azizi M, Schmieder RE, Mahfoud F, et al. Endovascular ultrasound renal denervation to treat hypertension (RADIANCE-HTN SOLO): A multicentre, international, single-blind, randomised, sham-controlled trial. *Lancet*. 2018;391:2335-2345.

How to cite this article: Al Raisi SI, Pouliopoulos J, Qian P, et al. Comparison of two different radiofrequency ablation systems for renal artery denervation: Evaluation of short-term and long-term follow up. *Catheter Cardiovasc Interv*. 2018;1-7. <https://doi.org/10.1002/ccd.28038>

Chapter 6

Assessment of Renal Artery Branch Denervation Using A Phantom Model

Al Raisi SI, Pouliopoulos J, Barry MT, Qian P, Thiagalingam A, Swinnen J, Koor P. Renal artery branch denervation: Evaluation of lesion characteristics using a thermochromic liquid crystal phantom model. *Heart, Lung and Circulation*. Under review.

Renal artery branch denervation: Evaluation of lesion characteristics using a thermochromic liquid crystal phantom model

Authors: Sara I. Al Raisi ^{a,b}, MB Bch, FRACP; Jim Pouliopoulos ^{a,b}, PhD; Michael T. Barry ^{a,b}, B.Sc; Pierre Qian ^{a,b}, MBBS, FRACP; Aravinda Thiagalingam ^{a,b}, MBBS, PhD; John Swinnen ^c, MBBS; Pramesh Kovoor ^{a,b*}, MBBS, PhD

^a Department of Cardiology, Westmead Hospital, Sydney, NSW, Australia

^b University of Sydney, NSW, Australia

^c Department of Vascular Surgery, Westmead Hospital, Sydney, NSW, Australia

Shot Title: Branch renal artery denervation in a phantom model

***Correspondence and Reprints Requests:** **Word count:** 3638

A/Professor Pramesh Kovoor

Senior Cardiology Staff Specialist

PO Box 533, Westmead Hospital, Cnr of Hawkesbury and Darcy Road

NSW, 2145, Australia

Phone: (+612) 8890 6030, Fax: (+612) 8890 8323

E-mail: pramesh.kovoor@sydney.edu.au

Declarations of interest

P. Qian and M T Barry are inventors of a microwave catheter for renal artery denervation. The intellectual property is owned by the University of Sydney and Westmead Hospital. Australian Patent AU2015902225 issued 12-06-2015. J Swinnen received an unconditional grant from Medtronic for a drug eluting balloon study in restenosis of the native hemodialysis access fistula (2014-2017). The other authors have no conflict of interests to declare.

Abstract

Background: Lately, combined main vessel and branch ablation has been recommended during radiofrequency (RF) renal artery denervation. Utilising a validated renal artery phantom model, we aimed (1) to determine thermal injury extent (lesion depth, width and circumferential coverage) and electrode-tissue interface temperature for branch renal artery ablation, and (2) to compare the extent of thermal injury for branch versus main vessel ablation using the same RF System.

Methods: We employed a gel based renal artery phantom model simulating variable vessel diameter and flow, which incorporated a temperature sensitive thermochromic-liquid-crystal (TLC) film for assessing RF ablation thermodynamics. Ablations in a branch renal artery model (n= 32) were performed using Symplicity Spyral. Lesion dimensions defined by the 51°C isotherm, circumferential injury coverage, and electrode-tissue interface temperature were measured for all ablations at 60 secs.

Results: Lesion dimensions were 2.13 ± 0.13 mm and 4.13 ± 0.18 mm for depth and width, respectively, involving 23% of the vessel circumference. Maximum electrode-tissue interface temperature was $68.31\pm 2.29^\circ\text{C}$. No significant difference in lesion depth between branch and main vessel ablations was found ($\Delta = 0.02$ mm, $p = 0.60$). However, lesions were wider in the branch ($\Delta = 0.49$ mm, $p < 0.001$) with a larger circumferential coverage compared to main vessel (arc angle of $82.02\pm 3.27^\circ$ versus $54.90\pm 4.36^\circ$, respectively).

Conclusions: In the phantom model, branch ablations were of similar depth but had larger width and circumferential coverage compared to main vessel ablations. Concerning safety, no overheating at the electrode-tissue interface was observed.

Keywords: Hypertension, renal denervation, radiofrequency ablation

Introduction

Traditionally, the delivery of radiofrequency (RF) ablation during renal artery denervation (RAD) had been limited to the main vessel only (between the ostium and the bifurcation) with no involvement of the branches [1-3]. This conventional method has been proven to be safe in all major clinical trials; however, the efficacy was found to be inconsistent [1-3]. Therefore, exploration of new procedural methods and techniques became essential in order to improve clinical outcomes. Moreover, a single method may not be suitable across all technologies and designs for RAD devices. As a result, recent work had demonstrated that RF ablation in renal artery branches and perhaps the accessory arteries combined with main vessel ablation could be more efficacious than ablation in the main vessel only [4, 5]. Biochemically, combined main vessel and branch ablation resulted in a greater reduction in norepinephrine concentration in the kidney compared to main vessel ablation alone in an animal model [4, 6]. In addition, ablation in the branches only resulted in a larger reduction in kidney norepinephrine concentration compared to main vessel ablation (83% versus 71%, respectively). This was accompanied with a reduction in cortical axonal density of 77% and 64%, respectively [4]. Clinically, better blood pressure response three months post RAD was observed with the combined method using the multi-electrode Symplicity Spyral System (Medtronic, Minneapolis, MN, USA) [5]. This approach has been supported by the finding of closer proximity of nerve fibres to the renal artery intima in distal segments and beyond the bifurcation compared to proximal segments [7]. Whilst early studies in this contemporary method are promising, it's important to recognise that physiological differences between the main vessel and the branches may impact RF lesion formation as well as raise some safety concerns.

We previously explored the biophysical properties of RF ablation using different RAD systems in a gel based phantom model of the main renal artery, involving thermochromic-liquid-crystal (TLC) based thermography [8, 9]. In this study, we aimed to evaluate the thermal properties of RF ablation using the Symplicity Spyril system in a phantom model of a renal artery branch and determine the extent of thermal injury produced, defined by lesion depth, lesion width and circumferential coverage. We also aimed to assess the maximum temperature at the electrode-tissue interface (modelled based on the electrode-TLC interface) for branch ablations. In addition, we compared lesion dimensions and the circumferential coverage of ablations in the branch to ablations performed previously in a main vessel model.

Material and Methods

Multi-electrode Symplicity Spyril RAD system was used to perform RF ablations on a gel based model of a renal artery branch (vessel diameter of 3 mm and flow rate of 100 ml/min). Details of the gel formulation and description of the experimental apparatus has been previously described [8, 10]. Clinically recommended ablation parameters were used (maximum power of 6.5 W and ablation duration of 60 secs). Lesion dimensions (depth and width) were measured for all RF ablations at 20 secs, 30 secs, 40 secs, 50 secs and at 60 secs, to assess the temporal lesion growth and to determine the size of complete lesions. The dimensions obtained were then used to calculate the circumferential coverage (arc angle) for a single RF ablation lesion. Additionally, maximum TLC temperature at the end of RF ablations were measured. Lesion dimensions and the circumferential coverage for branch ablations were compared with RF ablations previously performed in a main vessel phantom model (5 mm vessel diameter, flow rate of 500 ml/min, n= 16) using Symplicity Spyril.

Angiographic analysis of renal artery branches

To determine the arterial branch diameter required for the phantom model, a total of ten selective renal arteriograms from a cohort of patients who underwent RAD in our centre were analysed. Diameter of the main vessel, first order and second order branches were measured (Figure 1). The guiding catheter was used to calibrate the measured distances. Vessel diameters were 6.1 ± 0.6 mm, 4.4 ± 0.5 mm and 2.8 ± 0.3 mm for main vessel (site A), first order (site B) and second order branches (site C), respectively. Therefore, all gel models of the renal artery branch anatomy were formed with a 3 mm vessel diameter (minimum diameter required for Symplicity Spyril system).

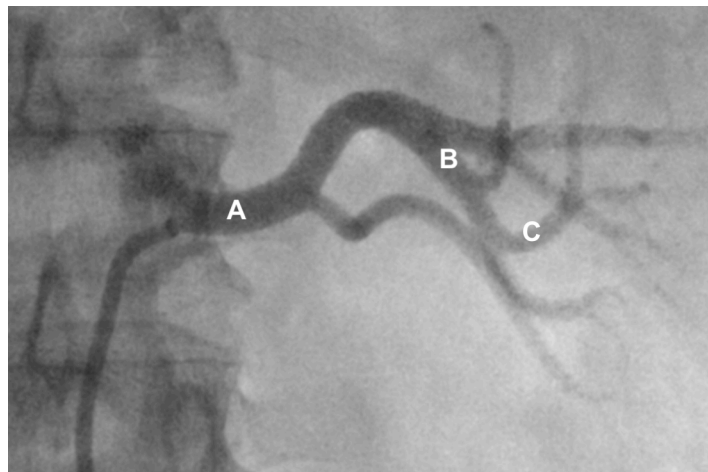


Figure 1. An arteriogram of a left renal artery demonstrating branching pattern. (A) Main vessel, (B) first order branch, (C) second order branch.

Thermochromic liquid crystal phantom model of the renal artery branch

A previously described renal artery phantom model [8] was modified to simulate the biophysical characteristics of renal artery branch. Briefly, a mixture of saline and agar substitute gel (Phytigel; Merck, St. Louis, MO, USA) was placed in a cast that contained a 3 mm cylindrical former, which was removed after gel solidification

creating phantom vessel lumen. Prior to pouring the gel, a TLC film (LCR Hallcrest LLC, Glenview, IL, USA) was centred in the cast, held vertically by the former. The TLC film has dual temperature sensitivity range (between 50-77°C and 80-103°C); thus, it changed colour accordingly during RF application creating a colour gradient (Figure 2). The gel was placed in a tank that constantly pumps normal saline around it and into the vessel lumen. We estimated the flow rate in the branch at 100 ml/min assuming main vessel flow rate of 500 ml/min, as human renal arteries often bifurcate into two divisions, which give rise to five segmental branches [11]. The tank temperature was regulated at physiological body temperature (37°C).

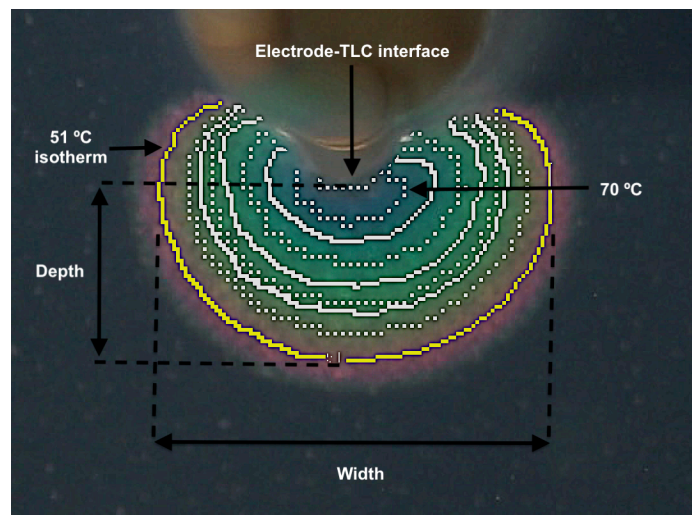


Figure 2. Colour gradient on TLC during application of RF energy (at 60secs) with superimposed temperature isotherms. The isotherm of interest (51°C) highlighted in yellow. The isotherm at the electrode-TLC interface corresponds to 70°C.

Radiofrequency ablation in the phantom model

The Symplicity Spyril catheter was introduced into the vessel lumen over a 0.014" guide wire under direct visualisation. The wire was then retracted to allow spiral configuration of the catheter. For all ablations, a single electrode was positioned in contact and on plane with the TLC film. Adequate electrode-TLC contact was visually

confirmed. Radiofrequency ablation was then commenced and continued for a duration of 60 secs. In case of a generator error, the catheter was repositioned to optimise contact with gel/TLC surface. Photographs of the TLC film were acquired (at baseline and every 10 secs during ablation) using a digital camera (Canon EOS 5D Mark II; Canon Inc., Tokyo Japan) and a flash light (Canon Speedlite 580EX; Canon) placed in front of the model.

Analysis of radiofrequency ablation lesions

Photographs of colour gradient produced on the TLC film during RF application were analysed using an in-house built software (i-Chrome Pro 1.5.19, Westmead Hospital, Australia). The software enabled the identification of a predetermined temperature isotherm for each lesion and automatically highlighted the preconfigured isotherm of interest (Figure 2). We used the 51°C isotherm to outline lesion margins as neural thermal injury occurs at temperature > 45-50°C [12, 13]. Lesion depth was defined as the length of a perpendicular line from the electrode tip to the maximum depth of the 51°C isotherm and the width was defined as the maximum width of the 51°C isotherm borders that is perpendicular to the depth line.

The circumferential coverage of RF thermal injury per energy application was calculated as follows (Figure 3):

Arc angle for each RF application = $2 \times \Theta$, where

$$\Theta = \tan^{-1} \left(\frac{\frac{1}{2} \times w}{r+l} \right),$$

w= mean lesion width, r=mean vessel radius and l= mean depth at maximum lesion width.

The circumferential coverage of each RF lesion (%) = $\left(\frac{\text{arc angle}}{360} \right) \times 100$

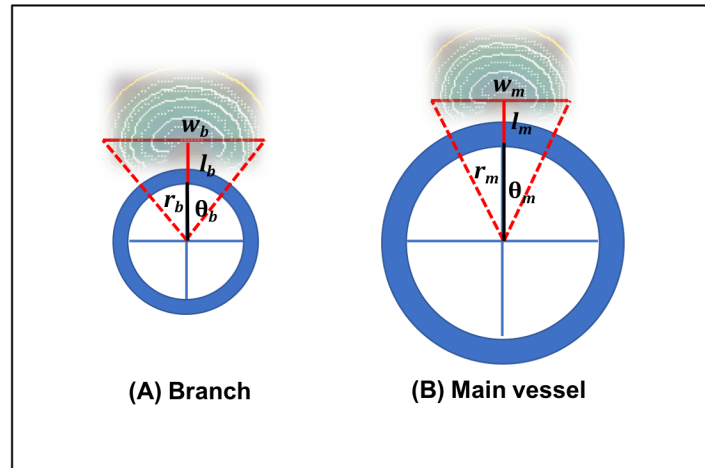


Figure 3. Illustration of circumferential coverage of thermal injury for branch and main vessel ablation. w_b ; lesion maximum width for branch, w_m ; lesion maximum width for main vessel, r_b ; branch radius, r_m ; main vessel radius, l_b ; depth where maximum width occurred for branch, l_m ; depth where maximum width occurred for main vessel, θ_b ; branch arc angle, θ_m ; main vessel arc angle.

Additionally, the temperature of the isotherm at the electrode-TLC interface was determined for all RF lesions at 60 secs using i-Chrome software (Figure 2).

Statistical analysis

GraphPad Prism (GraphPad Software, Inc., La Jolla, CA, United States) statistical analysis software was used to analyse the data. When similar model was used previously, six ablations in total (three in each group) was required to observe a significant difference in lesion depth and width between two groups with a power of 95% and a level of significance (α) of 0.05 [8]. An independent sample student t-test was used to compare mean lesion depth, lesion width, maximum electrode- TLC interface temperature and circumferential lesion coverage of RF lesions between branch versus main vessel RF lesions. Data was expressed as mean \pm standard deviation (mean \pm SD).

Results

A total of 32 RF ablations were performed on four blocks of gel, to avoid gel damage caused by overheating. A summary of RF ablation parameters is included in Table 1.

Table 1. Radiofrequency ablation parameters for branch and main vessel ablations

Group	Baseline impedance (Ω)	Impedance drop (%)	Maximum power (W)	Electrode tip Temperature ($^{\circ}\text{C}$)
branch (n= 32)	219.89 \pm 0.53	2.66 \pm 0.75	6.5	55.01 \pm 2.73
Main vessel (n= 16)	174.25 \pm 3.53	2.38 \pm 0.72	6.5	45.56 \pm 2.63
<i>p</i> -value	<0.001	0.23	-	<0.001

Lesion analysis for branch ablation

In the branch, mean lesion dimensions were 2.13 \pm 0.13 mm and 4.13 \pm 0.18 mm for depth and width, respectively, at 60 secs. At the depth where maximum lesion width occurred (Figure 3), lesion circumferential coverage (arc angle) per ablation was 82.02 \pm 3.27 $^{\circ}$. The maximum temperature at the electrode-TLC interface at 60 secs was > 10 $^{\circ}\text{C}$ higher than the maximum electrode tip temperature recorder by the generator (68.31 \pm 2.29 $^{\circ}\text{C}$

versus $55.01 \pm 2.73^\circ\text{C}$ for electrode-TLC interface and electrode tip temperature, respectively).

Comparison of branch versus main vessel ablation

There was no significant difference in lesion depth between ablations performed in the branch phantom model and those performed in the main vessel phantom model (mean difference of 0.02 mm, $p=0.60$). However, lesion width was larger for branch ablation compared to main vessel (mean difference of 0.49 mm, $p<0.001$), as shown in Figure 4A and 4B.

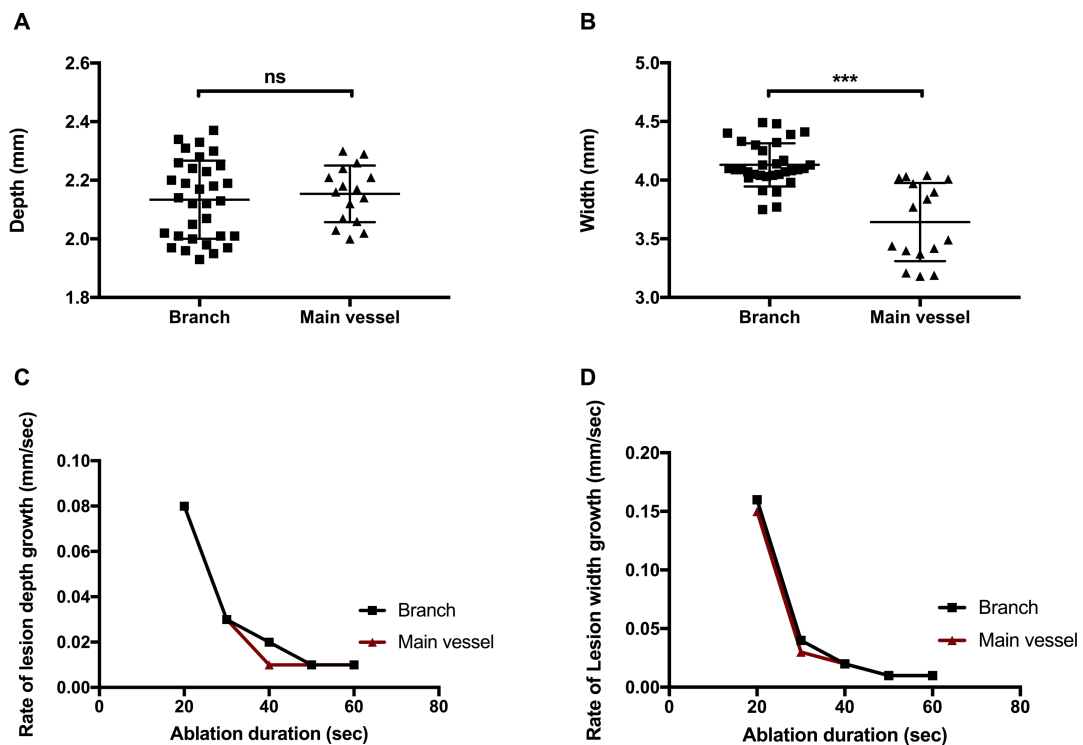


Figure 4. Scatter plot of lesion depth (A) and width (B) for branch and main vessel ablations. Lesion depth growth rate for branch and main vessel ablation (C), lesion width growth rate for branch and main vessel (D).

Lesion growth rate was the fastest in the first 20 secs of RF application for both branch and main vessel ablation. Thereafter, the growth rate significantly decreased until it reached a steady state at about 40-50 secs (Figure 4C and 4D). For a single RF application, the circumferential coverage of thermal injury based on the 51°C isotherm was larger for branch compared to main vessel ablation (arc angle of $82.02 \pm 3.27^\circ$ versus $54.90 \pm 4.36^\circ$, respectively) covering 23% versus 15% of the arterial wall circumference ($p < 0.001$).

Discussion

In the present study, RF ablation performed in a TLC model of renal artery branch produced lesions of similar depth to ablation performed in a TLC model of the main vessel using the same RF system. However, in the branch, lesions were larger in width compared to main vessel lesions. No overheating of the electrode-tissue interface occurred in branch ablation (max temperature of 68°C). Furthermore, a larger circumferential coverage of injury was achieved with RF ablation in the main vessel.

Amongst various factors, lesion size is a key determinant of procedural success in renal artery denervation. In the main vessel, the depth of thermal injury for different RF systems was reported to be between 3-6 mm in animal studies [14-16]. Variations in device choice and timing of histological assessment between the studies could account for this variability. Nonetheless, most of these devices are currently unavailable. We previously assessed RF ablation lesion size in a TLC phantom model of the main vessel using the Symplicity Spyral system, and found lesion depth to be 2.15 mm. Given the anatomical distribution of renal nerves, injury of this depth may be insufficient for effective denervation if ablations are confined to the main vessel [7, 9]. In the branch, lower blood flow rate is likely to reduce convective heat loss into the blood pool, increase power density at the electrode-tissue interface, and subsequently increase tissue heating and lesion size [17]. However, in the phantom model, we found no difference in lesion depth between ablations produced in the branch versus the main vessel. Of note, a study in a swine model reported comparable lesion depth (2 mm) for ablations performed in renal artery branches using Symplicity Spyral [14]. In contrast to the main vessel, this depth of thermal injury in the branches would result in more nerves being destroyed as distal to the bifurcation, 79% of nerve fibres were found to be located within 2 mm from the intima [7].

Regarding safety, a reduction in convective cooling in the branch, could lead to excessive heating at the electrode-tissue interface [17, 18]. Generator feedback mechanism would result in decreased power output if high electrode tip temperature is detected, thus preventing extreme heating. However, maximum electrode tip temperature does not reflect the true maximum tissue temperature. The discrepancy between the electrode tip and tissue temperature had been described in previous studies on RF myocardial ablation [19]. The TLC phantom model used in our study has the advantage of enabling rapid assessment of maximum temperature at the electrode-TLC interface as well as deeper within the lesion. In our study, we found a difference of 13°C between maximum electrode tip temperature and maximum TLC temperature. Nonetheless, maximum TLC temperature did not reach the threshold for dense microbubble, pop and coagulum formation (90-100°C) [17, 20]. Safety assessment during a study of combined main vessel and branch ablation in a swine model found no vessel wall injury or thrombosis with complete re-endothelialisation occurring at 28 days in the treated vessels [4]. Moreover, in a clinical study, evaluation with MR angiography and renal artery duplex sonography at three months showed no procedural related renal artery stenosis. In addition, no effect on kidney function test was observed [5].

Whilst lesion depth was similar in branch and main vessel ablation, RF ablation in the branch would result in a greater circumferential coverage of thermal injury due to a larger lesion width and a smaller vessel diameter (Figure 3). One set of ablations (four electrodes) using the Symplicity Spyril catheter would cover 91% of the arterial wall circumference of the branch versus 61% of the main vessel, assuming energy is delivered to four different vessel wall quadrants. Thus, a reduced number of ablations would be required in the branch to result in a complete circumferential denervation

compared to the main vessel. Nonetheless, energy application should ideally involve all branches to achieve complete denervation. Though, it is unknown if extensive ablation and larger circumferential injury would result in long-term complications.

Study limitation

Our study has several limitations. Firstly, the homogenous nature of the TLC phantom model does not account for the various components of the perinephric tissue. Therefore, the pattern of heat distribution may be more irregular than what is produced in the phantom model. In addition, the effect of acute physiological response to catheter manipulation and vessel wall injury can't be assessed in the phantom model (i.e. vessel spasms, change in flow, etc.). Nonetheless, the effect of different factors on ablation thermodynamics and lesion formation could be assessed under controlled conditions. Furthermore, the TLC enables more accurate assessment of temperature at the electrode-tissue interface and deeper within the lesion compared to electrode tip temperature. In addition, main vessel ablations data was historic. However, the experimental setup of the model is designed to enable precise control of parameters including gel composition, gel and saline conductivity, laminar flow rate and catheter positioning to ensure repeatability of results.

Conclusions

Despite similar lesion depth, increased lesion width with larger circumferential coverage in addition to the closer anatomical relationship to renal nerves could account for the better denervation efficacy observed using the contemporary approach of combined main vessel and branch denervation compared to main vessel ablation only.

Although no overheating occurred at the electrode-TLC interface, the long-term safety of this method is yet to be confirmed clinically.

References

1. Krum H, Schlaich M, Whitbourn R, Sobotka PA, Sadowski J, Bartus K, et al. Catheter-based renal sympathetic denervation for resistant hypertension: a multicentre safety and proof-of-principle cohort study. *Lancet*. 2009;373:1275-81.
2. Esler M, Krum H, Sobotka PA, Schlaich MP, Schmieder RE, Böhm M. Symplicity HTN investigators. Renal sympathetic denervation in patients with treatment-resistant hypertension (The Symplicity HTN-2 Trial): a randomised controlled trial. *Lancet*. 2010;376:1903-9.
3. Bhatt DL, Kandzari DE, O'Neill WW, D'Agostino R, Flack JM, Katzen BT, et al. A Controlled Trial of Renal Denervation for Resistant Hypertension. *N Engl J Med*. 2014;370:1393-401.
4. Mahfoud F, Tunev S, Ewen S, Cremers B, Ruwart J, Schulz-Jander D, et al. Impact of Lesion Placement on Efficacy and Safety of Catheter-Based Radiofrequency Renal Denervation. *J Am Coll Cardiol*. 2015;66:1766-75.
5. Fengler K, Ewen S, Hollriegel R, Rommel KP, Kulenthiran S, Lauder L, et al. Blood Pressure Response to Main Renal Artery and Combined Main Renal Artery Plus Branch Renal Denervation in Patients With Resistant Hypertension. *J Am Heart Assoc*. 2017;6:e006196.
6. Henegar JR, Zhang Y, Hata C, Narciso I, Hall ME, Hall JE. Catheter-Based Radiofrequency Renal Denervation: Location Effects on Renal Norepinephrine. *Am J Hypertens*. 2015;28:909-14.
7. Sakakura K, Ladich E, Cheng Q, Otsuka F, Yahagi K, Fowler DR, et al. Anatomic assessment of sympathetic peri-arterial renal nerves in man. *J Am Coll Cardiol*. 2014;64:635-43.

8. Al Raisi SI, Pouliopoulos J, Barry MT, Swinnen J, Thiagalingam A, Thomas SP, et al. Evaluation of lesion and thermodynamic characteristics of Symplicity and EnligHTN renal denervation systems in a phantom renal artery model. *EuroIntervention*. 2014;10:277-84.
9. Al Raisi SI, Barry MT, Qian P, Bhaskaran A, Pouliopoulos J, Kovoor P. Comparison of new generation renal artery denervation systems: Assessing lesion size and thermodynamics using a thermochromic liquid crystal phantom model. *EuroIntervention*. 2017;13:1242-1247.
10. Chik WW, Barry MA, Thavapalachandran S, Midekin C, Pouliopoulos J, Lim TW, et al. High spatial resolution thermal mapping of radiofrequency ablation lesions using a novel thermochromic liquid crystal myocardial phantom. *J Cardiovasc Electrophysiol*. 2013;24:1278-86.
11. Graves FT. The anatomy of the intrarenal arteries and its application to segmental resection of the kidney. *Br J Surg*. 1954;42:132-9.
12. Cosman ER, Jr., Cosman ER, Sr. Electric and thermal field effects in tissue around radiofrequency electrodes. *Pain Med*. 2005;6:405-24.
13. Cosman ER Jr CES. Radiofrequency Lesions. In: Lozano AM GP, Tasker RR, editors. Textbook of stereotactic and functional neurosurgery. 2nd ed. Berlin, Heidelberg, Germany: Springer Science & Business Media; 2009. p. 1359-80.
14. Mahfoud F, Pipenhagen CA, Boyce Moon L, Ewen S, Kulenthiran S, Fish JM, et al. Comparison of branch and distally focused main renal artery denervation using two different radio-frequency systems in a porcine model. *Int J Cardiol*. 2017;241:373-378.
15. Bertog S, Fischel TA, Vega F, Ghazarossian V, Pathak A, Vaskelyte L, et al. Randomised, blinded and controlled comparative study of chemical and

radiofrequency-based renal denervation in a porcine model. *EuroIntervention*. 2017;12:e1898-e906.

16. Sakaoka A, Terao H, Nakamura S, Hagiwara H, Furukawa T, Matsumura K, et al. Accurate Depth of Radiofrequency-Induced Lesions in Renal Sympathetic Denervation Based on a Fine Histological Sectioning Approach in a Porcine Model. *Circ Cardiovasc interv*. 2018;11:e005779.

17. Nath S, DiMarco JP, Haines DE. Basic aspects of radiofrequency catheter ablation. *J Cardiovasc Electrophysiol*. 1994;5:863-76.

18. Haines DE. The biophysics of radiofrequency catheter ablation in the heart: the importance of temperature monitoring. *Pacing Clin Electrophysiol*. 1993;16:586-91.

19. Wittkampf FH, Nakagawa H. RF catheter ablation: Lessons on lesions. *Pacing Clin Electrophysiol*. 2006;29:1285-97.

20. Wood MA, Shaffer KM, Ellenbogen AL, Ownby ED. Microbubbles during radiofrequency catheter ablation: composition and formation. *Heart Rhythm*. 2005;2:397-403.

Chapter 7

Discussion

DISCUSSION

7.1 Summary

Hypertension has a significant long-term clinical burden on our society. Various medical options are available to treat high BP, yet of those who are aware of their hypertension, only half of them have their BP controlled [1]. Interruption of renal sympathetic nerves, which are thought to play a critical role in the mechanism of hypertension through minimally invasive RAD has been considered for the management of resistant hypertension [3]. Nonetheless, inconsistent clinical trial results raised uncertainties regarding the efficacy of this procedure [3, 15, 16]. Thus, further research in the basic mechanisms of RAD was warranted. Amongst various factors, Ablation lesion size is an important determinant for effective denervation. Larger lesions are likely to result in more significant nerve injury. Several RF devices were developed for RAD [22]; however, information regarding their thermal properties and lesion characteristics were limited in the literature. The TLC renal artery phantom model allowed spatiotemporal assessment of RF ablation lesions produced by different RF devices used for RAD. The ability to control variables, and to visualise thermal profiles in real-time in the phantom model enabled comparison between devices under identical experimental settings, which may otherwise not be achievable to such an extent *in vivo*. We first assessed the thermodynamics and lesion dimensions of single electrode Symplicity Flex and multi-electrode EnligHTN systems in the phantom model. The results demonstrated that RF ablation using single electrode Symplicity Flex produced significantly larger lesions in both depth and width compared to multi-electrode EnligHTN, which was likely due to longer ablation duration and larger electrode surface area in contact with the phantom vessel wall (3.8 mm versus 3.4 mm,

and 7.2 mm versus 6.2 mm, p -value <0.001 , for depth and width, respectively). This work provided the first report of a direct comparison between two commercially available RAD devices and their thermal injury depth. A porcine model study later reported similar lesion depth for Symplicity Flex [17]. The significance of the findings from the phantom model were further explored in a clinical study that assessed office BP change after RAD using either systems. Whilst no significant difference in office BP reduction between the two systems was found, the total cohort showed a significant office BP reduction from baseline, which persisted up to 4 years, consistent with results of previous RAD studies (Symplicity HTN-1 & 2). Our study suggested that both systems are as effective in causing sufficient nerve injury to result in a clinical response, and the overall findings support the role of RAD in hypertension management. New generation multi-electrode Symplicity Spyral and EnligHTN systems were later developed to simplify the procedure and make it less operator dependant. Assessment of the new devices in the phantom model demonstrated that the new generation EnligHTN produced larger lesions in depth compared to Symplicity Spyral (2.32 mm versus 2.15 mm, p -value <0.001 , respectively). Moreover, lesion depth for the new generation devices were reduced by 30-40% compared to data we previously reported for the previous generation systems, when performed under similar experimental conditions, suggesting that the new devices may be less effective clinically. According to findings from a post-mortem study by Sakakura, lesion depth between 2.32 - 2.15 mm could potentially miss about 50% of nerve fibres around the main renal artery (proximal to bifurcation) [23]. Consequently, to overcome the limited heating depth of the new generation devices, RF ablation in renal artery branches where nerve fibres are found closer to the intima in addition to the main vessel was investigated as a new method for RAD [23-25]. This method resulted in a better reduction in kidney norepinephrine concentration in a porcine model, and a significant change in BP clinically compared to the conventional method [24, 25]. Initial randomised sham-controlled trials

demonstrated safety and efficacy up to 6 months [26, 27]. Nonetheless, concerns were raised regarding the safety of RF ablation in the branches. Smaller vessel diameter and lower flow rate in the branch could impact lesion size or cause excessive tissue heating resulting in vessel wall injury. Thus, we further developed the phantom model to incorporate renal artery branch anatomy and associated physiological parameters to assess ablation lesion characteristics and to understand the extent of thermal injury during renal branch ablation. In the phantom model, lesions produced in the branch were of similar depth, but had larger circumferential coverage compared to the main vessel. The similarity in lesion depth between the main vessel and the branch together with increased circumferential lesion coverage, and the shallower occurrence of nerve fibres in the branch explain the better efficacy observed with combined branch and main vessel ablation in clinical studies [25]. Additionally, the RF generator temperature-loop feedback mechanism prevented over heating of the electrode-TLC interface, as the maximum temperature observed did not exceed 68 °C. In regards to this, a recent porcine model study assessed the safety of branch ablation using the IberisBloom system (Terumo Corporation, Tokyo, Japan) incorporating a helical catheter design similar to Symplicity Spyril, and demonstrated no significant luminal narrowing based on angiographic assessment or medial damage on histology at up to 90 days post ablation [28].

7.2 Conclusion

The field of RAD continues to evolve. Refining the procedural technique and optimising devices is one aspect of improving the outcome. My work contributes to the field of RAD by helping to identify the limitations and to better understand the capabilities of devices used in managing resistant hypertension, by taking a bench-to bedside-to-bench approach in studying the various systems and feeding into the knowledge cycle required to progress the field. My

work adds to the constant refinement needed and illustrates the complexity faced by RAD as a tool in combating this chronic disease.

7.3 Future directions

It has become evident from the work performed in this thesis and other available data regarding injury depth of RF devices used in RAD, and localisation of renal sympathetic nerves that the current devices have limited thermal injury depth. This resulted in a shift from main vessel ablation as a method for RAD to branch ablation in addition to the main vessel [26]. Nonetheless, the reported magnitude of BP drop with this technique was much lower compared to previously reported and it requires extensive ablation within the smaller diameter branches, the long-term safety of which has not yet been confirmed [26]. It is possible that this could lead to higher complications rate related to catheter manipulation in smaller vessels. Therefore, future work can aim to improve the thermal injury profile for RF devices while maintaining safety. The renal artery phantom model described can be utilised to assess RF ablation, perhaps using an electrophysiology RF catheter to allow adjustments of parameter including ablation power and duration. RF ablations can be performed using escalated power protocol with images acquired at regular interval during RF ablation (e.g. every 10 sec, for 90 sec). Lesion dimension and maximum TLC temperature could then be measured for different power settings at each time interval. Ablation parameters that results in improved lesion depth without causing overheating at the TLC/electrode surface can be determined and can then be assessed in an animal study for validation of thermal injury depth on histology, and to assess safety as well as to confirm nerve fibre injury (both acutely and in medium term). If proven to be feasible and safe, a randomised controlled study in animal could be performed to compare it to the current standard RF systems and non-denervated control. Efficacy can be assessed by measuring

cortical axonal density and kidney norepinephrine concentration. Efficacy and safety can then be assessed in clinical trials with comparison to current standard system, as well as other denervation modalities.

8. Bibliography

1. Roger VL, Go AS, Lloyd-Jones DM, Benjamin EJ, Berry JD, Borden WB, et al. Heart disease and stroke statistics--2012 update: a report from the American Heart Association. *Circulation* 2012;125:e2-e220.
2. Calhoun DA, Jones D, Textor S, Goff DC, Murphy TP, Toto RD, et al. Resistant hypertension: diagnosis, evaluation, and treatment: a scientific statement from the American Heart Association Professional Education Committee of the Council for High Blood Pressure Research. *Circulation* 2008;117:e510-26.
3. Krum H, Schlaich M, Whitbourn R, Sobotka PA, Sadowski J, Bartus K, et al. Catheter-based renal sympathetic denervation for resistant hypertension: a multicentre safety and proof-of-principle cohort study. *Lancet* 2009;373:1275-81.
4. DiBona GF. Physiology in perspective: The Wisdom of the Body. Neural control of the kidney. *Am J Physiol Regul Integr Comp Physiol*. 2005;289:R633-41.
5. DiBona GF. Sympathetic nervous system and the kidney in hypertension. *Curr Opin Nephrol Hypertens* 2002;11:197-200.
6. DiBona GF, Kopp UC. Neural control of renal function. *Physiol Rev* 1997;77:75-197.
7. Esler M, Willett I, Leonard P, Hasking G, Johns J, Little P, et al. Plasma noradrenaline kinetics in humans. *J Auton Nerv Syst* 1984;11:125-44.
8. Esler M, Jennings G, Korner P, Willett I, Dudley F, Hasking G, et al. Assessment of human sympathetic nervous system activity from measurements of norepinephrine turnover. *Hypertension* 1988;11:3-20.
9. Esler M, Jennings G, Lambert G. Noradrenaline release and the pathophysiology of primary human hypertension. *Am J Hypertens* 1989;2:140s-6s.
10. Esler M, Jennings G, Korner P, Blombery P, Sacharias N, Leonard P. Measurement of total and organ-specific norepinephrine kinetics in humans. *Am J Physiol* 1984;247:E21-8.

11. DiBona GF. Functionally specific renal sympathetic nerve fibers: role in cardiovascular regulation. *Am J Hypertens* 2001;14:163s-70s.
12. Campese VM, Kogosov E, Koss M. Renal afferent denervation prevents the progression of renal disease in the renal ablation model of chronic renal failure in the rat. *Am J kidney Dis* 1995;26:861-5.
13. Ye S, Ozgur B, Campese VM. Renal afferent impulses, the posterior hypothalamus, and hypertension in rats with chronic renal failure. *Kidney Int.* 1997;51:722-7.
14. Katholi RE, McCann WP, Woods WT. Intrarenal adenosine produces hypertension via renal nerves in the one-kidney, one clip rat. *Hypertension.* 1985;7:188-93.
15. Esler MD, Krum H, Sobotka PA, Schlaich MP, Schmieder RE, Bohm M. Renal sympathetic denervation in patients with treatment-resistant hypertension (The Symplicity HTN-2 Trial): a randomised controlled trial. *Lancet* 2010;376:1903-9.
16. Bhatt DL, Kandzari DE, O'Neill WW, D'Agostino R, Flack JM, Katzen BT, et al. A controlled trial of renal denervation for resistant hypertension. *N Engl J Med* 2014;370:1393-401.
17. Bertog S, Fischel TA, Vega F, Ghazarossian V, Pathak A, Vaskelyte L, et al. Randomised, blinded and controlled comparative study of chemical and radiofrequency-based renal denervation in a porcine model. *EuroIntervention* 2017;12:e1898-e906.
18. Mahfoud F, Pipenhagen CA, Boyce Moon L, Ewen S, Kulenthiran S, Fish JM, et al. Comparison of branch and distally focused main renal artery denervation using two different radio-frequency systems in a porcine model. *Int J Cardiol.* 2017;241:373-8.
19. Sakakura K, Roth A, Ladich E, Shen K, Coleman L, Joner M, et al. Controlled circumferential renal sympathetic denervation with preservation of the renal arterial wall using intraluminal ultrasound: a next-generation approach for treating sympathetic overactivity. *EuroIntervention.* 2015;10:1230-8.

20. Pathak A, Coleman L, Roth A, Stanley J, Bailey L, Markham P, et al. Renal sympathetic nerve denervation using intraluminal ultrasound within a cooling balloon preserves the arterial wall and reduces sympathetic nerve activity. *EuroIntervention*. 2015;11:477-84.
21. Chik WW, Barry MA, Thavapalachandran S, Midekin C, Pouliopoulos J, Lim TW, et al. High spatial resolution thermal mapping of radiofrequency ablation lesions using a novel thermochromic liquid crystal myocardial phantom. *J Cardiovasc Electrophysiol*. 2013;24:1278-86.
22. Bunte MC, Infante de Oliveira E, Shishehbor MH. Endovascular treatment of resistant and uncontrolled hypertension: therapies on the horizon. *JACC Cardiovasc Interv*. 2013;6:1-9.
23. Sakakura K, Ladich E, Cheng Q, Otsuka F, Yahagi K, Fowler DR, et al. Anatomic assessment of sympathetic peri-arterial renal nerves in man. *J Am Coll Cardiol*. 2014;64:635-43.
24. Mahfoud F, Tunev S, Ewen S, Cremers B, Ruwart J, Schulz-Jander D, et al. Impact of Lesion Placement on Efficacy and Safety of Catheter-Based Radiofrequency Renal Denervation. *J Am Coll Cardiol*. 2015;66:1766-75.
25. Fengler K, Ewen S, Hollriegel R, Rommel KP, Kulenthiran S, Lauder L, et al. Blood Pressure Response to Main Renal Artery and Combined Main Renal Artery Plus Branch Renal Denervation in Patients With Resistant Hypertension. *J Am Heart Assoc*. 2017;6(8).
26. Townsend RR, Mahfoud F, Kandzari DE, Kario K, Pocock S, Weber MA, et al. Catheter-based renal denervation in patients with uncontrolled hypertension in the absence of antihypertensive medications (SPYRAL HTN-OFF MED): a randomised, sham-controlled, proof-of-concept trial. *Lancet*. 2017;390:2160-70.
27. Kandzari DE, Bohm M, Mahfoud F, Townsend RR, Weber MA, Pocock S, et al. Effect of renal denervation on blood pressure in the presence of antihypertensive drugs: 6-month

efficacy and safety results from the SPYRAL HTN-ON MED proof-of-concept randomised trial. *Lancet*. 2018. 391:2346-2355

28. Sakaoka A, Rousselle SD, Hagiwara H, Tellez A, Hubbard B, Sakakura K. Safety of catheter-based radiofrequency renal denervation on branch renal arteries in a porcine model. *Catheter Cardiovasc Interv*. 2018. doi:10.1002/ccd.27953. [Epub ahead of print]